CASCADING EFFECTS OF LAKE ERIE HARMFUL ALGAL BLOOMS (HABS) ON ZOOPLANKTON PREY PRODUCTION, LARVAL FISH ABUNDANCE, YOUNG-OF-YEAR FORAGE FISH AVAILABILITY, AND WALLEYE YEAR CLASS STRENGTH

By

Tomena K. Scholze

A THESIS

Submitted to
Michigan State University
in partial fulfillment of the requirements
for the degree of

Fisheries and Wildlife–Master of Science

2017

ABSTRACT

CASCADING EFFECTS OF LAKE ERIE HARMFUL ALGAL BLOOMS (HABS) ON ZOOPLANKTON PREY PRODUCTION, LARVAL FISH ABUNDANCE, YOUNG-OF-YEAR FORAGE FISH AVAILABILITY, AND WALLEYE YEAR CLASS STRENGTH

By

Tomena K. Scholze

In Lake Erie, walleye (*Sander vitreus*) fishery recruitment is controlled by physical and biological processes acting on early life history stages; however, the impacts of recent, recurring cyanobacterial (*Microcystis aeruginosa*) blooms on fishery ecosystem productivity are largely unknown. I hypothesized these harmful algal blooms (HABs) would negatively impact walleye recruitment in a trophic cascade framework by altering algal community species and size composition, limiting suitable food particles available to zooplankton and therefore decreasing zooplankton abundance and causing a shift in community composition. This would directly impact the prey resources available to larval fishes during critical life stages, affecting their growth, survival, and recruitment to the young-of-year (YOY) stage. I investigated the potential for Lake Erie HABs to impact YOY forage fish availability and walleye year class strength using fisheries-independent data from the annual western basin interagency bottom trawl survey and satellite-derived estimates of HAB severity for 2002-2014. I further assessed how HABs impact zooplankton and ichthyoplankton prey availability by sampling *Microcystis*, zooplankton, and larval fishes in the western basin in 2015 and 2016. HABs did not have a significant impact on walleye year class strength, but they did impact the distribution of YOY and larval fishes in the western basin, in particular clupeid species. However, HABs were associated with increased zooplankton production, suggesting HABs directly impact larval and planktivorous fishes, rather than indirectly decreasing their abundance by limiting the availability of zooplankton prey.

ACKNOWLEDGEMENTS

This thesis is the result of work funded by the Great Lakes Restoration Initiative and the U.S. Geological Survey.

I thank the members of my committee, Dr. Ed Roseman, Dr. Dan Hayes, and Dr. Mary Anne Evans for their advice throughout this project and their constructive criticism regarding this manuscript. I sincerely thank Dr. Bill Taylor for the opportunity to pursue my master's degree at Michigan State University and his encouragement and patient guidance throughout my program of study.

I am indebted to my many colleagues at the USGS Great Lakes Science Center in Ann Arbor, MI for their assistance in planning and executing two successful seasons of field sampling: Greg Kennedy, Jaquelyn Craig, Jason Fischer, Kevin Keeler, Robin DeBruyne, and Stacey Ireland. I appreciate those of you who joined me in the challenges and joys of field work on Lake Erie: Nathan Williams, Emily Galassini, Dana Castle, Dustin Bowser, Paige Wigren, and Rob Hunter. I would also like to thank Kevin Peterson for his guidance regarding data analysis techniques that were novel to me.

I extend a special thank you to my undergraduate research technicians: Alex Hondzinski, Katie Kierczynski, Zach Fyke, Andrew Pawloski, Julia Krohn, Joey Riedy, Michelle VanCompernolle, and Jessica Clark. Without your tireless work in the field and behind the microscope this undertaking would have proved truly endless.

I gratefully acknowledge the generosity of my colleagues who provided access to data in support of this project: Dr. Richard Stumpf, Dr. Tim Davis, Dr. Chris Vandergoot, Dr. Eric Weimer, Dr. Mike Thomas, and Dr. Jeff Tyson. In particular, Chapter 1 was produced under written agreement with Lake Erie Committee of the Great Lakes Fishery Commission.

I also extend my sincere gratitude to Nicole Jess of MSU's Center for Statistical Training and Consulting for her patience and insight into the world of sample selection models. Finally, I would like to thank my lab mates, friends, and family for your unending encouragement. Your support kept me motivated through the rough times along the way.

TABLE OF CONTENTS

LIST OF TABLES

LIST OF FIGURES

KEY TO ABBREVIATIONS

CI	cyanobacterial index
CI_i	cyanobacterial index during the i^{th} 10-day interval
CI_{max}	annual maximum cyanobacterial index
CPUE	catch per unit effort
DO	bottom dissolved oxygen
ECDF	empirical cumulative distribution function
GLM	generalized linear model
HAB	harmful algal bloom
IACUC	Institutional Animal Care and Use Committee
IMR	inverse Mills ratio
MERIS	medium resolution imaging spectrometer
MODIS	moderate resolution imaging spectroradiometer
NDBC	National Data Buoy Center
NOAA	National Oceanic and Atmospheric Administration
ODNR	Ohio Department of Natural Resources
OMNR	Ontario Ministry of Natural Resources
SE	standard error
USGS	United States Geological Survey
YOY	young-of-year

THESIS INTRODUCTION

In marine and freshwater environments, fish larvae experience high and variable rates of mortality (Houde 1997). For many populations, including Lake Erie walleye (*Sander vitreus*), fluctuations in larval mortality rates regulate recruitment, causing substantial interannual variability in year class strength. Larval growth and survival rates are driven by spatial and temporal overlap of larvae with patchily distributed habitat conditions, including zooplankton prey (Roseman et al. 2005). Currently, walleye recruitment in Lake Erie is thought to be regulated at the larval stage by biological and physical processes such as water warming rate and prey availability (Roseman 2000). A regression model incorporating spawning stock biomass, water warming rate, and prey abundance explained 92% of the observed variation in age-2 walleye recruitment to the fishery in western Lake Erie (Madenjian et al. 1996).

However, the size and frequency of harmful cyanobacterial (*Microcysits aeruginosa*) blooms has increased dramatically in Lake Erie in recent decades (Michalak et al. 2013, Obenour et al. 2014, Stumpf et al. 2012), spatially and temporally overlapping with larval fishes in the epilimnetic waters of the western basin. Though some studies (Landsberg et al. 2002) have assessed the direct effects of algal toxins on zooplankton (e.g. Weigand & Pflugmacher 2004) and fish (e.g. Acuña et al. 2012), few studies have characterized the effect of HABs on fish communities at an ecological scale, especially in freshwater ecosystems. In marine environments, HABs have been associated with decreases in fish density and species richness (Gannon et al. 2009) and species-specific changes in recruitment (Warlen et al. 1998). However, a lack of information on how HABs affect ecological communities remains a problem for aquatic and marine resource managers (Ramsdell et al. 2005).

In this thesis, I address two main questions: 1) How are Lake Erie HABs affecting age-0 walleye recruitment? 2) How are HABs affecting the abundance and distribution of zooplankton prey, ichthyoplankton, and young-of-year (YOY) forage fishes in the western basin of Lake Erie? I hypothesized Lake Erie HABs would affect aquatic biotic communities on multiple trophic levels, influencing fishery recruitment through food web interactions. Under this trophic cascade framework, I expected to see a disruption in food web dynamics where HABs are present. Consistent with a trophic cascade framework, I predicted HABs would alter algal community species and size composition, limiting suitable-sized food particles for zooplankton, which in turn would cause a shift in zooplankton community structure. This change in zooplankton availability would directly impact the growth and survival of prey resources available to larval fishes during critical life stages, decreasing forage fish production, and ultimately altering walleye fishery recruitment dynamics.

CHAPTER 1

IMPACTS OF HARMFUL ALGAL BLOOMS ON YOUNG-OF-YEAR FORAGE FISH PRODUCTION IN WESTERN LAKE ERIE AND IMPLICATIONS FOR WALLEYE YEAR CLASS STRENGTH

INTRODUCTION

Harmful algal blooms (HABs), rapid accumulations of algal cells associated with socio-economic or ecological impairment, are increasing globally (Ho & Michalak 2015) due to anthropogenic nutrient loading and climate change (Michalak et al. 2013). In recent years, blooms of *Microcystis aeruginosa* (hereafter *Microcystis*), a toxin-producing cyanobacteria, have been occurring with increasing frequency and severity in the western basin of Lake Erie (Obenour et al. 2014, Stumpf et al. 2012) due to re-eutrophication (Scavia et al. 2014). These HABs can produce microcystin, a hepatotoxin, which have been associated with a number of ill effects on people and wildlife, prompting beach closures and inhibiting other water-based recreational activities, decreasing property values (Baron et al. 2016), and impacting animal and human health by contaminating drinking water supplies (Backer et al. 2015). However, the impacts of HABs on freshwater ecosystems and fishery production are poorly understood.

Some studies have examined the direct effects of algal toxins present in the environment during HABs on select aquatic organisms (e.g. Wood et al. 2014, Landsberg 2002), but more work is needed to characterize the direct impacts of HABs on the myriad of species exposed to a variety of algal toxins in aquatic and marine environments. In Lake Erie, HABs are associated with the production of microcystin, a hepatotoxin. Ingestion of microcystin has been linked to decreased feeding, growth, survival, and reproduction rates in zooplankton (Wilson et al. 2006), and poor length-weight condition factor, hemorrhaging, liver and gonadal lesions, and a decline in reproductive potential in fishes (Acuña et al. 2012). Microcystin accumulation may occur in

primary consumers like gizzard shad (*Dorosoma cepedianum*), the preferred prey of walleye (*Sander vitreus*) (Knight et al. 1984), that unselectively filter feed on phytoplankton in the epilinion and metalimnion (Wiegand & Pflugmacher 2004). Microcystin can also bioaccumulate in fish tissues, increasing in concentration at higher trophic levels (Wituszynski 2014). These direct effects of Lake Erie *Microcystis* blooms and associated toxins may impact the condition, nutritional status, survival, recruitment, distribution, and abundance of important walleye prey species, which include gizzard shad, alewife (*Alosa pseudoharengus*), shiners (*Notropis* spp.), white perch (*Morone americana*), white bass (*M. chrysops*), and yellow perch (*Perca flavescens*) (Roseman 2000). Though the direct effects of microcystins on fish are relatively well-studied, few studies have investigated the indirect effects of HABs on fish communities at an ecosystem scale.

Though Warlen et al. (1998) observed species-specific changes in recruitment of marine fishes in response to a red tide dinoflagellate bloom, it is uncertain how changing limnological conditions in Lake Erie with increasingly frequent and severe cyanobacterial HABs will impact forage fish production and walleye recruitment. The factors driving the recruitment of age-2+ walleye into the fishery in past decades are relatively well understood; however, recruitment is highly variable and strong year classes are produced infrequently (Walleye Task Group 2016). Walleye fishery recruitment is determined during the first year of life, so walleye year class strength, an index of fishery recruitment, is measured during an annual western basin interagency bottom trawl survey in August that targets young-of-year (YOY) fishes. Currently, walleye recruitment to the YOY stage is thought to be regulated by biological and physical processes that create patchily distributed habitat conditions in western Lake Erie, mediating larval growth and survival rates (Roseman et al. 2005). These processes include: water warming rate, which

influence larval metabolism, starvation, and growth (Busch et al. 1975, Roseman 2000); frequency and intensity of storm events, which can dislodge eggs from western basin reefs (Roseman 2000); river discharge, which determines mortality rates and the speed of larval out-migration from rivers (Mion et al. 1998); and zooplankton and ichthyoplankton prey availability, which influence feeding and growth rates. A Ricker stock-recruitment model incorporating spawning stock biomass, water warming rate, and abundance of age-0 gizzard shad prey available in the fall explained 92% of the observed variation in age-2 walleye recruitment in western Lake Erie (Madenjian et al. 1996). However, HABs may spatially and temporally overlap with zooplankton and ichthyoplankton prey resources, YOY forage fishes, and YOY walleye in the western basin of Lake Erie. Therefore, it is uncertain how changing limnological conditions with increasingly frequent and severe HABs will impact fishery ecosystems and walleye year class strength.

I hypothesized Lake Erie HABs would affect aquatic biotic communities on multiple trophic levels, limiting the availability YOY prey and influencing walleye fishery recruitment in a trophic cascade (Ware & Thompson 2005). Consistent with a trophic cascade framework, I predicted HABs would alter algal community species and size composition, limiting suitable-sized food particles for zooplankton, which in turn would cause a decrease in zooplankton abundance and a shift in zooplankton community structure. This change in zooplankton prey availability would directly impact the growth and survival of larval fishes during their critical life stages, influencing larval and YOY forage fish production, and ultimately altering walleye fishery recruitment dynamics. The goal of this study was to determine if Lake Erie HABs have a detrimental impact on YOY forage fish abundance and growth and assess effect of HABs on walleye recruitment to inform fishery management and ensure sustainable harvest. In this study I

focused on three main objectives: 1) How does annual HAB severity impact walleye year class strength? I hypothesized that walleye year class strength would decrease with increasing HAB severity because severe HABs would limit the zooplankton prey available to larval and YOY forage fishes, causing YOY forage fish production to decline. 2) How does HAB cell density impact the distribution of walleye and their prey? I hypothesized the catch per unit effort (CPUE) of YOY walleye and YOY forage fishes would decrease with increasing HAB cell density, since I predicted YOY fishes would avoid areas affected by HABs and associated toxins. 3) How do HABs impact the growth of YOY fishes? I hypothesized, if HABs decrease the availability of prey resources, HABs would be associated with decreased growth rates, indicated by a negative shift in length-frequency distributions of YOY walleye and YOY forage fishes.

METHODS

YOY Catch Data

To assess the effect of HABs on walleye year class strength, YOY forage fish relative abundance, and YOY fish distribution in the western basin of Lake Erie, I obtained fisheries-independent catch data for YOY fishes in 2002 through 2015 from the annual western basin interagency bottom trawl survey conducted by the Ohio Department of Natural Resources (ODNR) and Ontario Ministry of Natural Resources (OMNR) (Figure 1, LEC 2015). Since walleye year class strength, an index of recruitment, is estimated in August (LEBS 2015), I calculated CPUE, a measure of relative abundance, of YOY fishes captured in August using Equation 1:

(1) $$CPUE = catch \div \frac{EffDist \times 1000 \times 6}{10000}$$

where CPUE is measured in fish/hectare, *catch* is the number of fish captured during the trawl, and *EffDist* is the distance in km sampled during trawling. The net opening measured 6 m across

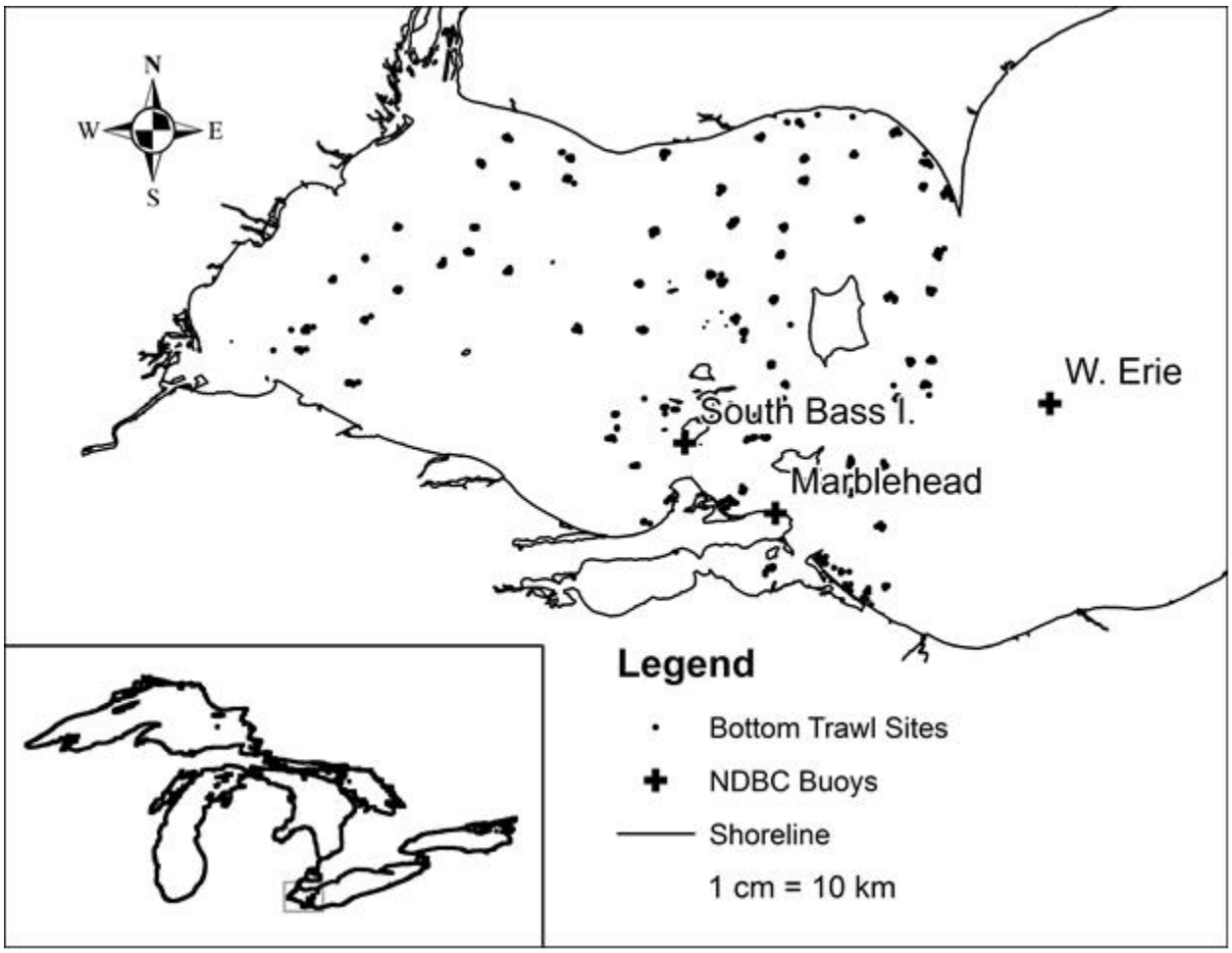

Figure 1: Map of Lake Erie western basin interagency bottom trawl sites and National Data Buoy Center stations.

on average (LEBS 2015). I used the annual average CPUE of YOY walleye in the August bottom trawl survey as an index of relative year class strength. I evaluated trends in the CPUE of YOY clupeids (alewife and gizzard shad) and shiners (*Notropis* spp.) captured during the August bottom trawl survey to determine the relative abundance and distribution of forage fishes that are the preferred prey of walleye (Knight et al. 1984). I also investigated trends in the relative abundance and distribution of other walleye prey species, including YOY yellow perch, white perch, white bass, and freshwater drum (*Aplodinotus grunniens*) (Scott & Crossman 1973).

Environmental data collected during the bottom trawl survey included water depth, bottom temperature, surface temperature, Secchi depth, and bottom dissolved oxygen (DO).

HAB Density Estimation

R.P. Stumpf provided 10-day composite images of HAB severity in western Lake Erie estimated from MERIS and MODIS satellite data for June through October in 2002 through 2014 (Wynne & Stumpf 2015). Wynne & Stumpf (2015) binned daily images into each 10-day composite to avoid underestimating algal biomass due to wind-induced mixing and reduce data loss due to clouds; each pixel in the 10-day composite image represents the maximum HAB severity observed over the 10 days included in the composite. In ArcGIS 10.4, I calculated the cyanobacterial index (CI), an estimate of HAB severity, during the western basin interagency bottom trawl survey at each bottom trawl site using Equation 2 (Wynne & Stumpf 2015):

(2) $$CI = 10^{scaled\ number \div 100 - 4}$$

where CI is the cyanobacterial index, and *scaled number* is the HAB severity value extracted from the 1.1 km^2 pixel corresponding to each western basin interagency bottom trawl site. In cases where no HAB severity data was available at the trawl site, the value from the nearest neighboring pixel was used. For ease of comparison with other studies, I converted CI to an estimate of HAB cell density at each trawl site, with one CI unit equaling approximately 10^8 cells/mL (Stumpf et al. 2012). I divided these estimates of HAB cell density into five categories: negligible, low, medium, high, and very high. I set the negligible category (≤10,000 cells/mL) near the detection threshold for HABs in the composite images: 0.0001 CI or approximately 2.5 x 10^4 cells/mL (Wynne & Stumpf 2015). I based the low category (10,000-100,000 cells/mL) on the World Health Organization's "significantly increased risk" threshold of 0.001 CI or 10^5 cells/mL (Chorus & Bartram 1999). I established the medium (100,000-300,000 cells/mL), high

(300,000-650,000 cells/mL), and very high (>650,000 cells/mL) categories by separating the remaining range of HAB density values using the Fisher-Jenks natural breaks algorithm in the R package "classInt" (Bivand 2015, R Core Team 2014) and rounding the values to the nearest 50,000 cells/mL. I expected to observe substantial declines in YOY fish CPUE at sites where the HAB cell density was greater than 100,000 cells/mL. In addition to estimating the density of HAB cells at each trawl site, I obtained estimates of lake-wide HAB severity (CI_i) for eleven 10-day intervals in 2002-2015 (Stumpf et al. 2016). Stumpf et al. (2016) calculated CI_i by summing the CI of all pixels in the western basin for each 10-day composite image, and proposed using the maximum CI_i (CI_{max}) as an index of yearly HAB severity. I considered blooms mild when $CI_{max} \leq 1$, moderate when CI_{max} is between 1 and 2.4, severe when CI_{max} is between 2.4 and 6, and extreme when $CI_{max} > 6$ (International Joint Commission 2014). I expected low YOY forage fish abundance and walleye year class strength when CI_{max} was greater than 2.4.

Spring Storm Events

In order to incorporate the frequency of severe spring storm events into my analysis of the factors which influence walleye year class strength, I obtained continuous wind data recorded on South Bass Island, OH for 1 April – 15 May 2002-2015 from National Oceanic and Atmospheric Administration (NOAA) National Data Buoy Center (Figure 1, NDBC 2017c). I supplemented missing data with measurements from a nearby station at Marblehead, OH (NDBC 2017b). I considered wind speed observations exceeding 4.028 ms^{-1} from the E-NE (45^o – 90^o), 4.861 ms^{-1} from the S-SW (180^o – 225^o), or 5.694 ms^{-1} from the NW (270^o – 315^o) storm events that could disturb walleye egg and larval development on western basin reefs (Busch et al. 1975, Roseman et al. 1996). I used the proportion of storm observations in each year as an annual index of spring storm events.

Water Warming Rate

In order to incorporate water warming rate into my analysis of the factors which influence walleye year class strength, I obtained hourly measurements of surface water temperature in western Lake Erie from NOAA National Data Buoy Center (Figure 1, NDBC 2017a). I calculated the daily mean water temperature and used linear regression to determine the water warming rate during 1 April – 15 May of each year, a critical period for walleye egg and larval development (Roseman et al. 1996).

YOY Walleye Year Class Strength Regression Tree

To determine which biotic and abiotic variables had the greatest influence walleye year class strength, I built and pruned a regression tree using the R package "rpart" (Therneau et al. 2014, R Core Team 2014). YOY walleye year class strength was the dependent variable in the model, and independent variables included the average bottom temperature, average surface temperature, average DO, average Secchi depth and average depth measured at western basin interagency bottom trawl sites, CI_{max}, the proportion of storm observations 1 April – 15 May, the water warming rate 1 April – 15 May, and the average CPUE of YOY yellow perch, *Notropis* spp., *Morone* spp., clupeids, and freshwater drum captured in the western basin interagency bottom trawl survey.

YOY Walleye CPUE Regression Tree

To determine which biotic and abiotic variables had the greatest influence on YOY walleye CPUE at each bottom trawl site, I built and pruned a regression tree using the R package "rpart" (Therneau et al. 2014, R Core Team 2014). YOY walleye CPUE was the dependent variable in the regression tree, and independent variables included the CPUE of YOY yellow perch, freshwater drum, clupeid, *Notropis* and *Morone* species, site location (latitude and

longitude), depth, DO, Secchi depth, bottom temperature, surface temperature, and HAB cell density at each western basin interagency bottom trawl site.

Modeling YOY Walleye CPUE

To determine how YOY walleye CPUE at each trawl site was influenced by HAB cell density, site location, temperature, water clarity, depth, and dissolved oxygen, I used R (R Core Team 2014) to fit a Heckman selection model to predict YOY walleye CPUE using data from 2002-2014. Heckman's selection model is widely used in economics and sociology to address selection biases that occur when modeling two-stage processes, including farmers' perception of and adaptation to climate change (Tilahun & Bedemo 2014), the probability and scale of corporate acquisitions in the stock market (Peng et al. 2013), and the elderly's utilization and cost of health care (Lim et al. 2011). This approach accounts for selection biases, since the outcome equation which models the second stage (e.g. adaptation to climate change) is conditional on the selection equation which models the first stage (e.g. perception of climate change). In natural resources, Heckman's selection model has similarly been applied to datasets in which selection bias occurs because corner solutions (i.e. observations of $y = 0$) are prevalent (Wooldridge 2012). Though using the Poisson distribution can address selection bias when y is a discrete count variable, Heckman's selection model has been used to model continuous independent variables including participation in and value of sportfishing (Bockstael et al. 1990) and non-consumptive wildlife recreation (Rockel & Kealy 1991). Here, I applied Heckman's selection model to YOY walleye CPUE, a continuous variable which exhibits a corner solution response (CPUE = 0 at 55.5% of trawl sites). Using all 845 observations, I fit a probit model as the selection equation to model the probability that YOY walleye CPUE $\neq 0$. I then calculated the inverse Mills ratio (IMR) and included it as a sample selection correction factor in the

outcome equation, which models non-zero CPUE. I fit the outcome equation as a linear model with ln-transformed dependent variable, including only observations where CPUE > 0 (n = 376). The global probit selection equation included the latitude, longitude, surface temperature, bottom temperature, Secchi depth, DO, and HAB cell density at each trawl site in each year as independent variables. In addition, the global linear outcome equation included the IMR to account for selection bias (i.e. using only non-zero CPUE observations to build the model). I did not include surface temperature as an independent variable in the outcome equation to avoid issues with multicollinearity.

Modelling YOY Forage Fish CPUE

To determine how YOY forage fish (clupeid and *Notropis* species) CPUE at each trawl site was influenced by HAB cell density, site location, temperature, water clarity, depth, and DO, I built a model predicting YOY forage fish CPUE using data from 2002-2014 in R (R Core Team 2014). Since YOY forage fish CPUE is a continuous variable which exhibits a corner solution response (CPUE = 0 at 22% of trawl sites), I again decided to model the probability that CPUE ≠ 0 and non-zero CPUE separately with Heckman's selection model. I used a probit model as the selection equation and a linear regression with a ln-transformed dependent variable as the outcome equation. I included the latitude, longitude, surface temperature, bottom temperature, Secchi depth, bottom dissolved oxygen DO, and HAB cell density at each trawl site as independent variables in the global probit selection model. In addition, the global linear outcome equation included the IMR to account for sample selection.

YOY Length-frequency Analysis

To investigate if the size structure of YOY walleye, yellow perch, clupeids, *Notropis* spp., *Morone* spp., or freshwater drum sampled in 2002-2015 differed among years or among

HAB cell density categories, I constructed length-frequency histograms of YOY fishes captured during the August western basin interagency bottom trawl survey in each year using length intervals of 10 mm for walleye, clupeids, *Morone* species, and freshwater drum (Neumann et al. 2012) and 5 mm for yellow perch and *Notropis* spp., which were shorter on average. Using R (R Core Team 2014), I fit an empirical cumulative distribution function (ECDF), which shows the proportion of fish that are shorter than each observed length (Neumann & Allen 2007), to compare each length-frequency distribution and assess differences between years and among HAB cell density categories. I compared length-frequency distributions for each species between years and among HAB severity categories using pairwise bootstrapped Kolomogorov-Smirnoff tests, which are insensitive to ties associated with non-continuous or binned data (Sekhon 2011). I adjusted p-values for multiple comparisons.

RESULTS

Annual Trends in HAB Severity and YOY CPUE

869,381 YOY fishes were captured during 916 bottom trawls (Figure 2) that were conducted by ODNR and OMNR in the western basin of Lake Erie from 2002 through 2015, representing 30 species (Table A1). YOY walleye year class strength was highest in 2003; the annual average CPUE of YOY walleye during the August bottom trawl was 249.6 ± 41.8 fish/hectare (Figure 2A). A relatively strong year class of walleye was produced in 2015, when YOY walleye CPUE averaged 110.5 ± 19 fish/hectare. In other years, YOY walleye CPUE averaged less than 50 fish/hectare. Similarly, a strong year class of yellow perch was produced in 2003, when an average 2739.4 ± 536.2 fish/hectare were captured during the August bottom trawl survey (Figure 2B). Unlike walleye, the second-strongest year class of yellow perch was

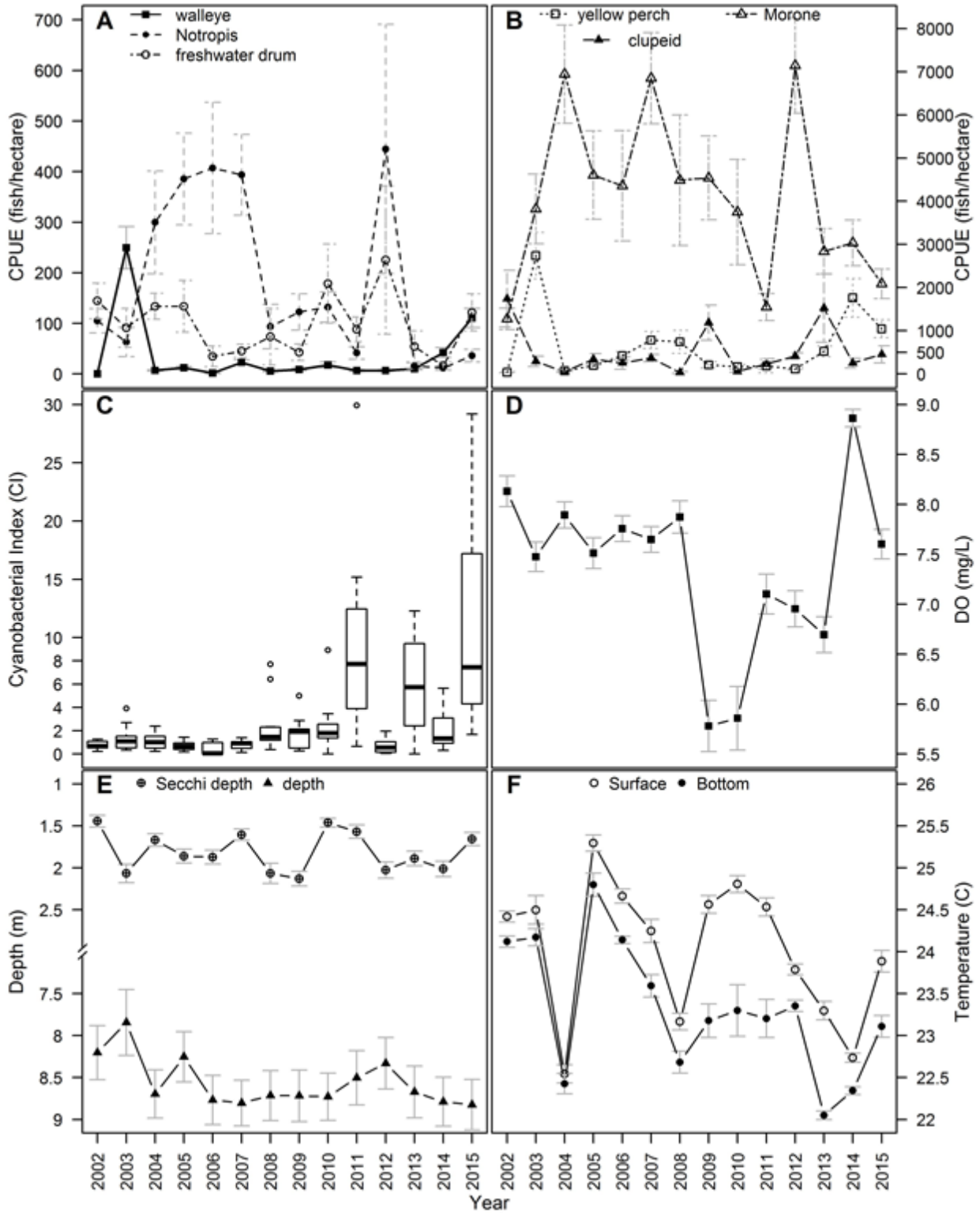

Figure 2: Western basin annual interagency bottom trawl trends 2002-2015. Gray bars indicate 1 SE. A-B: Annual average CPUE of YOY walleye, *Notropis* spp., freshwater drum, yellow perch, clupeid, and *Morone* spp in the August bottom trawl survey. C: Lake wide CI_i during each 10-day interval (Stumpf et al. 2016). D: Annual average DO at trawl sites. E: Annual average depth at trawl sites. F: Annual average temperature at trawl sites.

produced in 2014, with an average YOY yellow perch CPUE of 1762.3 ± 446.8 fish/hectare; however, a relatively strong year class was also produced in 2015, when the annual average CPUE was 1045.4 ± 208.2 fish/hectare. The relative abundance of YOY clupeid forage fishes (alewife and gizzard shad) was highest in 2002, 2009, and 2013, when an average of 1741.8 ± 657, 1186.3 ± 406, and 1526 ± 794 fish/hectare were captured, respectively (Figure 2B). YOY shiner (*Notropis* spp.) relative abundance was highest from 2004 through 2007, when the annual average CPUE ranged from 300 ± 101.6 to 407.3 ± 129.8 fish/hectare (Figure 2A). The largest year class of shiners was produced in 2012, when an average of 444.8 ± 246.5 fish/hectare were captured in the August bottom trawl survey. *Morone* spp. (*Morone americana* and *M. chrysops*) were the most abundant species captured in the August bottom trawl survey, comprising 68% of the total catch during this time period; the annual average CPUE of *Morone* spp. was less than 2000 fish/hectare only in 2002 and 2011 (Figure 2B). Freshwater drum year class strength was highest in 2012, with an annual average CPUE of 225.1 ± 146.5 fish/hectare, although the annual average CPUE also exceeded 100 fish/hectare in 2002, 2004, 2005, 2010, and 2015 (Figure 2A).

The annual average water depth and Secchi depth at bottom trawl sites were similar in all years 2002-2015 (Figure 2E). Annual average water temperature ranged from 22 to almost 26 ^{o}C (Figure 2F). Annual average DO ranged from 5.5-9 mg/L (Figure 2D), with anoxic conditions very rarely observed at western basin interagency bottom trawl sites. HAB severity generally increased from 2002-2015. HABs were most severe in 2011, 2013, and 2015, with CI_{max} values greater than 10 (Figure 2C). In 2002-2015, 19-44% of wind observations recorded near South Bass Island, OH had the potential to disturb walleye egg and larval development on western basin reefs in the spring (1 April – 15 May) (Figure 3). Water warming rates in the spring ranged from 0.1107 to 0.2849 ^{o}C/day; though water temperature decreased in the western basin during

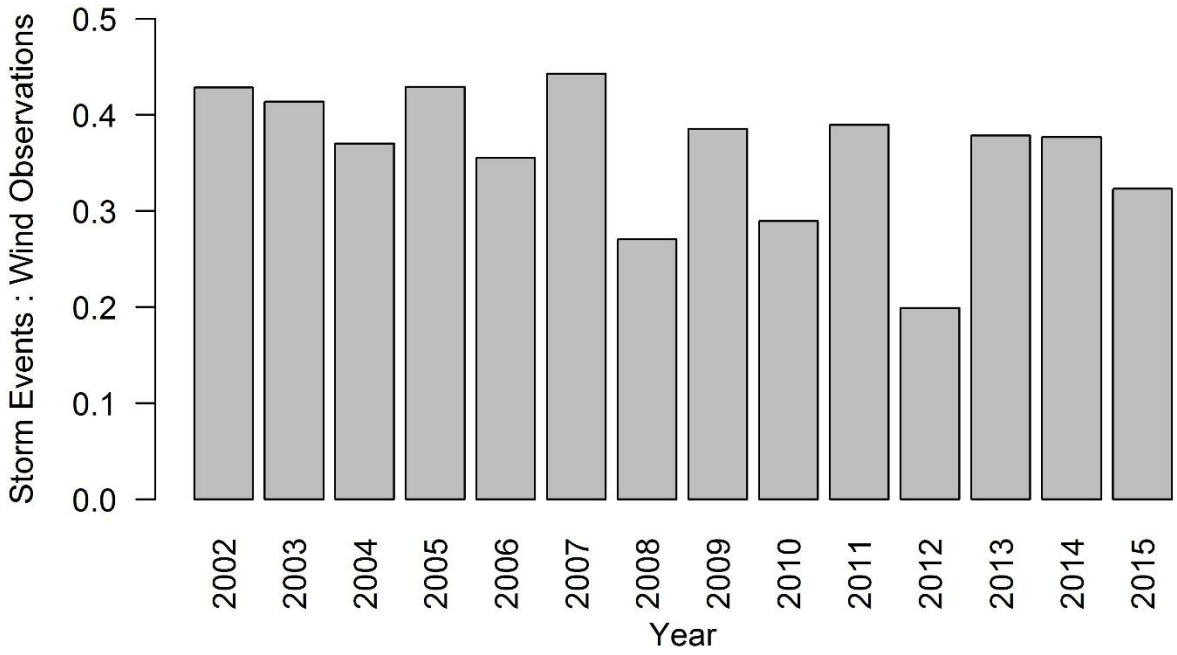

Figure 3: Proportion of wind observations severe enough to disturb walleye egg and larval development on western basin reefs 1 April – 15 May, 2002-2015.

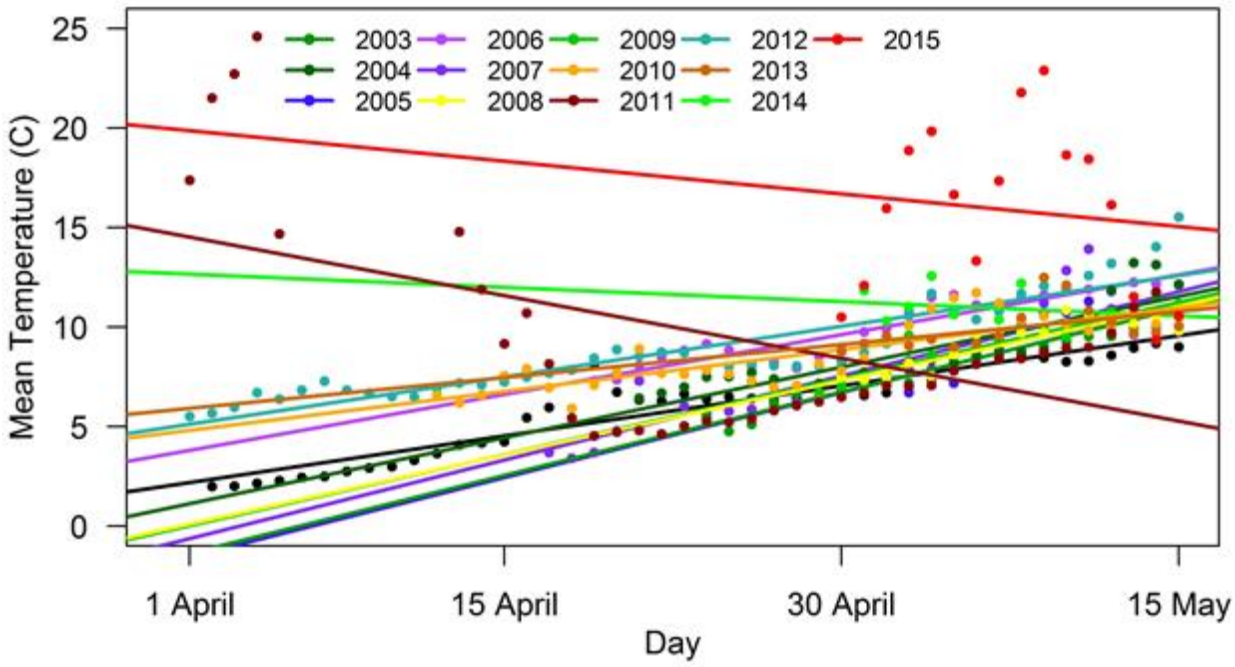

Figure 4: Spring water warming rates in the western basin of Lake Erie, 2002-2015. Points represent daily mean temperature recorded by NOAA National Data Buoy Center (NDBC 2017a).

this period in 2011, 2014, and 2015 (Table A2), though this was likely an artifact of incomplete or inaccurate water temperature measurements in early April. Water temperatures were highest in 2011 and 2015, two years when extremely severe HABs formed in the western basin (Figure 4).

Walleye Year Class Strength Regression Tree

The walleye year class strength regression tree (Figure 5) suggests the annual average CPUE of YOY yellow perch was the most important predictor of walleye year class strength. Strong walleye year classes were produced when the annual average yellow perch CPUE was greater than 914 fish/hectare, while annual average DO and depth had a fine-scale influence on the formation of moderate and weak year classes. These results suggest walleye year class strength and annual average yellow perch relative abundance are highly correlated (Pearson's $r = 0.869$, $p < 0.0001$), which is reasonable considering their similar life histories. When annual

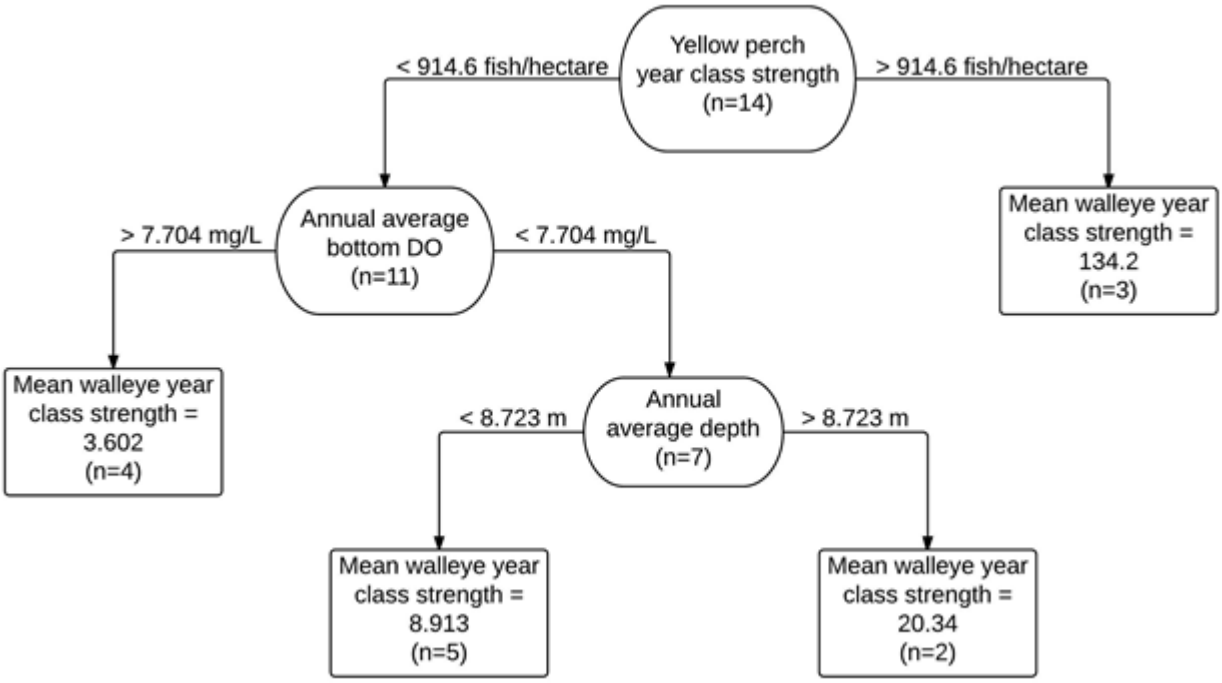

Figure 5: Pruned regression tree depicting factors influencing walleye year class strength.

average CPUE of yellow perch, *Notropis* spp., *Morone* spp., clupeids, and freshwater drum were excluded from the regression tree, the model had difficulty converging. This suggests abiotic factors, including CI_{max}, are not good predictors of highly variable walleye year class strength, or there was not enough variation in this relatively small (n = 14) dataset for model convergence.

Bottom Trawl Trends

Total YOY CPUE varied widely among years and trawl sites 2002-2014 (Figure 6). During the August bottom trawl survey 2002-2014, the water depth at trawl sites ranged from 1.2-12.7 m, with an overall mean of 8.5 m, water temperature ranged from 14.7-26.6 ºC with a mean of 23.3 ºC at the bottom and from 21-27.3 C with a mean of 24 ºC at the surface, Secchi depth ranged from 0.3-4.9 m, with an overall mean of 1.8 m, and DO ranged from 0.4-13.1 mg/L, with an overall mean of 7.3 mg/L.

HAB density (cells/mL) at trawl sites increased from June through August in all years. Estimates of HAB density at trawl sites in June, July, and August were highly positively correlated with each other, though the strength of the correlation decreased as the temporal interval between density estimates increased ($0.286 \leq r \leq 0.626$, $p < 0.001$). In addition, estimates of HAB cell density during the August bottom trawl was highly positively correlated with CI_i during August ($r = 0.41$, $p < 0.001$). HAB density was often highest along the Ohio shoreline (Figure 6).

YOY Walleye CPUE Regression Tree

The YOY walleye CPUE regression tree (Figure 7) suggests the CPUE of another percid, YOY yellow perch, at each bottom trawl site was the most important predictor of YOY walleye CPUE. CPUE of YOY walleye was low when YOY yellow perch CPUE was less than 1526 fish/hectare. Surface temperature at each bottom trawl site exerted a fine-scale influence on YOY

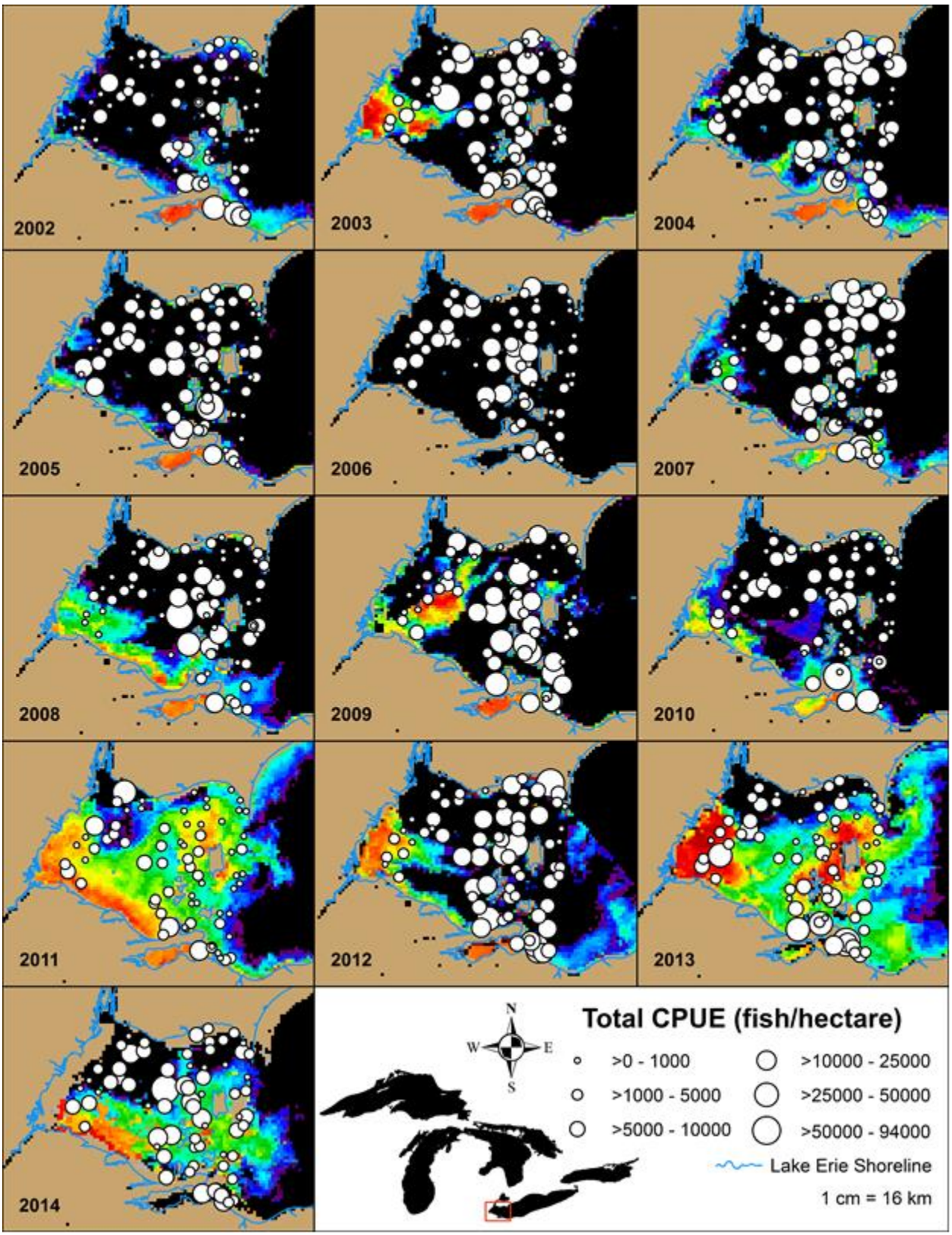

Figure 6: Estimated HAB density in western Lake Erie (Wynne & Stumpf 2015) and total CPUE of YOY fishes during the August bottom trawl survey 2002-2014 (LEC 2015). Warm colors represent high HAB cell density; black indicates HAB cell density below the detection threshold.

walleye CPUE; YOY walleye CPUE was highest when YOY yellow perch CPUE > 1526 fish/hectare and surface temperature > 25.2 ºC. When YOY yellow perch, freshwater drum, clupeid, *Notropis*, and *Morone* species were excluded from the regression tree, the model had difficulty converging. This suggests abiotic factors and HAB cell density alone are not good predictors of YOY walleye CPUE.

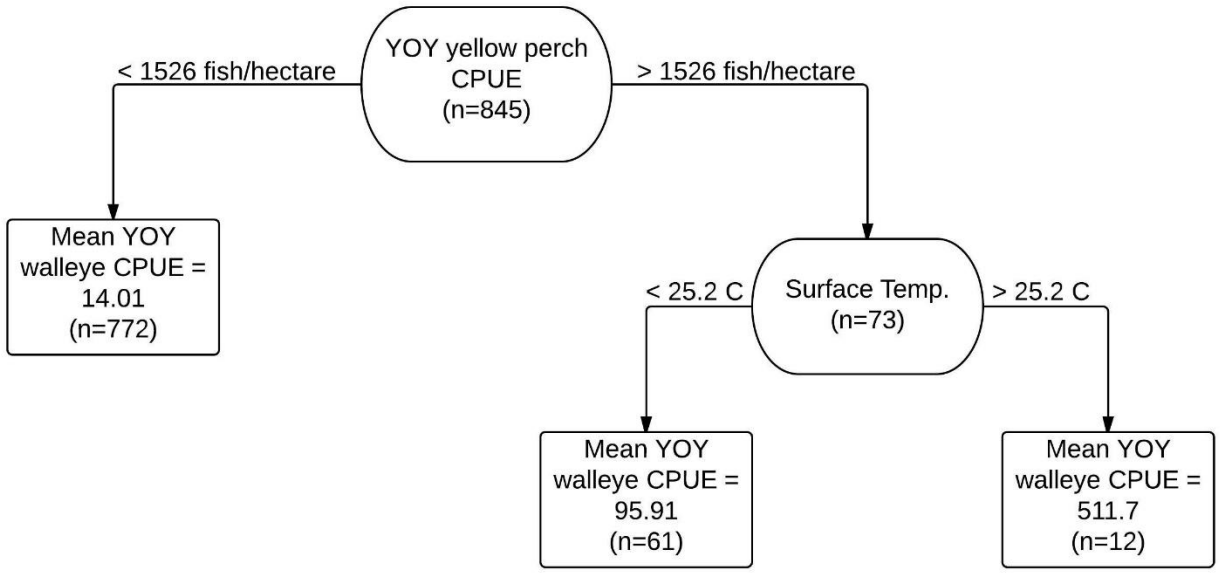

Figure 7: Pruned regression tree depicting factors that influence YOY walleye CPUE.

YOY Walleye CPUE Model

The probit selection equation (Equation 3) explained 5.5% of the variation in YOY walleye presence-absence ($p < 0.0001$, McFadden pseudo-$R^2 = 0.0547$.) The location of the trawl site, water temperature, site depth, and Secchi depth had a significant effect on the probability that YOY walleye CPUE $\neq 0$ (Table 1). The probability that YOY walleye CPUE $\neq 0$ decreased with increasing latitude (i.e. was lower at northern sites), longitude (i.e. was lower at eastern sites), Secchi depth (i.e. decreased as water clarity increased), and surface temperature, but increased with increasing depth and bottom temperature. DO and HAB cell density did not have a significant effect on the probability that YOY walleye CPUE $\neq 0$.

(3) $$P(CPUE \neq 0|x_k) = 12.07 - 1.65\ Latitude - 0.6803\ Longitude + 0.08247\ depth + 0.1948\ BTemp - 0.1838\ STemp - 0.2386\ Secchi - 0.01132\ DO + 2.908 \times 10^{-7} HAB\ density$$

When YOY walleye CPUE > 0, the linear outcome equation (Equation 4) explained 5% of the variation in ln-transformed walleye CPUE (p = 0.0006896, $R^2_{adj.}$ = 0.05028). Site latitude and bottom temperature were significant predictors of YOY walleye CPUE, while Secchi depth and DO were significant at α = 0.1 (Table 1). YOY walleye CPUE increased by 14% with each ºC increase in bottom temperature and by 99% with each 0.1º decrease in latitude.

(4) $$\ln(CPUE)|CPUE > 0, x_k = 42.17 - 2.296\ Latitude - 0.6263\ Longitude + 0.03871\ Depth + 0.1325\ BTemp + 0.2952\ Secchi - 0.0792\ DO - 1.024 \times 10^{-7} HAB\ density - 0.4285\ IMR$$

Table 1: YOY walleye Heckman selection model. *Denotes statistical significance at α = 0.1. **Denotes statistical significance at α = 0.05.

Variable	Probability CPUE ≠ 0			CPUE		
	Coefficient	SE	p-value	Coefficient	SE	p-value
Intercept	12.07	19.12	0.5279	42.17	28.93	0.1459
Latitude	-1.65	0.3404	1.26E-6**	-2.296	0.8721	0.00882**
Longitude	-0.6803	0.2475	0.005989**	-0.6263	0.4438	0.159
Depth	0.08247	0.0243	0.00069**	0.03871	0.0507	0.44572
Bottom Temp.	0.1948	0.05149	0.000154**	0.1325	0.05947	0.02653**
Surface Temp.	-0.1838	0.05694	0.001246**			
Secchi	-0.2386	0.07287	0.001059**	0.2952	0.1624	0.06998*
DO	-0.01132	0.0339	0.7384	0.0792	0.04702	0.09297*
HAB cell density	2.91E-07	2.82E-07	0.3026	1.02E-07	3.97E-07	0.7963
IMR				0.4285	0.7207	0.5525

YOY Forage Fish CPUE Model

The fitted probit selection equation (Equation 5) explained 10.8% of the variation in YOY forage fish (clupeid and *Notropis* species) presence-absence (p < 0.0001, McFadden pseudo-R^2 = 0.1083). The Secchi depth and HAB cell density at each trawl site had a significant effect on the probability that forage fish CPUE ≠ 0 (Table 2). The probability that forage fish

CPUE ≠ 0 decreased with increasing HAB cell density and Secchi depth (i.e. decreased with increasing water clarity). The location of the trawl site, site depth, water temperature, and DO did not have a significant effect on the probability that forage fish CPUE ≠ 0.

(5) $$P(CPUE \neq 0|x_k) = 0.4057\ Latitude - 0.2525\ Longitude - 0.04332\ Depth + 0.06325\ BTemp + 0.09686\ STemp - 0.4661\ Secchi + 0.04425\ DO - 9.433 \times 10^{-7} HAB\ cell\ density - 39.83$$

When YOY forage fish CPUE > 0, the linear outcome equation (Equation 6) explained 12.2% of the variation in ln-transformed forage fish CPUE ($p < 0.0001$, $R^2_{adj.} = 0.1218$). Site longitude, depth, bottom temperature, and DO were significant predictors of YOY forage fish CPUE (Table 2). YOY forage fish CPUE increased by 23.5% with each 0.1° increase in longitude (i.e. was higher at eastern sites) and by 36% with each °C increase in bottom temperature, but decreased by 17% with each meter increase in depth and by 19% with each 1 mg/L increase in DO. Latitude, surface temperature, Secchi depth, and HAB cell density did not have a significant impact on non-zero forage fish CPUE predictions at each trawl site.

(6) $$\ln(CPUE)|CPUE > 0, x_k = 53.14 + 0.5059\ Latitude + 0.8547 Longitude - 0.1559 Depth + 0.3074 BTemp - 0.08407\ STemp - 0.6451\ Secchi - 0.1765 DO - 1.129 \times 10^{6}\ HAB\ cell\ density + 0.07465\ IMR$$

Table 2: YOY forage fish Heckman selection model. *Denotes statistical significance at α = 0.1. **Denotes statistical significance at α = 0.05.

Variable	Probability CPUE > 0			CPUE		
	Coefficient	SE	p-value	Coefficient	SE	p-value
Intercept	-39.83	23.26	0.08682*	53.14	45.97	0.2481
Latitude	0.4057	0.3744	0.2786	0.5059	0.6629	0.4457
Longitude	-0.2525	0.2892	0.3827	0.8547	0.4309	0.04775**
Depth	-0.04332	0.02807	0.1228	-0.1559	0.05126	0.00245**
Bottom Temp.	-0.06325	-0.05036	0.2092	0.3074	0.1022	0.00273**
Surface Temp.	0.09686	-0.06146	0.1151	-0.08407	0.106	0.4279
Secchi	-0.4661	0.07836	2.71E-9**	-0.6451	0.4369	0.1403
DO	0.04425	0.03813	0.2458	-0.1765	0.06561	0.00731**
HAB cell density	-9.43E-07	3.10E-07	0.00235**	-1.13E-06	9.41E-07	0.2306
IMR				0.07465	2.076	0.9713

YOY Length-Frequency Trends

The median TL of YOY walleye captured during the August western basin interagency bottom trawl survey 2002-2015 was 131 mm. The length-frequency distribution (Figure A1) of YOY walleye in 2003 was significantly different from any year 2004-2015 ($p < 0.0001$). The median TL of YOY walleye was lower in 2003 than any year 2004-2015 (Figure 8A). The strongest year class of walleye observed during this study was produced in 2003, with an annual average CPUE of 249.6 ± 41.8 fish/hectare, and HABs were relatively mild, with a CI_{max} of 3.92. The median TL of YOY walleye was highest in 2012. The length-frequency distribution in 2012 differed significantly from every year 2003-2015 ($p < 0.0001$) except 2006, the year with the second-highest median TL. HABs were mild in 2006, with a CI_{max} value of 1.27, and walleye year class strength was very low with an annual average CPUE of 1.6 ± 0.7 fish/hectare. HABs were also mild in 2012, with a CI value of 1.96, the lowest recorded since 2007, and walleye year class strength was low, with an annual average CPUE of 6.8 ± 1.5 fish/hectare. Years with extreme HABs, 2011 and 2015, both had average median TL values compared to other years 2003-2014. The median TL of YOY walleye was slightly lower in 2015, when the second largest year class of walleye was produced (110.5 ± 19 fish/hectare), compared to 2011 when the average annual CPUE of YOY walleye was relatively low (6.7 ± 1.6 fish/hectare). The length-frequency distribution (Figure A2) of YOY walleye was significantly different among categories of HAB density estimated for each trawl site in 2002-2014 ($p < 0.018$). The median TL of YOY walleye captured at each trawl site increased with increasing HAB density (Figure 8B). The median TL was lowest when HAB density at the trawl site was negligible and highest when the density of HAB cells was high or very high.

The length-frequency distributions (Figure A3) of YOY yellow perch were

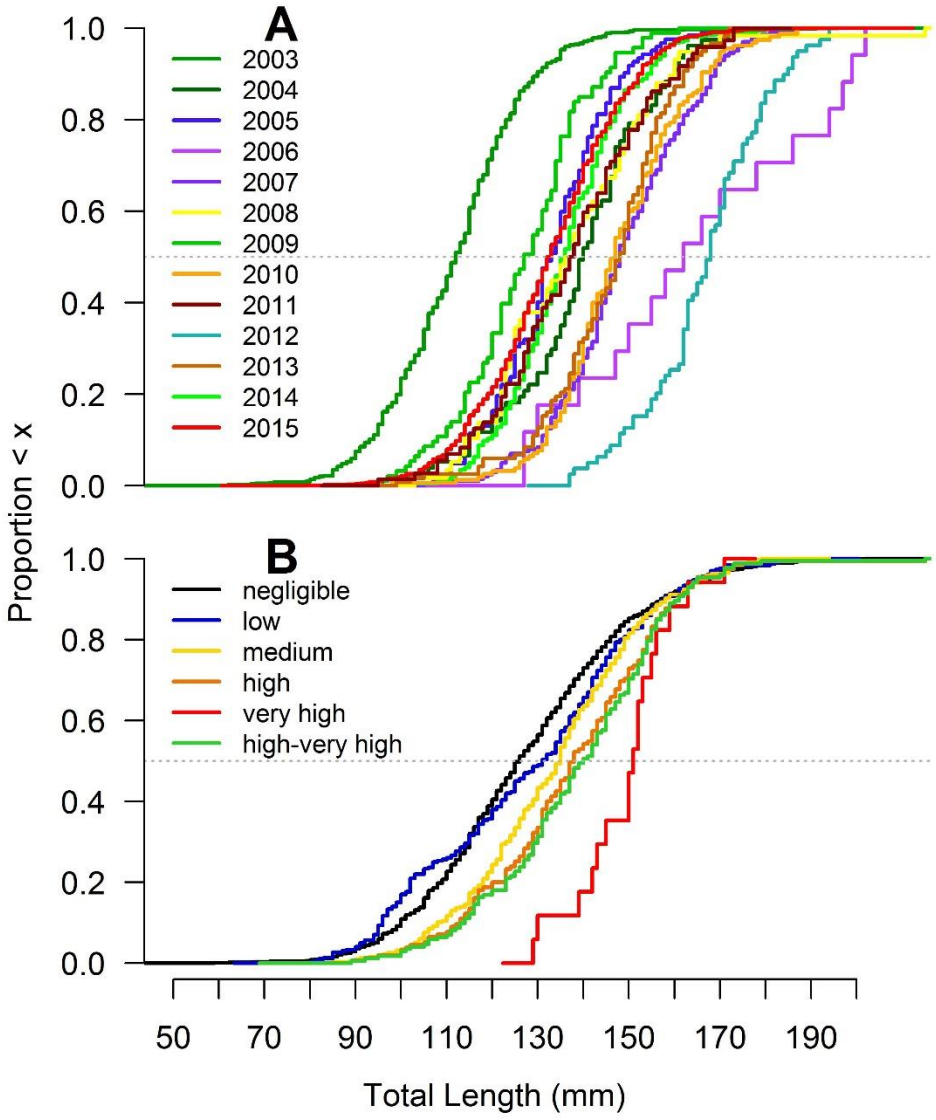

Figure 8: YOY walleye ECDF. The dotted gray line denotes the median TL. A: YOY walleye ECDF curves for each year 2003-2015. Cool colors represent years with low CI_{max}. B: YOY walleye ECDF curves for each HAB cell density category. High-very high categories were combined due to relatively low sample size in the very high category.

significantly different among all years 2002-2015 ($p \leq 0.0402$) with the exception of 2002 and 2007, which were not significantly different from each other ($p = 0.2368$). The median TL of YOY yellow perch captured during the August western basin interagency bottom trawl survey 2002-2015 was 66 mm. The median TL of YOY yellow perch was lowest in 2003 (Figure 9A), when HABs were mild and the strongest year class of yellow perch observed during this study

was produced (2739.4 ± 536.2 fish/hectare), similar to walleye. However, the second-lowest median TL occurred in 2015, a year of extreme HABs the third-highest yellow perch year class strength (1045.4 ± 208.1 fish/hectare). Also similar to walleye, 2006 had the second-highest median TL, although YOY yellow perch median TL was highest in 2010. In 2006 yellow perch year class strength and HAB severity were modest; in 2010 HABs were more severe but year class strength was low. The length-frequency distribution of YOY yellow perch captured at each trawl site in 2002-2014 was significantly different among the negligible, low, and medium HAB cell density categories ($p < 0.0014$) and among the negligible, low, high-very high cell density categories ($p < 0.0006$), but there was no significant difference in length-frequency distribution between the medium and high-very high cell density categories ($p = 0.6562$, Figure A4). Like walleye, the median TL of YOY yellow perch was lowest at trawl sites with negligible HAB density (Figure 9B). However, the median TL of YOY yellow perch captured at each trawl site did not monotonically increase with increasing HAB density; it was highest at sites with medium to high HAB density. Sites with very high density had an average median TL compared to other HAB density categories.

The length-frequency distributions of YOY clupeid species differed significantly among most years 2002-2015 ($p \leq 0.0036$), with the exception of 2003 and 2004 ($p = 0.4428$), 2008 and 2012 ($p = 0.0768$), 2008 and 2015 ($p = 0.108$), and 2009 and 2011 ($p = 0.499$), which were not significantly different from each other (Figure A5). The median TL of YOY clupeid species captured during the August western basin interagency bottom trawl survey 2002-2015 was 81 mm. The median TL of YOY clupeid species was lowest in 2006, a year with moderate clupeid year class strength (256 ± 145.5 fish/hectare) and a mild HAB with a $CI_{max} = 1.27$ (Figure 10A). The second-lowest median TL was observed in 2002, when the strongest clupeid

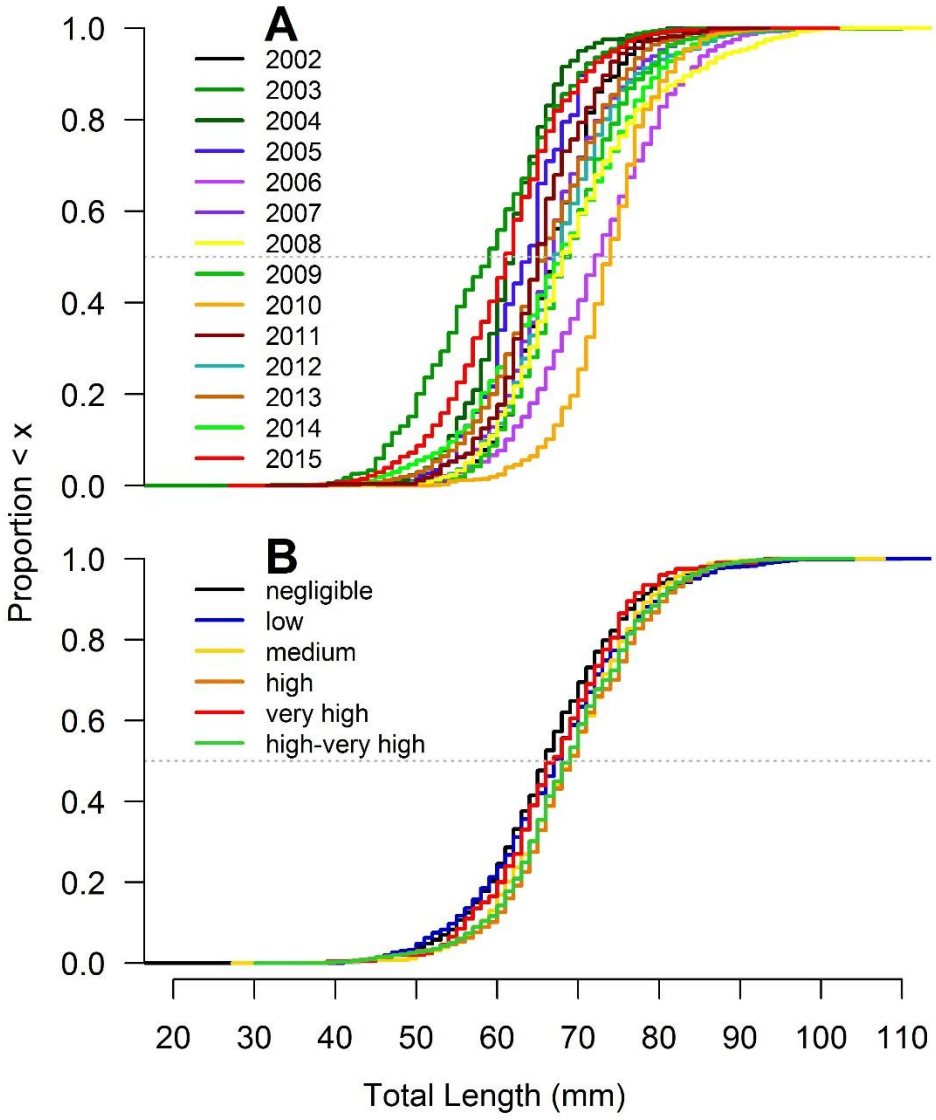

Figure 9: YOY yellow perch ECDF. The dotted gray line denotes the median TL. A: YOY yellow perch ECDF curves for each year 2002-2015. Cool colors represent years with low CI_{max}. B: YOY yellow perch ECDF curves for each HAB cell density category. High-very high categories were combined due to relatively low sample size in the very high category.

year class 2002-2015 was produced (1741.8 ± 657 fish/hectare) and HABs were mild (CI_{max} = 1.27). The median TL of YOY clupeid species was highest in 2010, a year with low clupeid year class strength (59.3 ± 22.9 fish/hectare) and a severe HAB, with a CI_{max} = 8.93. The second-highest median TL was observed in 2014, a year with moderate clupeid year class strength (252.3 ± 113.8 fish/hectare) and a relatively severe HAB (CI_{max} = 5.65). The length-frequency

distribution of YOY clupeid species were significantly different among categories of HAB density estimated for each trawl site in 2002-2014 ($p \leq 0.0232$, Figure A6). When the high and very high HAB cell density categories were combined due to relatively low sample size in the very high category, the median TL of YOY clupeids decreased with increasing HAB density, with the greatest difference between sites with negligible and low HAB density (Figure 10B).

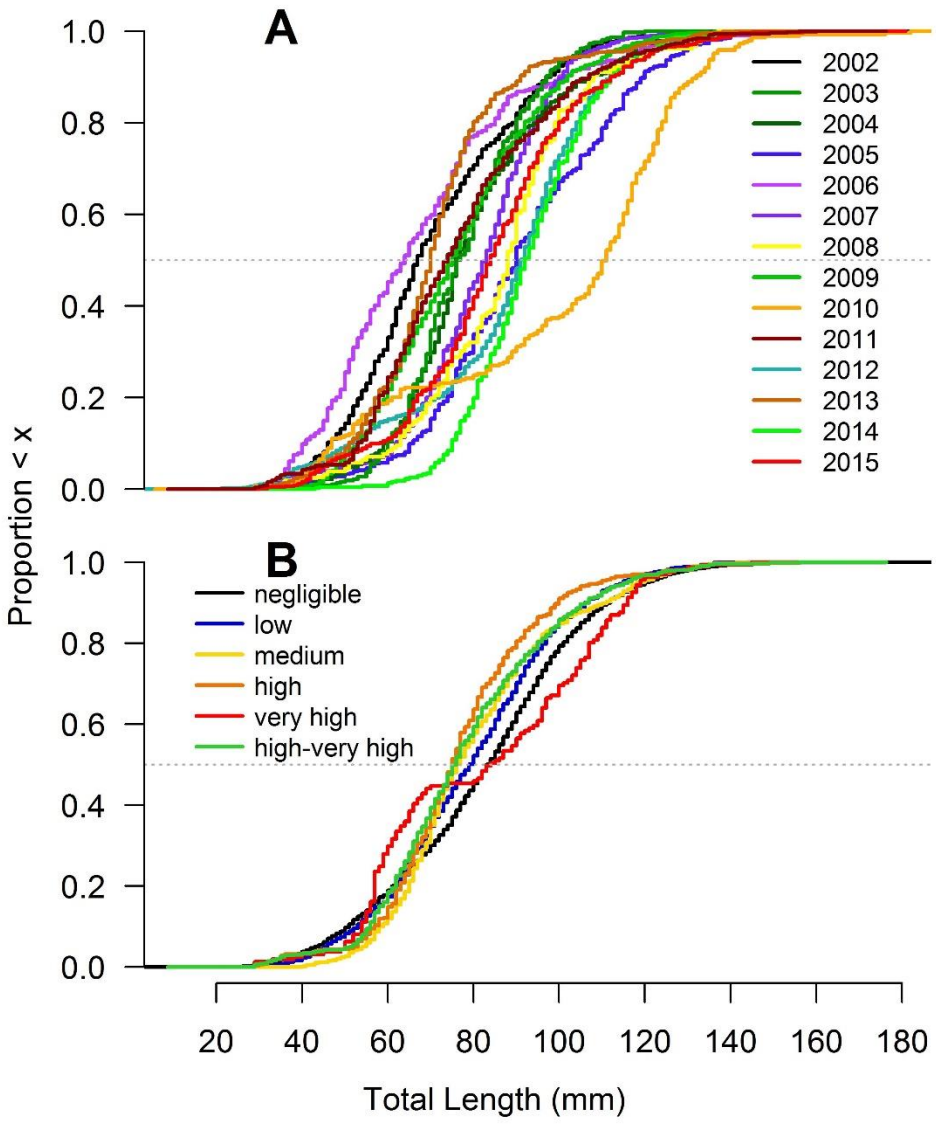

Figure 10: YOY clupeid ECDF. The dotted gray line denotes the median TL. A: YOY clupeid ECDF curves for each year 2002-2015. Cool colors represent years with low CI_{max}. B: YOY clupeid ECDF curves for each HAB cell density category. High-very high categories were combined due to relatively low sample size in the very high category.

The length-frequency distributions (Figure A7) of YOY *Notropis* species were significantly different among all years 2002-2015 ($p \leq 0.0048$). The median TL of YOY *Notropis* spp. captured during the August western basin interagency bottom trawl survey 2002-2015 was 47 mm. The median TL of YOY *Notropis* was lowest in 2003 (Figure 11A), when both *Notropis* year class strength and HAB severity were relatively low (63.2 ± 29 fish/hectare and CI_{max} = 3.92, respectively). The second-lowest median TL occurred in 2004, when HABs were mild (CI_{max} = 2.39) and a strong year class of *Notropis* was produced, with an average CPUE of 300 ± 101.6 fish/hectare captured during the August bottom trawl survey. YOY *Notropis* median TL was highest in 2010, when year class strength was moderate (132.1 ± 30.1 fish/hectare) and CI_{max} was 8.93. The second-highest median TL was observed in 2014, when the annual average *Notropis* CPUE was the lowest observed during this study (11.8 ± 3.9 fish/hectare) and a moderate HAB occurred (CI_{max} = 5.65). The length-frequency distribution of YOY *Notropis* species was significantly different among categories of HAB cell density estimated for each trawl site in 2002-2014 ($p \leq 0.0292$, Figure A8). YOY *Notropis* median TL was lowest at sites with very high or negligible HAB cell densities, and highest at sites with high HAB cell density (Figure 11B).

The length-frequency distributions of YOY *Morone* species (Figure A9) were significantly different among all years 2002-2015 ($p \leq 0.0012$). The median TL of YOY *Morone* spp. captured during the August western basin interagency bottom trawl survey 2002-2015 was 59 mm. The median TL of YOY *Morone* species was lowest in 2004, a year with high *Morone* year class strength and (6942.6 ± 1139.3 fish/hectare) and moderate HAB severity with CI_{max} = 2.39 (Figure 12A). The second-lowest TL was observed in 2007, a year with high *Morone* year

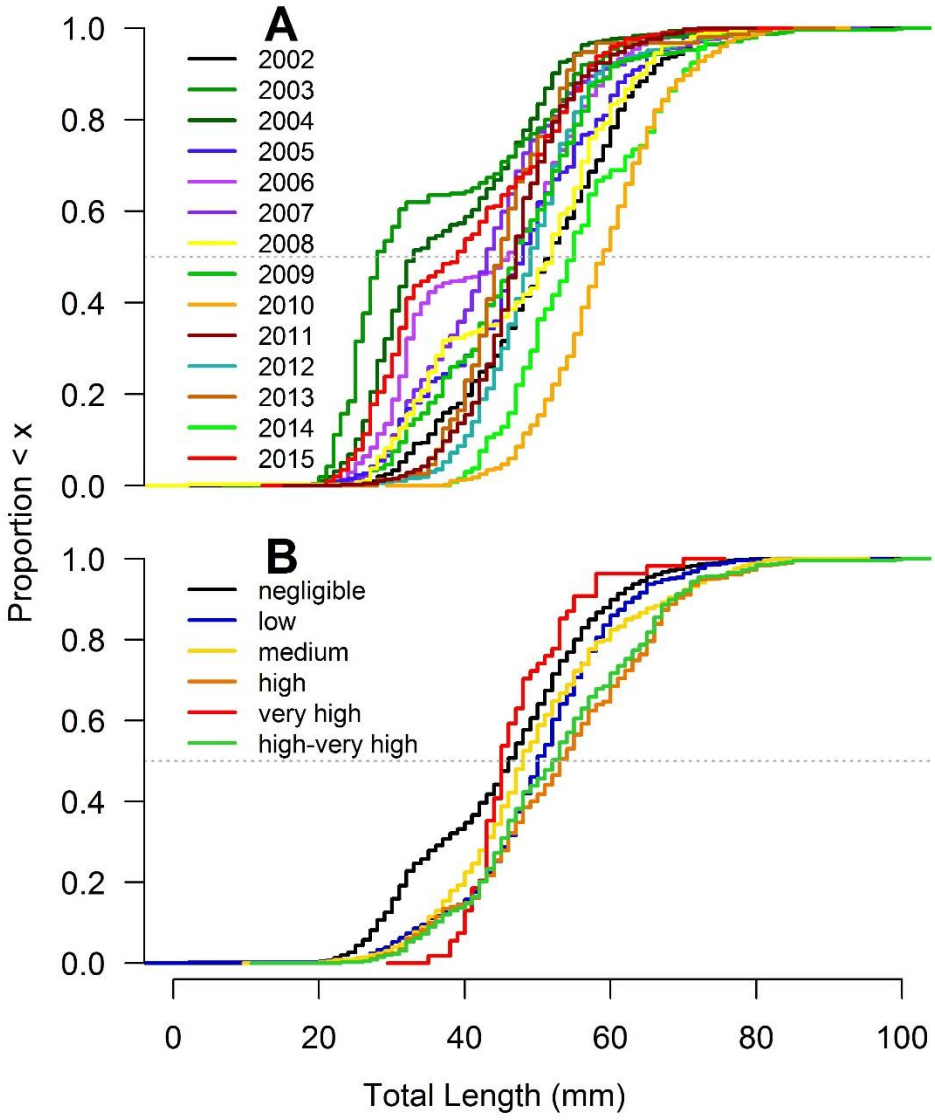

Figure 11: YOY *Notropis* ECDF. The dotted gray line denotes the median TL. A: YOY *Notropis* ECDF curves for each year 2002-2015. Cool colors represent years with low CI_{max}. B: YOY *Notropis* ECDF curves for each HAB cell density category. High-very high categories were combined due to relatively low sample size in the very high category.

class strength (6850.7 ± 1055.7 fish/hectare) and a mild HAB (CI_{max} = 1.39). The median TL of YOY *Morone* species was highest in 2010, a year with moderate year class strength (3749.7 ± 1220.2 fish/hectare) and a severe HAB with a CI_{max} = 8.93. The second-highest TL was observed in 2002, a year with low *Morone* year class strength (1273.9 ± 249 fish/hectare) and a mild HAB (CI_{max} = 1.27). The length-frequency distribution of YOY *Morone* species were

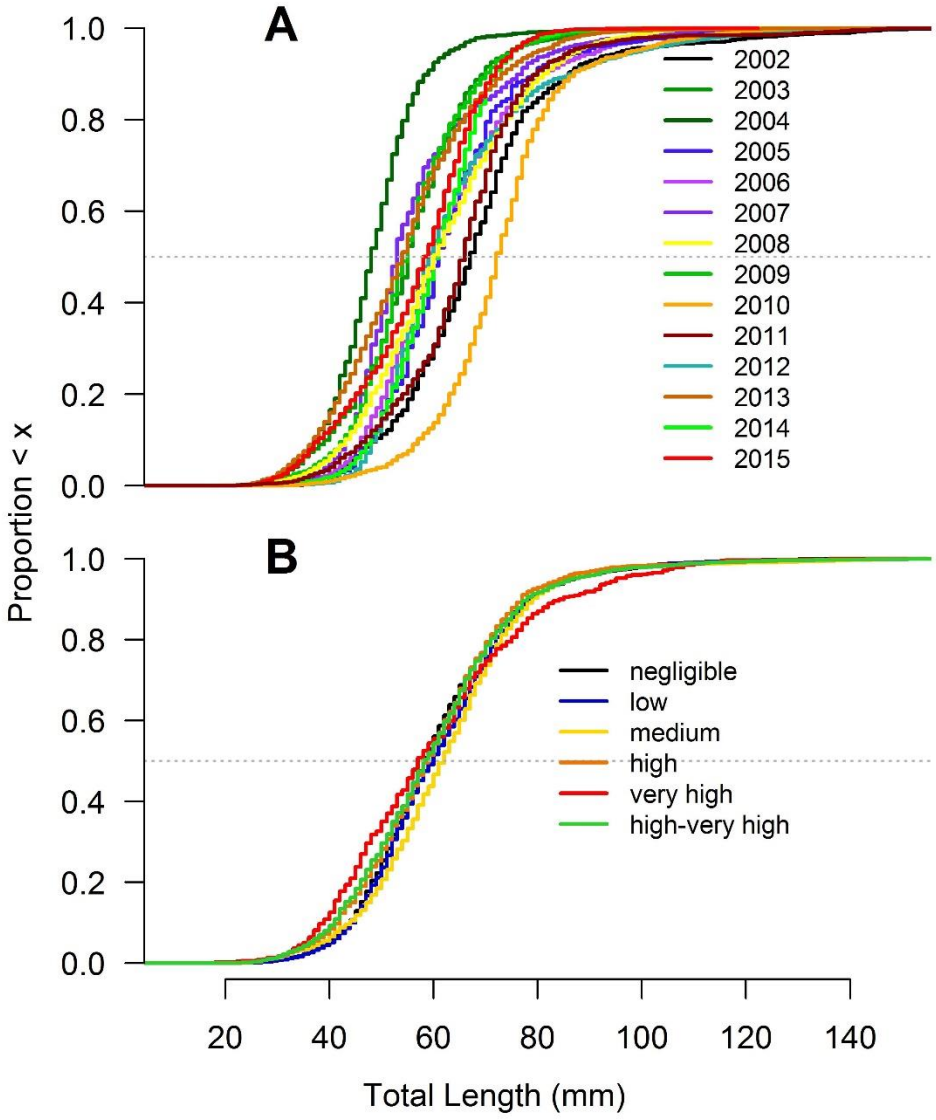

Figure 12: YOY *Morone* ECDF. The dotted gray line denotes the median TL. A: YOY *Morone* ECDF curves for each year 2002-2015. Cool colors represent years with low CI_{max}. B: YOY *Morone* ECDF curves for each HAB cell density category. High-very high categories were combined due to relatively low sample size in the very high category.

significantly different among categories of HAB density estimated for each trawl site in 2002-2014 ($p \leq 0.0038$, Figure A10), though the median TL of YOY *Morone* captured at bottom trawl sites was similar across HAB cell density categories (Figure 12B). The median TL was highest at sites with medium or low HAB cell density, and lowest at sites with high-very high or negligible HAB cell density.

The length-frequency distributions of YOY freshwater drum (Figure A11) differed significantly among most years 2002-2015 ($p \leq 0.0372$), with the exception of 2003 and 2015 ($p = 0.183$), 2007 and 2009 ($p = 0.2744$), 2007 and 2012 ($p = 0.062$), 2007 and 2013 ($p = 0.2572$), and 2009 and 2013 ($p = 0.1672$), which were not significantly different from each other.

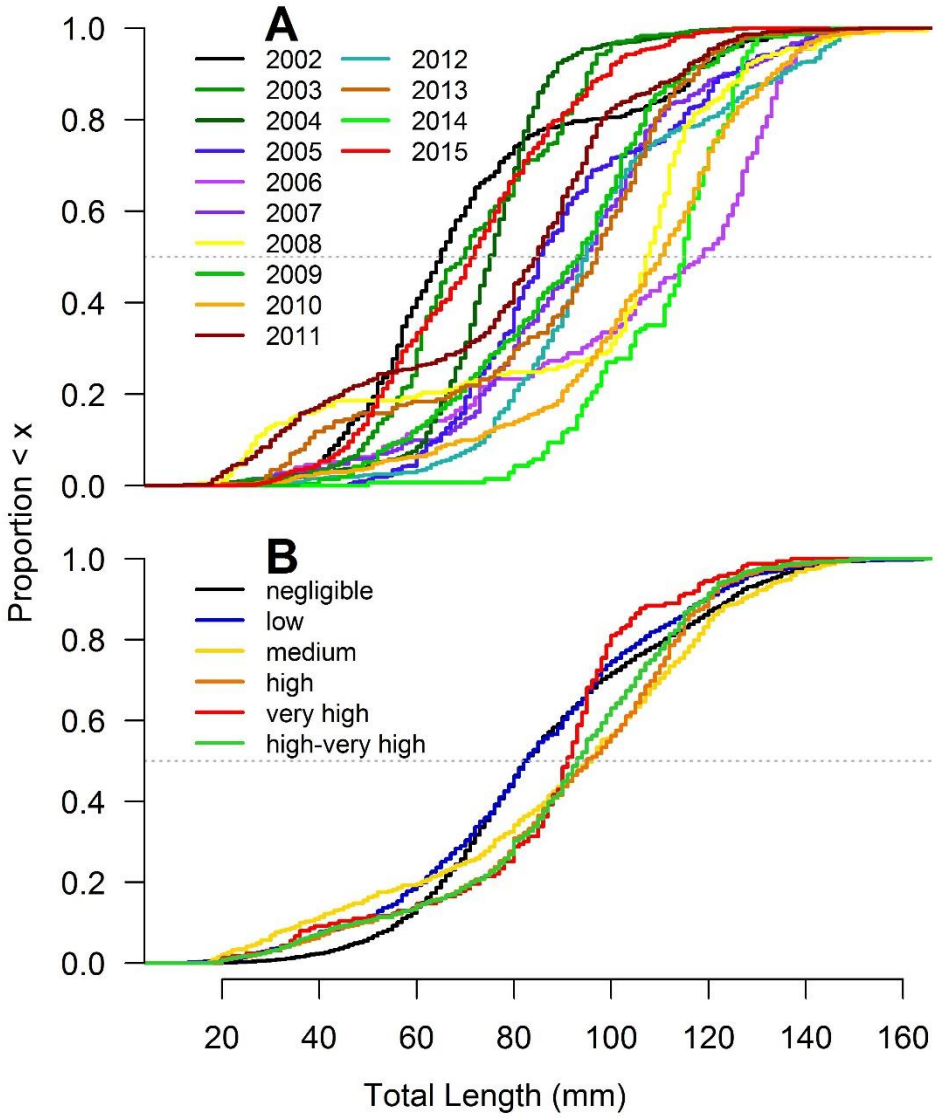

Figure 13: YOY freshwater drum ECDF. The dotted gray line denotes the median TL. A: YOY freshwater drum ECDF curves for each year 2002-2015. Cool colors represent years with low CI_{max}. B: YOY freshwater drum ECDF curves for each HAB cell density category. High-very high categories were combined due to relatively low sample size in the very high category.

The median TL of YOY freshwater drum captured during the August western basin interagency bottom trawl survey 2002-2015 was 84 mm. The median TL of YOY freshwater drum was lowest in 2002 and 2003 (Figure 13A), when the annual average CPUE of YOY freshwater drum was relatively high (114.3 ± 35.1 and 91 ± 38.4 fish/hectare, respectively) and HABs were mild (CI_{max} = 1.27 amd 3.92, respectively). The median TL was highest in 2006, when the annual average CPUE of YOY freshwater drum in the August bottom trawl survey was relatively low (34.6 ± 20.5 fish/hectare) and a mild HAB occurred (CI_{max} = 1.27). The second highest median TL was observed in 2014, when the annual average CPUE was the lowest observed 2002-2015 (16.4 ± 7.3 fish/hectare) and a moderately severe HAB occurred (CI_{max} = 5.65). The length-frequency distribution of YOY freshwater drum were significantly different among categories of HAB density estimated for each trawl site in 2002-2014 ($p \leq 0.0152$, Figure A12). The median TL of YOY freshwater drum was lowest at sites with negligible to low HAB density and highest at sites with medium to high HAB density (Figure 13B).

CONCLUSIONS

Overall, I found little evidence to support my hypothesis that HABs have a negative influence on walleye year class strength. Only two large year classes of walleye were produced during the time period considered by this study (2002-2015). Large walleye year classes were produced in 2003 and 2015, years characterized by mild and extremely severe HABs, respectively. These years were similar in terms of other potential predictors of year class strength considered in this study (i.e. site depth, Secchi depth, bottom DO, water temperature, spring storm events, and the abundance of other YOY fishes). Regression tree analysis demonstrated that the annual average CPUE of YOY yellow perch was the best indicator of walleye year class strength out of the variables I investigated; strong year classes of walleye were only produced

when yellow perch annual abundance was also high (Figure 5). Considering the similar life histories of these two percid species, I expect similar biological and physical factors would influence year class production. Though I was unable to identify reliable abiotic predictors of walleye year class strength, Madenjian et al. (1996) explained 92% of the variation in Lake Erie walleye recruitment using a Ricker stock recruitment model that included YOY gizzard shad abundance the previous fall, spawner abundance, and water warming rate in the spring. I conclude that Madenjian et al.'s (1996) walleye recruitment model is still valid under changing ecological conditions associated with increasingly frequent and severe HABs in western Lake Erie.

I found little evidence that HABs impacted the distribution and relative abundance of YOY walleye directly; however, the results of this study lend support to my hypothesis that HABs influence walleye indirectly by affecting the distribution and availability of their prey. The two-step Heckman YOY walleye CPUE model (Equation 3) did not explain much of the observed variance in YOY walleye CPUE and none of the independent variables included in the outcome equation (Equation 4) were significant predictors of YOY walleye relative abundance when CPUE > 0. Considering the YOY walleye CPUE regression tree (Figure 7), which identified YOY yellow perch CPUE as the most important variable influencing YOY walleye CPUE, these results suggest that HAB cell density and the environmental factors considered in this study are poor predictors of YOY walleye relative abundance. Rather, it seems on a coarse scale (i.e. the probability that CPUE $\neq 0$), YOY walleye are distributed according to characteristics of their life history. For example, non-zero catches were more likely at southern and western sites, near walleye-producing rivers and reefs, and in deeper and more turbid waters, which favor walleye feeding. It also seems that YOY walleye associate with other YOY fishes,

in particular yellow perch. Walleye are highly migratory and follow schools of prey fishes from the western basin to the central and eastern basins of Lake Erie (Reiger et al. 1969), so there should be a direct relationship between YOY walleye CPUE and the relative abundance of other YOY fishes. YOY walleye are also demersal, which further reduces their spatio-temporal overlap with HABs and their direct exposure microcystin.

Though the relative abundance and distribution of walleye in Lake Erie seems unrelated to the spatio-temporal extent of HABs and the other environmental variables I considered, I found evidence to support my hypothesis that HABs impact the availability of YOY forage fishes, with potential indirect effects on YOY walleye. The forage fish CPUE model shows that forage fishes (clupeid and *Notropis* species) avoid both areas affected by HABs and areas with low turbidity (Equation 5). YOY forage fishes may avoid areas severely affected by HABs to avoid toxicity associated with the ingestion of HAB cells and toxins and increase foraging efficiency (Engström-Öst et al. 2006), while inhabiting turbid areas may offer a refuge from predation (Engström-Öst et al. 2009, Reichert et al. 2010). Abiotic factors, such as depth, bottom temperature, and DO, have a fine-scale impact on the relative abundance of YOY forage fishes (Equation 6), compared to the impact HAB cell density and turbidity have on YOY forage fish presence-absence at bottom trawl sites in the western basin (Equation 5).

I found both HAB severity and the year class strength of YOY fishes influenced YOY length-frequency distributions. In contrast to my hypothesis, I found a clear inverse relationship between annual abundance estimates and annual median TL, but a direct relationship between HAB cell density and median TL at bottom trawl sites for most species. Therefore, I conclude on an annual scale, increased productivity associated with HABs (Larson et al. 2016) promotes the growth of YOY fishes, and competition associated with large year classes, rather than HABs,

limits growth by decreasing prey availability. I found an inverse relationship between the annual median TL of walleye and year class strength, perhaps due to competition for limited food resources (Knight & Vondracek 1993). There was no clear influence of yearly HAB severity on YOY walleye length-frequency distributions, though there was a direct relationship between the median TL of YOY walleye and HAB cell density at bottom trawl sites. At a yearly, basin-wide scale, YOY walleye growth is determined by year class strength and the subsequent severity of competition for food resources, as Knight et al. (1984) hypothesized. However, the distribution of these fishes in the western basin in bottom trawl survey is determined by both HAB density and the distribution of prey resources. Similar to walleye, I found an inverse relationship between yellow perch length and year class strength, but no clear influence of yearly HAB severity on length-frequency distribution at an annual scale. The median TL of yellow perch was highest at sites with moderate HAB densities. Considering yellow perch are omnivorous and inhabit shallow, open water (Scott & Crossman 1973), this suggests yellow perch are at greater risk of direct exposure to HABs and indirect exposure to algal toxins than demsersal, piscivorous walleye.

I found evidence of a direct relationship between yearly HAB severity and annual clupeid length-frequency distributions and an inverse relationship between annual abundance estimates and median TL. However, clupeid median TL decreased with increasing HAB cell density at bottom trawl sites. These results suggest clupeids, the preferred prey of walleye (Knight et al. 1984), are negatively impacted by exposure to HAB cells and toxins (Wiegand & Pflugmacher 2004), yet increased primary and secondary productivity associated with eutrophication and HABs benefits their growth. There is not a clear relationship between *Notropis* spp. annual length-frequency distributions and annual abundance indices or yearly HAB severity. In

addition, there is no clear trend between the median TL of *Notropis* spp. and HAB cell density at bottom trawl sites. The factors influencing the growth and length-frequency distribution of this important group of forage fishes warrants further investigation. I also found a clear inverse relationship between annual abundance and annual length-frequency distributions of two other ecologically important fishes, freshwater drum and *Morone* spp., though HAB severity had no clear influence. The results of the length-frequency analysis in this study suggest, for most YOY fishes considered, competition and prey availability are more important than HABs in determining length-frequency distributions at an annual scale, though HAB cell density has a size-specific influence on the distribution of YOY fishes throughout the western basin. The costs associated with HAB and algal toxin exposure are more severe for smaller fishes (Malbrouck & Kestemont 2005) yet YOY fishes may benefit from increased productivity associated with HABs.

Overall, HABs do not seem to impact YOY walleye year class strength, relative abundance, or distribution directly; rather, prey availability is an important factor driving year class strength, growth, and distribution of YOY walleye in western Lake Erie. However, HABs do have a direct impact on the distribution two important groups of YOY forage fishes, clupeid and *Notropis* species. If this spatial mismatch between YOY walleye and their preferred prey (due to their disparate responses to HABs) persists as HABs continue to increase in severity and spatio-temporal extent, I expect YOY walleye feeding, growth, and survival rates to decrease according to the match-mismatch hypothesis (Cushing 1990). It is essential to consider this impact of HABs on YOY forage fish distribution in interjuristictional walleye fishery management, as highly migratory walleye will follow schools of prey fish throughout Lake Erie. Though HAB severity had no impact on the relative abundance of YOY forage fishes, and may

contribute to increased growth rates by increasing primary and secondary productivity (Larson et al. 2016), it is also important to consider the direct effects of algal toxins on forage fish populations, as microcystin can bioaccumulate at higher trophic levels (Wituszynski 2014). Though preliminary studies show microcystin conentrations are below WHO guidelines in Lake Erie fish tissue (Ludsin et al. 2016), continued monitoring is needed to protect human health and identify emerging impacts on fish reproduction (e.g. Acuña et al. 2012) and stock-recruitment dynamics as the occurrence of severe HABs continues to increase. In the modern era of ecosystem-based management, it is important to consider the direct and indirect impacts HABs will have on fishery ecosystem productivity to assure sustainable harvest and the wellbeing of coastal communities under changing limnological conditions.

CHAPTER 2

INFLUENCE OF HABS IN WESTERN LAKE ERIE ON ZOOPLANKTON AND ICHTHYOPLANKTON PRODUCTION IN A TROPHIC CASCADE

INTRODUCTION

Harmful algal blooms (HABs), rapid accumulations of algal cells associated with socio-economic or ecological impairment, are increasing globally (Ho & Michalak 2015) due to anthropogenic nutrient loading (Michalak et al. 2013) and climate change (Paerl & Huisman 2008). In recent years, blooms of toxic cyanobacteria *Microcystis aeruginosa* (hereafter *Microcystis*) have been occurring with increasing frequency and severity in the western basin of Lake Erie (Obenour et al. 2014, Stumpf et al. 2012) due to re-eutrophication (Scavia et al. 2014). These HABs can produce microcystin, a hepatotoxin, and are associated with a number of ill effects on people and wildlife, prompting beach closures and inhibiting other recreational activities, decreasing property values (Baron et al. 2016), and impacting animal and human health by contaminating drinking water supplies (Backer et al. 2015). Some studies (Landsberg 2002) have demonstrated the negative effects of algal toxins on zooplankton (Wilson et al. 2006) and fish (Acuña et al. 2012) feeding, growth, and survival rates as well as the bioaccumulation of microcystin in their body tissues (Lehman et al. 2010, Wituszynski 2014). In marine environments, HABs have been associated with decreases in fish density and species richness (Gannon et al. 2009) and species-specific changes in recruitment (Warlen et al. 1998), though the mechanisms driving these trends remain unclear. A general lack of information on how HABs affect ecological communities remains a problem for aquatic and marine resource managers (Ramsdell et al. 2005).

This study addresses this research gap by investigating how spatio-temporal overlap with Lake Erie HABs influences larval and juvenile fishes during critical periods in their life history.

Hjort (1914) defined a critical period as an early life history stage which experiences high and variable rates of mortality. These fluctuations in larval mortality rates regulate recruitment (Houde 1997), contributing to inter-annual variability in year class strength. Mortality and sub-lethal effects of HABs are of particular concern during early life history stages, which are more sensitive to toxins due to their thin epithelial layer, large surface area to volume ratio, and high metabolic rate (Malbrouck & Kestemont 2005). In addition, larval fish have limited motility (Houde 1969), relying heavily on currents and other physical processes for transport (Mion et al. 1998); therefore, they are often restricted to nearshore nursery areas (Roseman et al. 2005) where cyanobacterial HABs are likely to form (Wynne & Stumpf 2015).

Feeding during the larval stage, and the onset of exogeneous feeding in particular, constitutes a critical period as defined by Hjort (1914). Larval feeding, growth, and survival rates, and ultimately recruitment (Miller et al. 1988), are driven by spatial and temporal overlap of larvae with patchily distributed habitat conditions, e.g. HABs and suitable concentrations and types of zooplankton prey (Cushing 1990). In Lake Erie, large-bodied cladocerans and copepods are the principle prey of larval fishes, including clupeid, *Notropis*, *Morone*, and percid species (Hartman et al. 1992, Scott & Crossman 1973). Roseman (2000) found larval walleye growth rates were limited when zooplankton prey concentrations were less than 20 zooplankton/L.

Lake Erie HABs have the potential to affect the availability of zooplankton prey for larval fishes. During a Lake Erie HAB, *Microcystis* affects phytoplankton community composition through allelopathic interactions, quickly becoming dominant (Legrand et al. 2003). Dissolved and ingested microcystin decrease the growth and survival rates of copepods, cladocerans, and rotifers (Wilson et al. 2006). In addition, *Microcystis* is a nutrient-poor food source for zooplankton, and colonies are difficult to ingest due to their large size, which inhibits

zooplankton grazing and growth during HABs (Ghadouani et al. 2004). Indiscrimiminat filter feeders such as cladocerans do not avoid ingesting toxic *Microcystis* cells (Fulton & Paerl 1987), exacerbating the impacts of microcystin on their growth and survival rates compared to selective, raptorial copepods (Ger et al. 2016, Landsberg 2002). Subsequent impacts of ingested toxins and poor nutritional quality may lead to altered community structure and reduced zooplankton densities in areas experiencing HABs, decreasing the zooplankton prey available to larval fishes.

I hypothesized Lake Erie HABs would affect aquatic biotic communities on multiple trophic levels, limiting the availability of zooplankton prey and thereby influencing larval fish production via a trophic cascade (Ware & Thomson 2005). Consistent with a trophic cascade framework, I predicted HABs would alter the algal community species and size composition, limiting suitable-sized food particles for zooplankton, which in turn would cause a decrease in zooplankton abundance and a shift in zooplankton community structure. This change in zooplankton prey availability would directly impact the growth and survival of larval fishes during their critical life stages, ultimately altering prey fish abundance and thus walleye fishery recruitment dynamics. My goal was to determine if Lake Erie HABs have a detrimental impact on the availability of suitable zooplankton prey and assess the implications for larval fish abundance and growth to inform fish recruitment models under changing limnological conditions. In this study I focused on three main objectives: 1) How does spatio-temporal variability in HAB severity influence the abundance and distribution of larval fishes in western Lake Erie? I hypothesized that larval fish abundance would decrease with increasing HAB cell density due to a decrease in feeding and survival rates associated with HABs. 2) How does spatio-temporal overlap with HABs in the epilimnion influence larval fish length-frequency distributions? I expected decreased feeding and growth rates would be indicated by a general

decrease in larval fish length where HABs persisted. 3) How does spatio-temporal variability in HAB severity influence zooplankton abundance, size distribution, and community composition? I hypothesized zooplankton abundance, particularly large-bodied cladocerans, would decrease with increasing HAB cell density.

METHODS

To characterize effects of HABs on larval fish production via a trophic cascade, I conducted weekly sampling at 14 sites located throughout the western basin of Lake Erie from June through August in 2015 and 2016, when larval fish and their zooplankton prey overlap with HABs (Figure 14). Physical factors that could influence larval fish growth, distribution, and relative abundance including water depth, Secchi depth, and water temperature within 1 m of the surface were also recorded at each sampling site. Samples were taken to estimate HAB density, zooplankton abundance, community composition, and length-frequency, and larval fish relative abundance and length-frequency as described below.

HAB and Zooplankton Sampling

I conducted duplicate vertical tows of a 0.5 m diameter, 112μm mesh zooplankton net at each site to estimate *Microcystis* bloom density (Bridgeman et al. 2013) and zooplankton relative abundance (Roseman et al. 2005). I attached a flow meter in the center of the net opening to estimate net efficiency and avoid biased samples due to clogging. I retrieved the zooplankton net at a rate < 1 ms^{-1} from 1 m above the lake bottom. I rinsed the outside of the net with lake water to concentrate each plankton sample to a volume of $\leq$ 150mL. I then preserved plankton samples in 350 mL collection bottles with an equal or greater volume of 10% sugar buffered formalin for transport to the laboratory (Haney & Hall 1973).

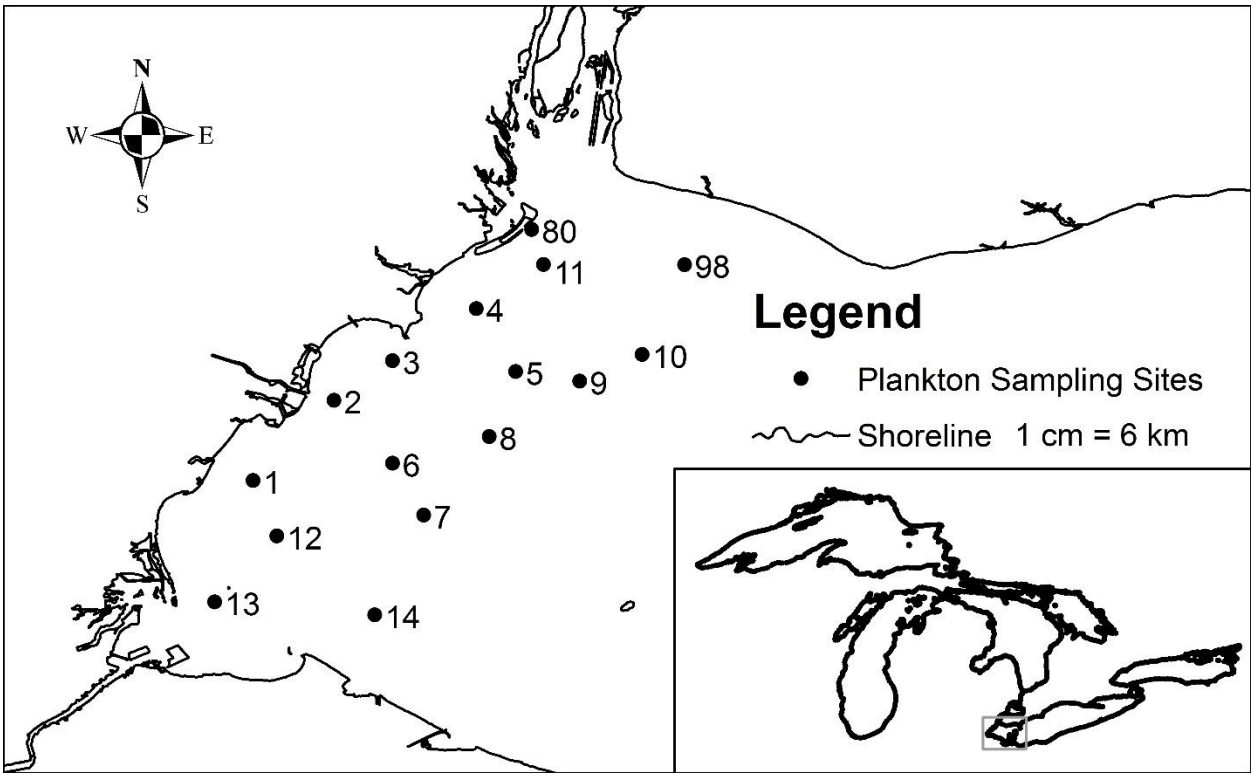

Figure 14: Map of *Microcystis*, zooplankton, and larval fish sampling sites in the western basin of Lake Erie. Sites 80 and 98 were sampled only in 2016, and larval fish were not sampled at these sites.

I estimated HAB density following Bridgeman et al. (2013). I diluted the entire plankton sample with tap water up to 1000 mL, depending on the amount of algae and debris in the sample, and allowed positively buoyant *Microcystis* colonies to separate from the remaining plankton in graduated 1 L Imhoff cones. I let the plankton samples settle for 24 hours, after which I removed settled zooplankton and non-buoyant phytoplankton from the bottom of the Imhoff cone. After a second 24-hour settling period, I recorded the biovolume of buoyant *Microcystis* to the nearest 1 mL. For ease of comparison with other studies, I converted non-zero *Microcystis* biovolume measurements to estimates HAB cell density using Equation 6 (Bridgeman et al. 2013), where *biovolume* is the volume of buoyant *Microcystis* in the settled

(6) $$\frac{cells}{m^3} = 252{,}469{,}314\ biovolume - 73{,}589{,}175$$

sample in mL. I converted this estimate of HAB cell density to cells/mL for ease of comparison with other studies.

To estimate the relative abundance of zooplankton at each site, I withdrew 1 mL subsamples of zooplankton from a known volume of settled plankton sample using a Hensen-Stemple pipette. I identified zooplankton to the order, or the family level when possible, in 1 mL subsamples following Balcer et al. (1984) until at least 150 individual zooplankters were counted. Using a digital micrometer, I measured up to 20 individual zooplankters from each taxa along their longest body axis. I estimated the relative abundance of zooplankton at each site using Equation 7, where

$$\frac{zooplankton}{L} = \frac{zooplankton_{subsample} \times \left(\frac{sample\ volume}{subsample\ volume}\right)}{volume\ sampled \times 1000} \quad (7)$$

$zooplankton_{subsample}$ is the number of zooplankton counted in the subsample(s), the *sample volume* is the total volume of the settled sample in mL, the *subsample volume* is the number of 1-mL subsamples counted, and the *volume sampled* is the total volume of water sampled during the trawl, in m^3. The volume of water sampled was calculated using the flowmeter readings as described in Equation 8, where *flow start* and *flow end* are the flowmeter readings at the start and end of the trawl, respectively, and the net radius is given in m.

$$volume\ sampled = (flow\ end - flow\ start) \times 0.00759816 \times \pi \times net\ radius^2 \quad (8)$$

Larval Fish Sampling

To evaluate the growth, distribution, and relative abundance of larval fishes in relation to HAB and zooplankton densities, I concurrently sampled pelagic ichthyoplankton at each site by towing a pair of 0.6 m diameter, 500µm mesh bongo nets in the upper 1 m of the water column at approximately 1 ms^{-1} for 5 minutes or less (Pritt et al. 2014). I attached a flow meter at the center of each net opening to estimate the volume of water sampled with each tow and avoid biased

samples due to net clogging. Following the procedure outlined in the IACUC Animal Use Form (Application #07/15-113-00), I euthanized and preserved larval fishes in 95% ethanol (Roseman et al. 2011).

I identified larval fishes to the lowest taxonomic level possible under a dissection microscope following Auer (1982). Using an optical or digital micrometer, I measured the total length of up to 20 individuals of each taxon to assess length-frequency distributions. I calculated catch per unit effort (CPUE), a measure of relative abundance, of larval fishes using Equation 9, where *catch* is the number of larval fishes captured in each bongo net and the *volume sampled* is the total volume of water sampled during the trawl, derived from Equation 8.

(9) $$\frac{larvae}{m^3} = \frac{catch}{volume\ sampled}$$

Modeling Larval Fish Relative Abundance

To determine how spatio-temporal variation in biological, i.e. HAB density, and physical habitat conditions, i.e. water temperature, Secchi depth, site depth and water clarity, influence the distribution and relative abundance of larval fishes in western Lake Erie, I fit a Heckman selection model (Wooldridge 2012) to predict larval fish CPUE using data from 2015 and 2016 using R (R Core Team 2014). Heckman's selection model is widely used in economics and sociology to address selection biases that occur when modeling two-stage processes, including farmers' perception of and adaptation to climate change (Tilahun & Bedemo 2014), the probability and scale of corporate acquisitions in the stock market (Peng et al. 2013), and the elderly's utilization and cost of health care (Lim et al. 2011). This approach thus accounts for selection biases, since the outcome equation which models the second stage (e.g. adaptation to climate change) is conditional on the selection equation which models the first stage (e.g. perception of climate change). In natural resources, Heckman's selection model has similarly

been applied to datasets in which selection bias occurs because observations of $y = 0$, i.e. corner solutions, are prevalent (Wooldridge 2012). Though using the Poisson distribution can address selection bias when *y* is a discrete count variable, Heckman's selection model has been used to model continuous independent variables including participation in and value of sportfishing (Bockstael et al. 1990) and non-consumptive wildlife recreation (Rockel & Kealy 1991). Here, I applied Heckman's selection model to larval fish CPUE, a continuous variable which exhibits a corner solution response (CPUE = 0 at 17.6% of trawl sites). Using all 754 observations, I fit a probit model as the selection equation to model the probability that larval fish CPUE $\neq 0$. I then calculated the inverse Mills ratio (IMR) and included it as a sample selection correction factor in the outcome equation, which models non-zero CPUE. I fit the outcome equation as a linear regression with ln-transformed dependent variable, including only observations where CPUE > 0 ($n = 621$). The global probit selection equation included site latitude, longitude, and depth, the Secchi depth, water temperature, and HAB cell density at each sampling site, and the week the sample was collected. In addition, the global linear outcome equation included the inverse Mills ratio to account for selection bias (i.e. using only non-zero CPUE observations to build the model).

Larval Fish Length-frequency Analysis

To infer how HABs impact the growth rates of larval fishes, I investigated yearly trends in larval fish length-frequency distributions by constructing length-frequency histograms for larval percids, clupeids, *Notropis* spp., and *Morone* spp. captured in 2015 and 2016 using 2 mm length intervals. I fit an empirical cumulative distribution function (ECDF), which shows the proportion of fishes shorter than each observed length (Neumann & Allen 2007), to each length-frequency distribution. To determine the impact of annual HAB severity on larval fish length-

frequency distributions, I compared the two ECDFs for each taxon between years using a bootstrapped Kolomogorov-Smirnoff test, which is insensitive to ties associated with non-continuous or binned data (Sekhon 2011, R Core Team 2014). I also fit an ECDF to larval percid, clupeids, *Notropis* spp., and *Morone* spp. length-frequency distributions for each week June through August to determine how these species' length-frequency distributions changed as HABs developed over the course of the sampling season. To investigate how larval length-frequency distributions changed across latitudinal and longitudinal gradients and gradients of HAB severity in 2015 and 2016, I binned larval fishes by site of capture and fit an ECDF to each length-frequency distribution for larval percids, clupeids, *Notropis* spp., and *Morone* spp. In this case, I combined length-frequency data from 2015 and 2016 for each species to increase sample size. I compared the ECDFs among sampling sites using pairwise bootstrapped Kolomogorov-Smirnoff tests, and adjusted the resulting p-values for multiple comparisons (R Core Team).

Modeling Zooplankton Relative Abundance

To investigate the impact of spatio-temporal variability in HAB cell density, water temperature, depth, and turbidity on the distribution and relative abundance of zooplankton in western Lake Erie, I fit a general linear model with a ln-transformed dependent variable using data from 2015 and 2016 (n = 787) (R Core Team 2014). The global model included site latitude, longitude, and depth, the Secchi depth, water temperature, and HAB cell density at each sampling site, and the week the sample was collected as independent variables. I used an exhaustive search procedure for variable selection (Lumley & Miller 2009, R Core Team 2014).

Zooplankton Community Composition

I examined the zooplankton community composition in 2015 and 2016 to investigate the influence of spatio-temporal variation in HAB density, water temperature, Secchi depth, and site

depth on specific zooplankton taxa, especially cladocerans and copepods, which are important prey items for many fish species (Balcer et al. 1984, Scott & Crossman 1973). To examine temporal trends, I combined data from all sites and calculated the proportion of major zooplankton taxa captured in each week of the sampling season at each site and over time. To examine spatial trends, I calculated the proportion of major zooplankton taxa captured at each sampling sites, combining data from all weeks sampled.

Zooplankton Length-frequency Analysis

To investigate yearly trends in zooplankton length-frequency distributions, I constructed length-frequency histograms for bosminids, Daphnidae, calanoid copepods, and cyclopoid copepods sampled in 2015 and 2016 using 0.1 mm length intervals. I fit an ECDF to the length-frequency distribution for each taxon in each year, and compared length-frequency distributions between years using a boostrapped Kolomogorov-Smirnoff test (Seckhon 2011, R Core Team 2014) to determine the impact of annual HAB severity on zooplankton length-frequency distributions. To investigate the impacts of spatio-temporal variation in HAB cell density on zooplankton length-frequency distributions, and subsequently the size distribution of prey available to larval fishes, I compared the length-frequency distributions of bosminids, Daphnidae, calanoid copepods, and cyclopoid copepods among sites and among sampling weeks using pairwise bootstrapped Kolomogorov-Smirnoff tests. I adjusted the resulting p-values for multiple comparisons (R Core Team 2014).

RESULTS

A total of 59,937 larval fishes were captured during 754 paired bongo trawls conducted in the western basin of Lake Erie in 2015 and 2016, representing 18 taxa (Table B1). Larval fishes were significantly more abundant in 2015 than in 2016 (Figure 15A, Figure 15B), when

the mean CPUE was 7.23 ± 2.63 fish/m^3 and 2.26 ± 0.56 larvae/m^3, respectively ($p < 0.0001$, $t = 4.334$). The relative abundance of larval fish generally decreased over the course of the sampling season in both years.

The total abundance of zooplankton was similar in both years (Figure 15C, Figure 15D), though the mean relative abundance was significantly higher in 2015 than in 2016 ($p = 0.001998$, $t = 3.103$), when the mean relative abundance was 226.9 ± 32.57 and 171.9 ± 22.21, respectively. In both years, the relative abundance of zooplankton peaked in late August. Zooplankton densities were rarely below the 20 zooplankton/L required for larval fish survival (Roseman 2000); this occurred only at sites near the mouth of the Detroit River, wherein zooplankton densities are much lower than in the western basin (Mion et al. 1998).

HAB cell density was higher in 2015 than in 2016 (Figure 15E, Figure 15F). In both years, I began collecting detectable amounts of HAB cells near 1 July. HAB density increased throughout July in both years, reaching a maximum near 1 August with substantial densities of HAB cells persisting through the end of August. There was a strong north-south gradient in HAB cell density; HAB cells were rarely if ever detected at sites near the mouth of the Detroit River (Figure 16). Along with the trends in zooplankton density, this trend in HAB cell density demonstrates a clear north-south gradient in primary production in western Lake Erie.

The water temperature, recorded within 1 m of the surface at each site, ranged from 14.7–27.9 ^{o}C. The weekly mean water temperature (Figure 15G) was similar in both years, and generally increased at similar rates throughout each sampling season. Site depth ranged from 3.1–10.5 m, with an overall mean of 6.9 m. The Secchi depth measured at each site ranged from 0.25–5.5 m, with an overall mean of 1.86 m. Both mean site depth and mean Secchi depth were similar across years (Figure 15H).

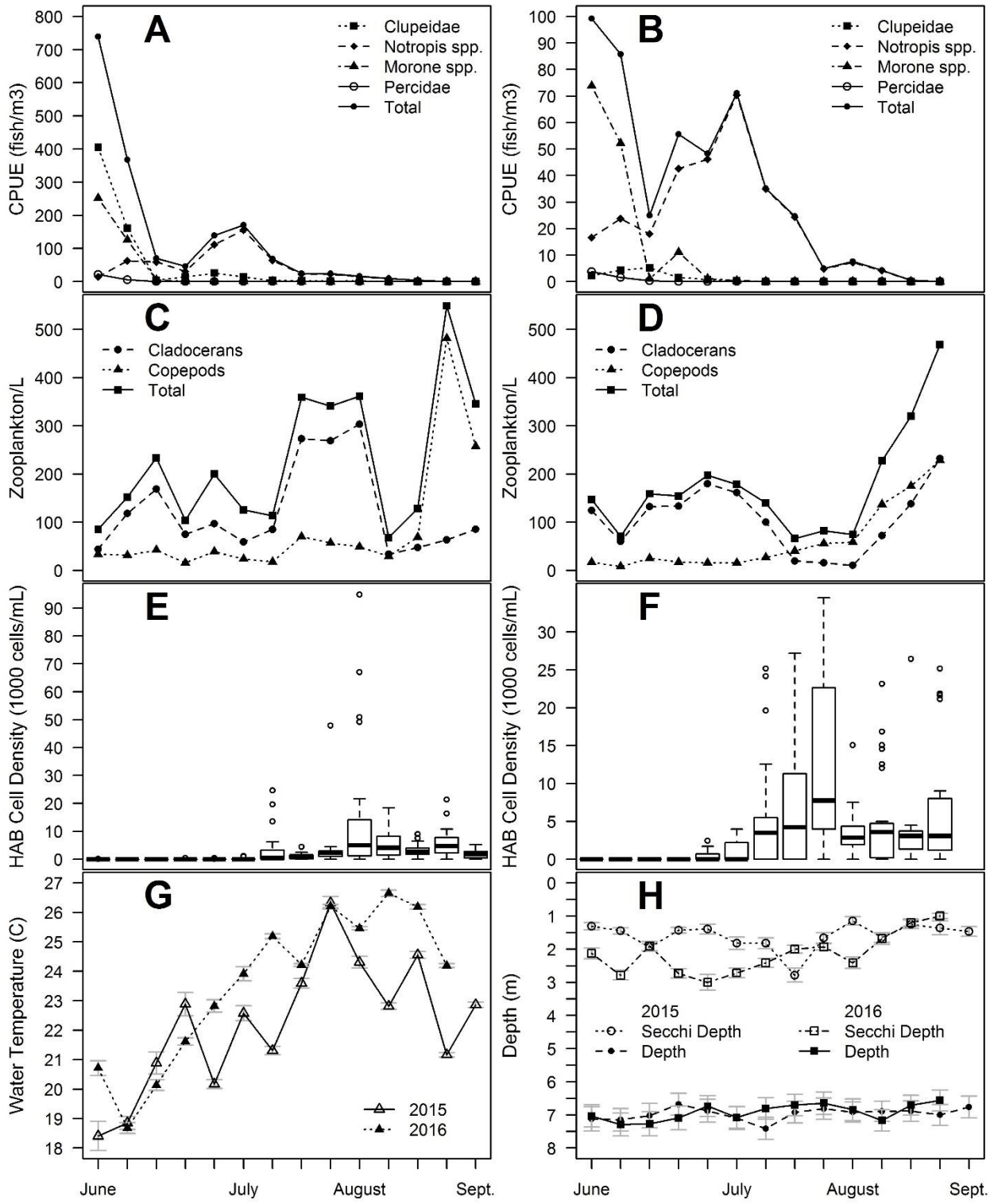

Figure 15: Weekly plankton sampling trends in 2015 and 2016. Gray bars indicate 1 SE. A: Weekly mean CPUE of larval fishes in 2015. B: Weekly mean CPUE of larval fishes in 2016. C: Weekly zooplankton density in 2015. D: Weekly mean zooplankton density in 2016. E: Weekly mean HAB cell density in 2015. F: Weekly mean HAB cell density in 2016. G: Weekly mean water temperature 2015-2016. H: Weekly mean site depth and Secchi depth 2015-2016.

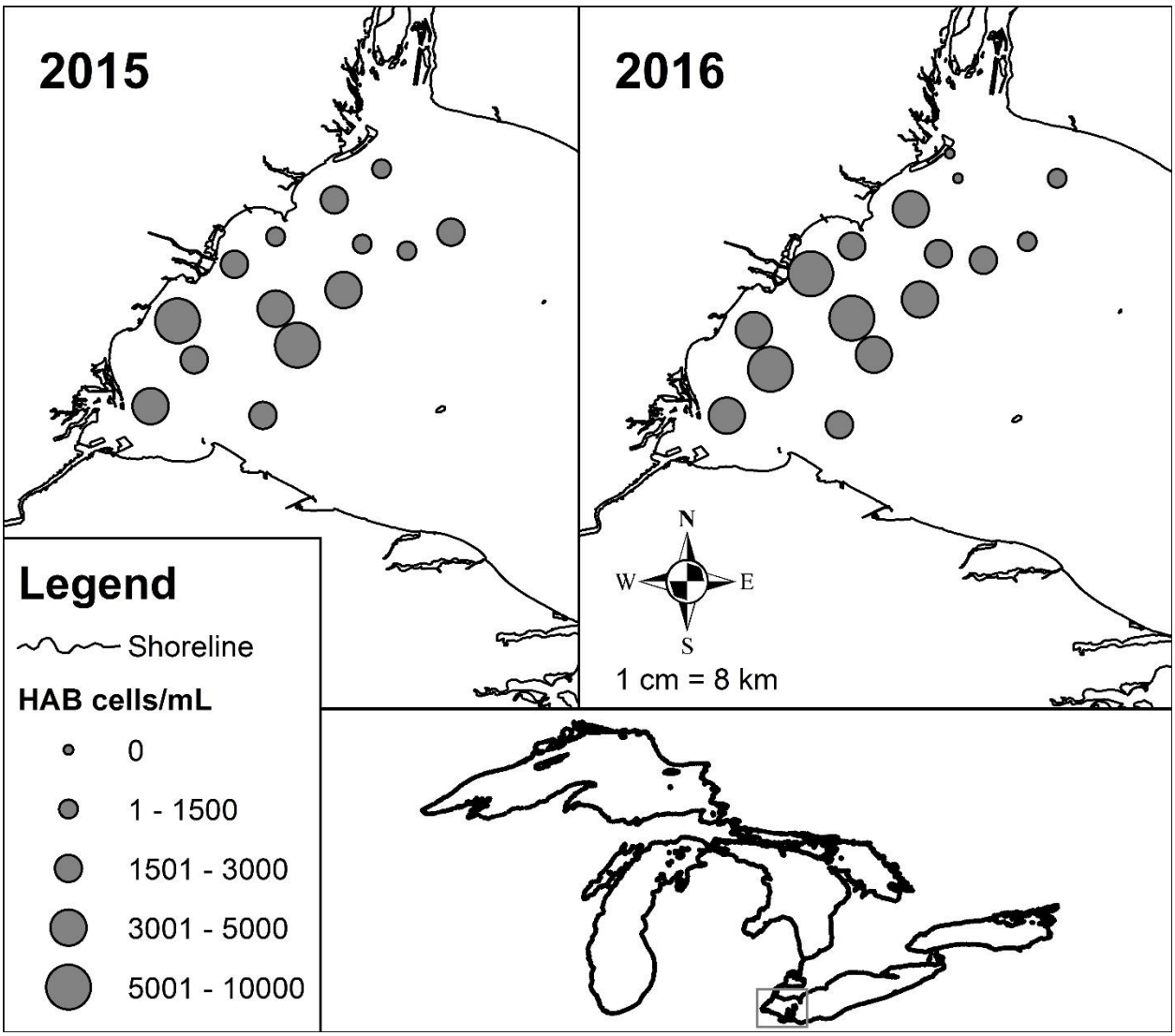

Figure 16: Mean HAB cell density at western basin plankton sampling sites in 2015 and 2016.

Larval Fish Relative Abundance Model

The probit selection equation (Equation 10), used to model the probability that larval fish CPUE ≠ 0, explained 48.1% of the variation in larval fish presence-absence ($p < 0.0001$, McFadden pseudo-$R^2 = 0.4812$). The week the sample was taken and HAB cell density at the sampling site had a significant effect on the probability that larval fish CPUE ≠ 0, while water depth was significant at $\alpha = 0.1$ (Table 3). The probability that larval CPUE ≠ 0 decreased with increasing HAB cell density and as weeks passed (i.e. was highest early in the sampling season).

Site location, Secchi depth, and water temperature did not have a significant effect on the probability that larval CPUE ≠ 0.

$$(10) \quad P(CPUE \neq 0|x_k) = 47.89 - 0.4627\,Week + 1.391\,Latiutude + 1.212\,Longitude - 0.1182\,Secchi - 0.02\,Temp + 0.14\,Depth - 1.722 \times 10^5\,HAB\ density$$

The linear outcome equation with a ln-transformed dependent variable (Equation 11) explained 40.9% of the variation in larval fish relative abundance ($p < 0.0001$, $R^2_{adj} = 0.4086$) when larval

Table 3: Larval fish Heckman selection model. *Denotes statistical significance at α = 0.1. **Denotes statistical significance at α = 0.05.

Variable	Probability CPUE > 0			CPUE		
	Coefficient	SE	p-value	Coefficient	SE	p-value
Intercept	47.89	21.7	0.8253	-28.12	14.92	0.05999*
Week	-0.4627	0.04749	< 2E-16**	-0.06263	-0.03785	0.09851*
Latitude	1.391	1.568	0.3748	-0.5657	1.143	0.6209
Longitude	1.212	2.068	0.5578	-3.703	1.361	0.00669**
Secchi	-0.1182	0.1217	0.3312	-0.2135	0.06111	0.00051**
Water Temp.	-0.02	0.04524	0.6584	-0.1072	0.03462	0.00204**
Depth	0.14	0.07932	0.0776*	0.08786	0.05119	0.08663*
HAB cell density	-1.72E-05	8.09E-06	0.0332**	-1.55E-05	9.68E-06	0.1111
IMR				-2.338	0.3458	3.22E-11**

fish CPUE > 0. Site longitude, the Secchi depth and water temperature measured at each site were significant predictors of non-zero larval fish CPUE, while the week samples were collected

$$(11) \quad \ln(CPUE)|CPUE > 0, x_k = 0.08786\,Depth - 0.06263\,Week - 0.5657\,Latitude - 3.703\,Longitude - 0.2135\,Secchi - 0.1072\,Temp - 1.54 \times 10^5\,HAB\ density - 2.338\,IMR - 281.2$$

and site depth were significant at α = 0.1 (Table 3). Larval fish CPUE decreased by 406% fish/m^3 with each 0.1° increase in longitude (i.e. CPUE was lower at eastern sites), by 24% with each meter increase in Secchi depth (i.e. CPUE was lower in clear water), and by 11% with each °C increase in water temperature. Site latitude and HAB cell density were not significant predictors of larval fish CPUE.

Larval Fish Length-frequency Analysis

The length-frequency distributions of clupeid species were significantly different in 2015 and 2016 ($p = 0.008984$), though the sample size was much smaller in 2016. Though the median TL of larval clupeids was similar in both years (approximately 7.9 mm), larval clupeids were generally longer in 2016 compared to 2015 (Figure 17A). Both the mean CPUE of larval clupeids and mean HAB cell density were lower in 2016 than 2015, suggesting a negative relationship between clupeid growth rates and both HAB cell density and clupeid abundance.

The length-frequency distributions of *Notropis* spp. were not significantly different between 2015 and 2016, with an overall median TL of approximately 7.6 mm (Figure 17B). Though the mean CPUE of larval *Notropis* spp. and mean HAB cell density were higher in 2015, these factors did not have a negative impact on *Notropis* spp. growth as I hypothesized. Zooplankton prey was more abundant in 2015 than 2016; adequate amounts of zooplankton prey in both years likely increased *Notropis* spp. growth rates.

The length-frequency distributions of *Morone* spp. were significantly different in 2015 and 2016 ($p < 0.0001$); the median TL of *Morone* spp. in 2015 was longer than in 2016 (8.2 mm and 7.2 mm, respectively) (Figure 17C). Both the mean CPUE of larval *Morone* spp. and mean HAB cell density were higher in 2015 than in 2016; however, the relative abundance of prey (zooplankton and larval clupeid spp.) was higher in 2015 than 2016. *Morone* spp. growth rates seemed to increase from abundant zooplankton prey and increased primary productivity associated with HABs in 2015.

There was no significant difference in the length-frequency distribution of percid species (walleye, yellow perch, and log perch) in total ($p = 0.0692$), but larval yellow perch, the vast majority of percid catch, were, in general, longer in 2015 than 2016 ($p = 0.0022$, Figure 17D).

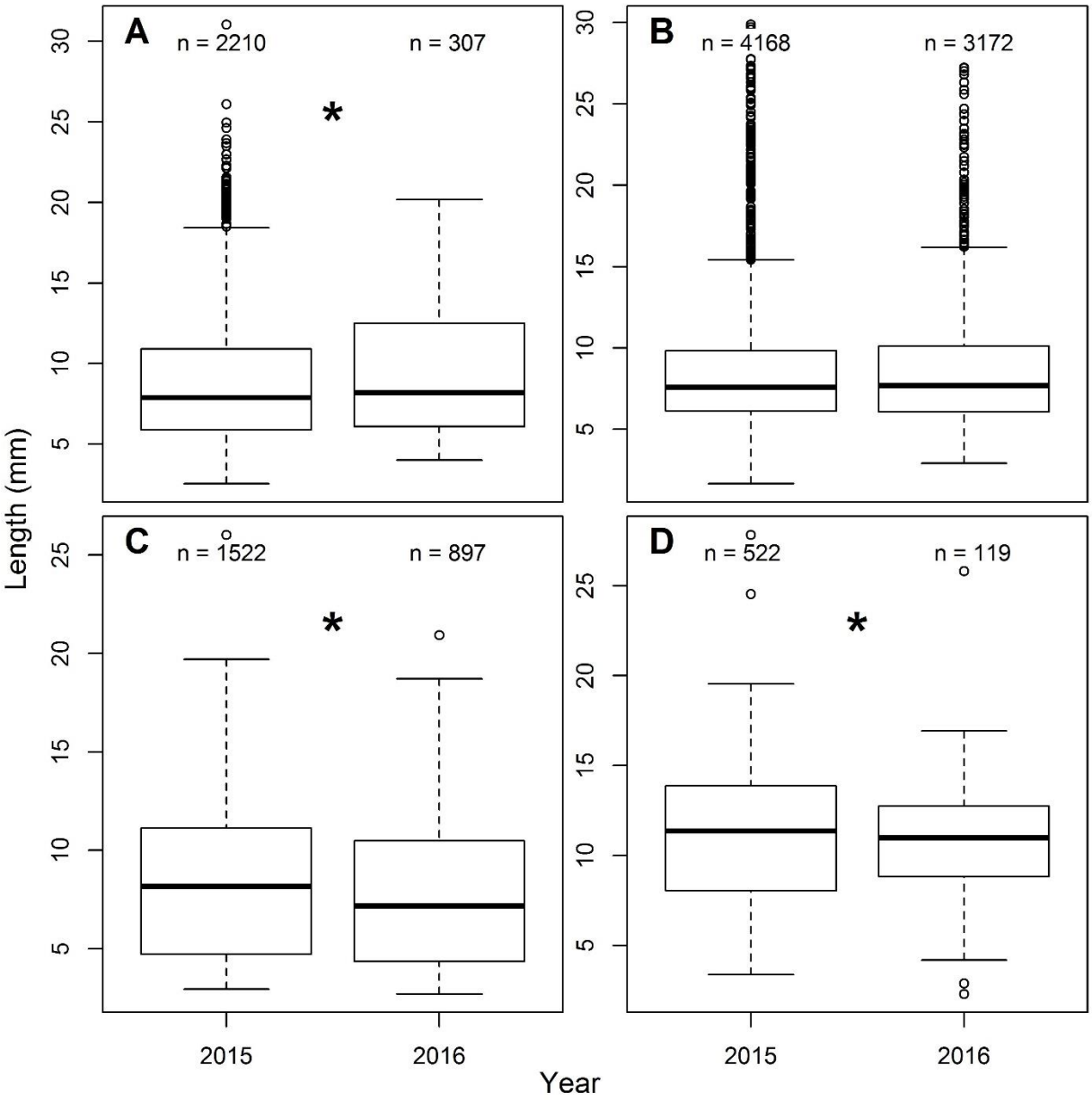

Figure 17: Comparison of larval length-frequency distributions in 2015 and 2016. *Denotes significance at α = 0.05. A: Larval clupeid spp. B: Larval *Notropis* spp. C: Larval *Morone* spp. D: Larval yellow perch.

Considering these results and the potential bias introduced when aggregating multiple species, I decided to only evaluate yellow perch, rather than a combination of percid species, in further length-frequency analyses. The median TL of larval yellow perch was 11.4 mm in 2015 and 11 mm in 2016. Like *Morone* spp., yellow perch were more abundant in 2015 than 2016, but

increased productivity and abundant zooplankton and ichthyoplankton prey in 2015 created favorable conditions for growth despite a severe HAB.

The abundance of larval clupeids, *Notropis* spp., *Morone* spp., and yellow perch generally decreased in successive weeks of sampling, while the median TL and overall length-frequency distribution of these species increased (Figure 18). Due to decreasing sample size in successive weeks, and the obvious nature of the length-frequency trends over time, I did not formally test these ECDFs with bootstrapped pairwise Kolomogorov-Smirnof tests.

There were strong spatial gradients in the length-frequency distributions of larval clupeids, *Notropis* spp., *Morone* spp., and yellow perch in 2015 and 2016. Generally, length decreased with increasing latitude and with increasing distance from shore. This trend is consistent with trends in zooplankton abundance, which decreased with increasing latitude and longitude (i.e. was highest at southern and nearshore sites), and trends in HAB cell density, which was highest at southern sites near the Maumee River mouth (Figure 16). There were strong spatial gradients in length-frequency distributions of larval prey fishes, with significantly longer larval clupeids captured at southern sites compared to northern sites ($p \leq 0.0464$) and at nearshore sites compared to offshore sites ($p \leq 0.0186$, Figure 19A, Figure 19B). There were similar trends in *Notropis* spp. length-frequency distributions; *Notropis* spp. were longest at southern nearshore sites and shortest at northern offshore sites (Figure 19C, Figure 19D). There was a strong nearshore-offshore gradient in *Morone* spp. length-frequency distributions, with the shortest *Morone* spp. captured at offshore sites (Figure 19E, Figure 19F). There was a weaker north-south gradient in *Morone* length-frequency distributions, with the longest *Morone* spp. captured at southern nearshore sites. There was also a strong north-south gradient in yellow perch length-frequency distributions, with the shortest yellow perch captured at the northernmost

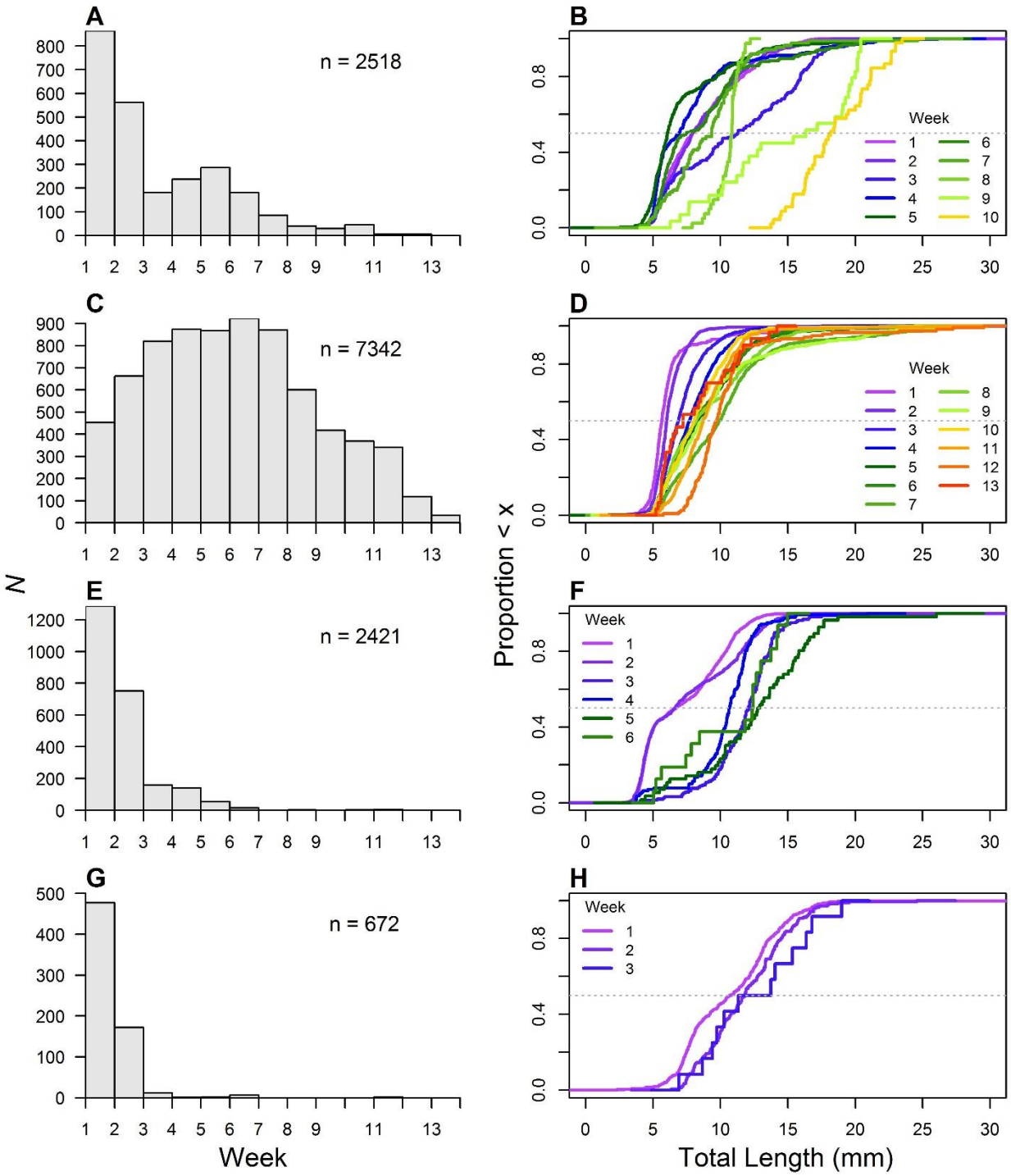

Figure 18: Larval fish length-frequency distributions over the course of the sampling season in 2015 and 2016. A: Number of clupeids collected and measured. B: Larval clupeid ECDF. C: Number of *Notropis* spp. collected and measured. D: Larval *Notropis* spp. ECDF. E: Number of *Morone* spp. collected and measured. F: Larval *Morone* spp. ECDF. G: Number of yellow perch collected and measured. H: Larval yellow perch ECDF.

sites (Figure 19G, Figure 19H). There was a weaker nearshore-offshore gradient in yellow perch length-frequency distributions; the longest yellow perch were captured at southern nearshore sites. In general, these differences in larval fish length-frequency distribution between sites were significant ($p < 0.05$); however, occasionally there was no significant difference in length-frequency distribution between adjacent sites, particularly those near the mouth of the Detroit River. These trends i.e. shorter larval fishes at northern, offshore sites mirrors the north-south gradient in primary i.e. HABs and secondary productivity i.e. zooplankton that I observed in the western basin. This suggests that larval fish growth rates are positively correlated to zooplankton prey availability and warm, nutrient-rich conditions that promote HAB formation.

Zooplankton Relative Abundance Model

The linear model with ln-transformed dependent variable (Equation 12) explained 56.6% of the variation in zooplankton relative abundance ($p < 0.0001$, $R^2_{adj} = 0.5657$). Site location, the Secchi depth, water temperature, and depth at each site, and the week samples were collected were all significant predictors of zooplankton relative abundance (Table 4), while HAB cell density at each site was significant at $\alpha = 0.1$. Holding all other variables constant, zooplankton

$$\ln(zoops\ L^{-1})\,|x_k = 0.02661\ Week - 3.737\ Latitude - 10.43\ Longitude - 0.2235\ Secchi + 0.07087\ Temp + 0.2478\ Depth + 9.177 \times 10^{-6}\ HAB\ density - 0.07106 \quad (12)$$

relative abundance increased by 7% with each ^{o}C increase in water temperature, by 28% with each meter increase in depth, and by 3% with each passing week, but decreased by 25% with each meter increase in Secchi depth (i.e. zooplankton abundance was lower in clearer water), by 420% with each 0.1^{o} increase in latitude (i.e. zooplankton were less abundant at northern sites), and by 3,386% with each 0.001^{o} increase in longitude (i.e. zooplankton were less abundant at eastern offshore sites).

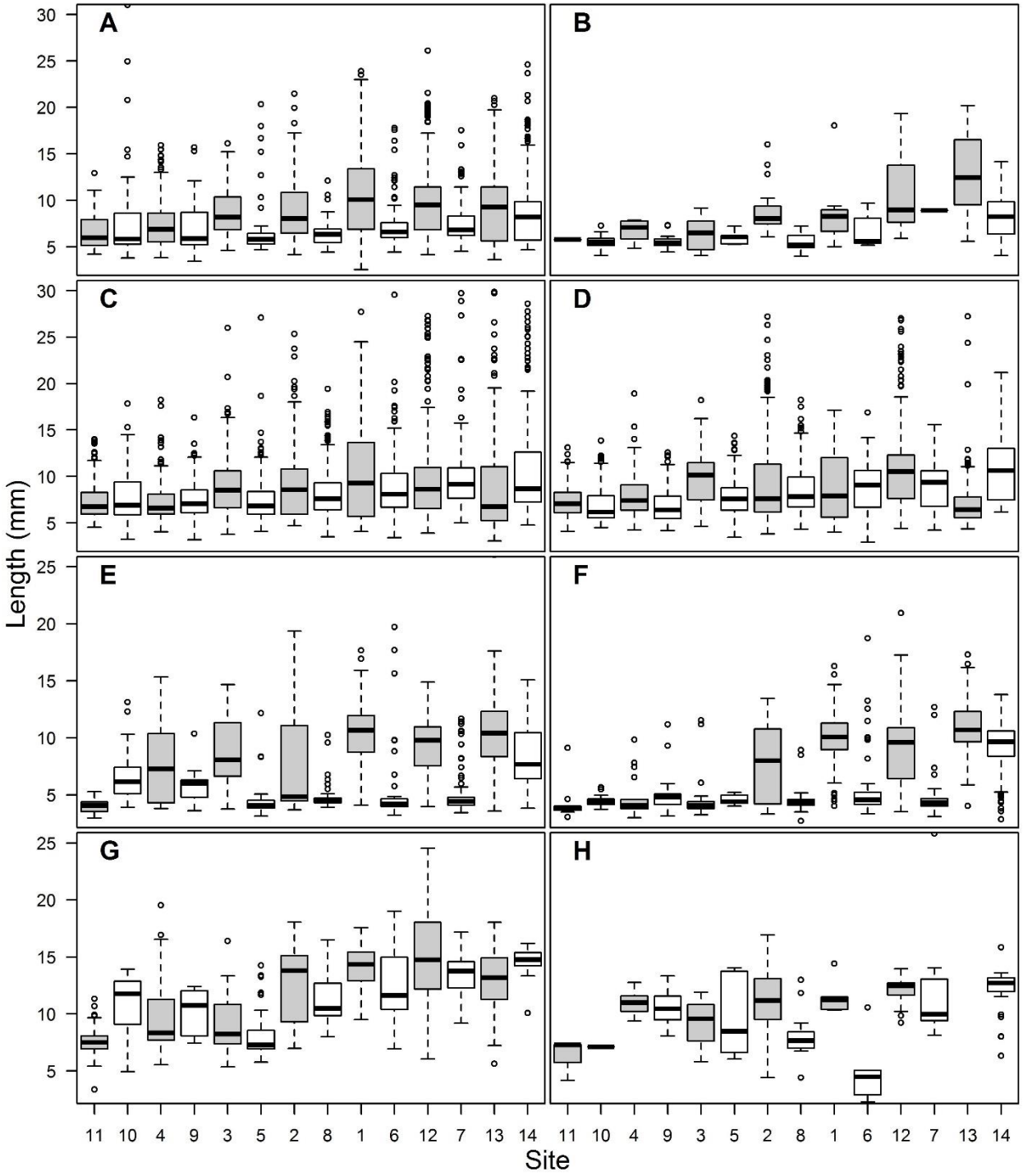

Figure 19: Spatial trends in larval fish length-frequency distributions. Sites on the x-axis are arranged from north to south. Gray boxes indicate nearshore sites; white boxes indicate offshore sites. A: Spatial trends in larval clupeid spp. length in 2015. B: Spatial trends in larval clupeid spp. length in 2016. C: Spatial trends in larval *Notropis* spp. length in 2015. D: Spatial trends in larval *Notropis* spp. length in 2016. E: Spatial trends in larval *Morone* spp. length in 2015. F: Spatial trends in larval *Morone* length in 2016. G: Spatial trends in yellow perch length in 2015. H: Spatial trends in larval yellow perch length in 2016.

Table 4: Zooplankton relative abundance GLM. *Denotes statistical significance at $\alpha = 0.1$. **Denotes statistical significance at $\alpha = 0.05$.

Variable	Coefficient	SE	p-value
Intercept	-71.06	96.66	4.97E-13**
Week	0.02661	0.01309	0.04244**
Latitude	-3.737	0.7456	6.68E-7**
Longitude	-10.43	0.8661	< 2E-16**
Secchi	-0.2235	0.04241	1.76E-7**
Water Temp.	0.07087	0.01976	0.000356**
Depth	0.2478	0.03369	4.85E-13**
HAB cell density	9.18E-06	5.47E-06	0.094163*

Zooplankton Community Composition

Zooplankton community composition was similar in 2015 and 2016. In June and July, the majority of zooplankton were cladocerans, primarily bosminids and Daphnidae, with calanoid and cyclopoid copepods accounting for ≤ 10% of the total zooplankton (Figure 20). Copepods and their nauplii larvae became the predominant members of the zooplankton community in late July (in 2016) to August (in 2015). In general, Daphnidae comprised a larger proportion of the cladocerans than bosminids, although bosminids increased in early July (in 2016) and late July (in 2015), as Daphnidae decreased and copepods became the most abundant group of zooplankton. The zooplankton community did not vary widely between sites (Figure 21). In general, 50% of zooplankton at each site were cladocerans, 40% were copepods and nauplii, and 10% were other taxa. Daphnidae typically outnumbered bosminids, accounting for 30% and 20% of the total zooplankton, respectively. Site 11, nearest the mouth of the Detroit River, was the exception; almost all cladocerans collected at this site were bosminids. Despite these spatial and temporal changes, the zooplankton community composition matched larval fish prey preferences for large-bodied cladocerans and copepods.

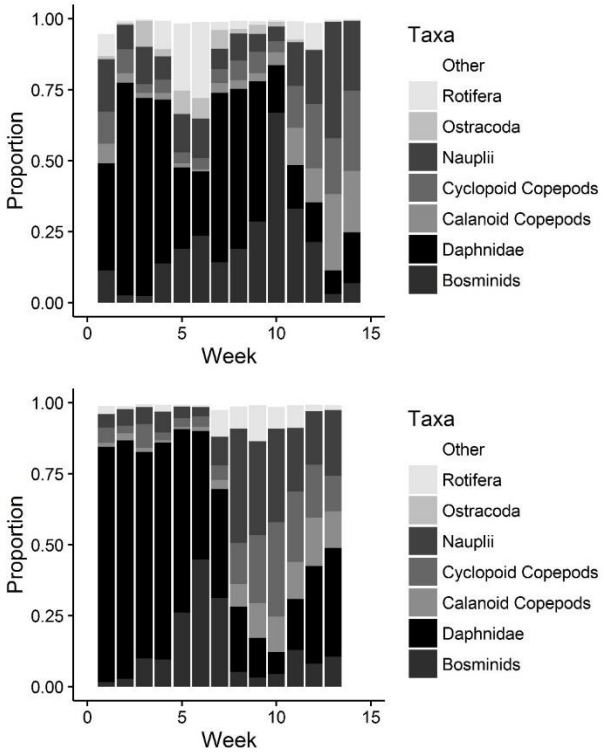

Figure 20: Changes in zooplankton community composition throughout the course of the sampling season, 2015 (top) and 2016 (bottom).

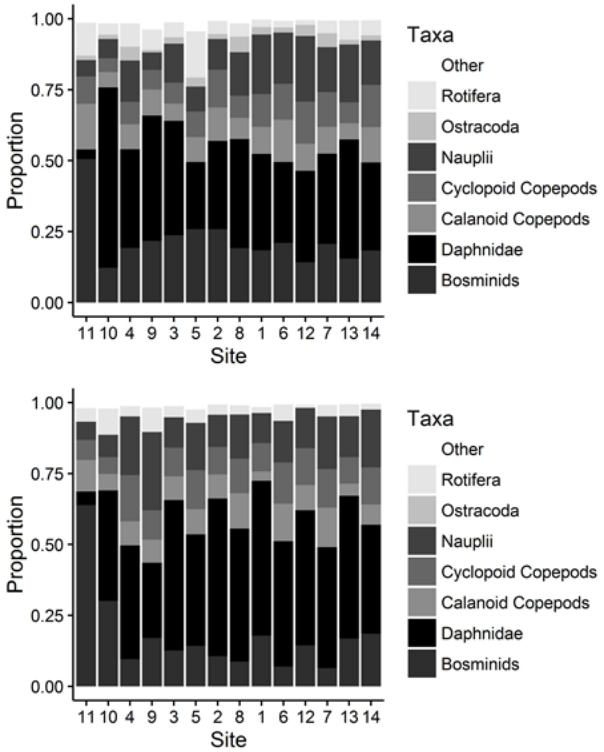

Figure 21: Zooplankton community composition at western basin plankton sampling sites, 2015 (top) and 2016 (bottom). Sites on the x-axis are arranged from north to south.

Zooplankton Length-frequency Analysis

Though the length-frequency distributions of bosminid spp. (Bosmina spp., Eubosmina spp., and Chydorus spp.; hereafter bosminds), Daphnidae, and calanoid copepods were significantly different in 2015 compared to 2016, these differences were very small and probably not biologically relevant (Table 5). In general, these zooplankton were slightly longer in 2016, when HAB severity and fish abundance and therefore predation were comparatively lower.

Table 5: Zooplankton length trends in 2015 and 2016.

2015	Length (mm)		
Taxa	Minimum	Mean	Maximum
Bosminid	0.12	0.3116	1.01
Daphnidae	0.16	0.7871	2.83
Calanoid	0.21	0.7331	2.32
Cyclopoid	0.12	0.5558	1.52
2016	Length (mm)		
Taxa	Minimum	Mean	Maximum
Bosminid	0.14	0.3125	1.15
Daphnidae	0.16	0.784	2.72
Calanoid	0.22	0.7594	1.88
Cyclopoid	0.19	0.5567	1.53

There was no significant difference in cyclopoid copepod length-frequency in 2015 compared to 2016, suggesting these selective feeders were not impacted by high densities of toxic *Microcystis*.

There were few significant spatio-temporal trends in zooplankton length-frequency distributions, and the differences in length were so small they may not be biologically relevant (i.e. the increase in zooplankton length is unlikely to cause zooplankton predators to become gape-limited). In 2015 and 2016, bosminids were significantly shorter at northern sites near the Detroit River mouth (Figure 22A, Figure 22B). Bosminid length-frequency distributions were

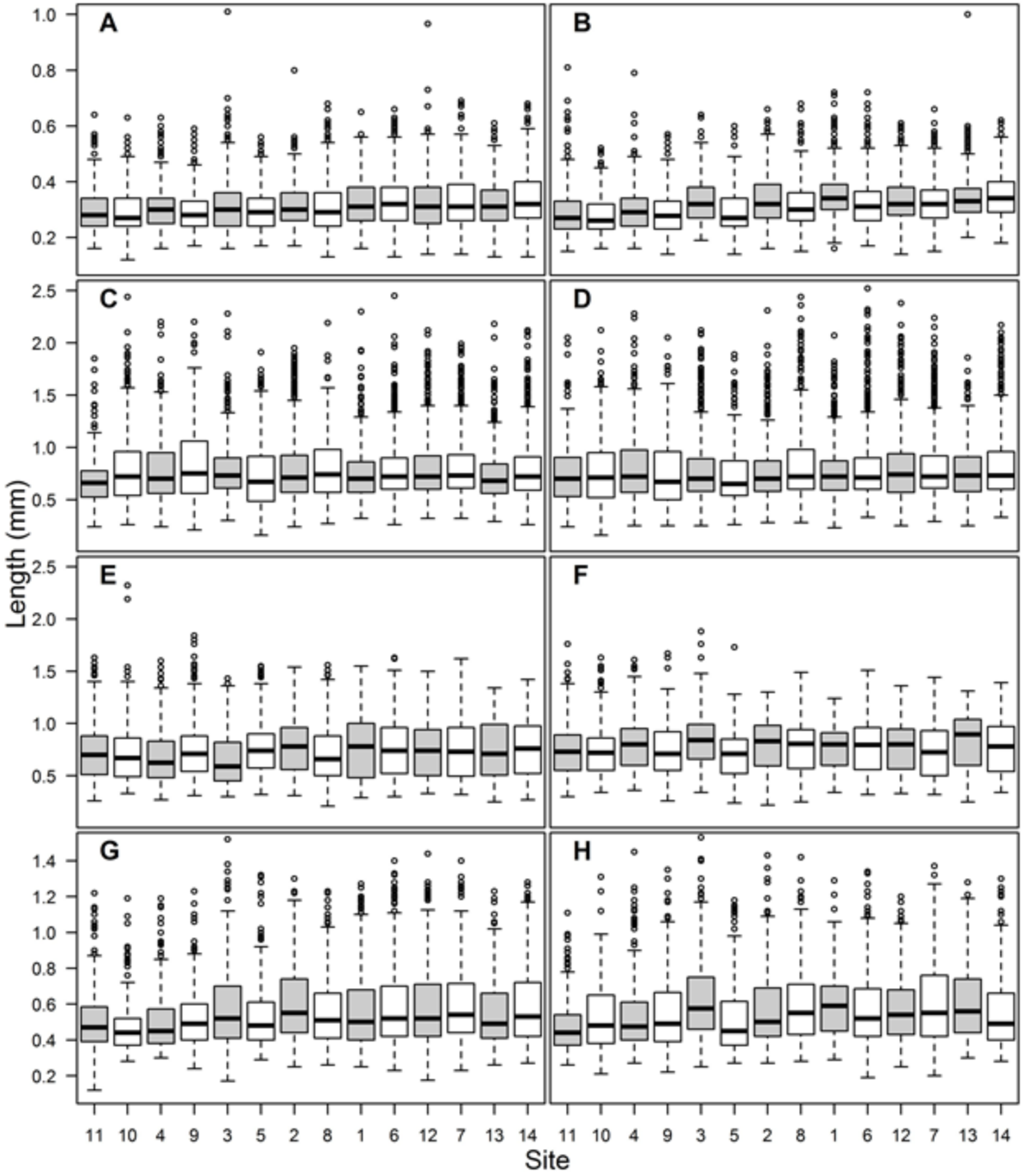

Figure 22: Spatial trends in zooplankton length-frequency distributions. Sites on the x-axis are arranged from north to south. Gray boxes indicate nearshore sites; white boxes indicate offshore sites. A: Spatial trends in bosminid length in 2015. B: Spatial trends in bosminid length in 2016. C: Spatial trends in Daphnidae length in 2015. D: Spatial trends in Daphnidae length in 2016. E: Spatial trends in calanoid copepod length in 2015. F: Spatial trends in calanoid copepod length in 2016. G: Spatial trends in cyclopoid copepod length in 2015. H: Spatial trends in cyclopoid copepod length in 2016.

similar at nearshore and offshore sites, though bosminids are typically most abundant in nearshore littoral and eutrophic waters (Balcer et al. 1984). There were no clear, significant spatial trends in Daphnidae length-frequency distributions, although Daphnidae length was more variable at offshore sites (Figure 22C, Figure 22D). Similarly, there was weak evidence that calanoid copepods were longer at inshore sites (Figure 22E, Figure 22F). In 2015, calanoid copepods were significantly shorter at southern sites near the Maumee River mouth, where HAB cell density tended to be highest, often forming surface scums; however, this trend did not hold in 2016. There were no clear, significant spatial trends in cyclopoid copepod length-frequency distributions, although cyclopoid copepods were slightly longer at southern sites (Figure 22G, Figure 22H).

Temporal trends in zooplankton length-frequency were stronger than spatial trends. The length-frequency distribution of bosminids significantly changed throughout the course of the sampling season (Figure 23A, Figure 23B) Bosminid lengths decreased on average during pulses of parthenogenic reproduction, which occur a few times each summer, particularly in early July and late summer (Balcer et al. 1984, Selgeby 1975). These pulses of reproduction introduced small bosminids into the population, whose length on average increased during the course of the approximately 5-week lifespan of the cohort. Daphnidae have a similar life history, and length-frequency trends (Figure 23C, Figure 23D), with each cohort of parthenogenic offspring growing for 4-5 weeks (Hall 1964). A large increase in bosminid and Daphnidae length occurred in July, coincident with a peak in water temperature and increasing HAB cell density, with lengths reaching a maximum in late July – early August, concurrent with peak HAB cell density. These trends in bosminid and Daphnidae length-frequency distributions are most obvious in 2015, when HAB severity was comparatively higher. Similarly, calanoid copepod length on average

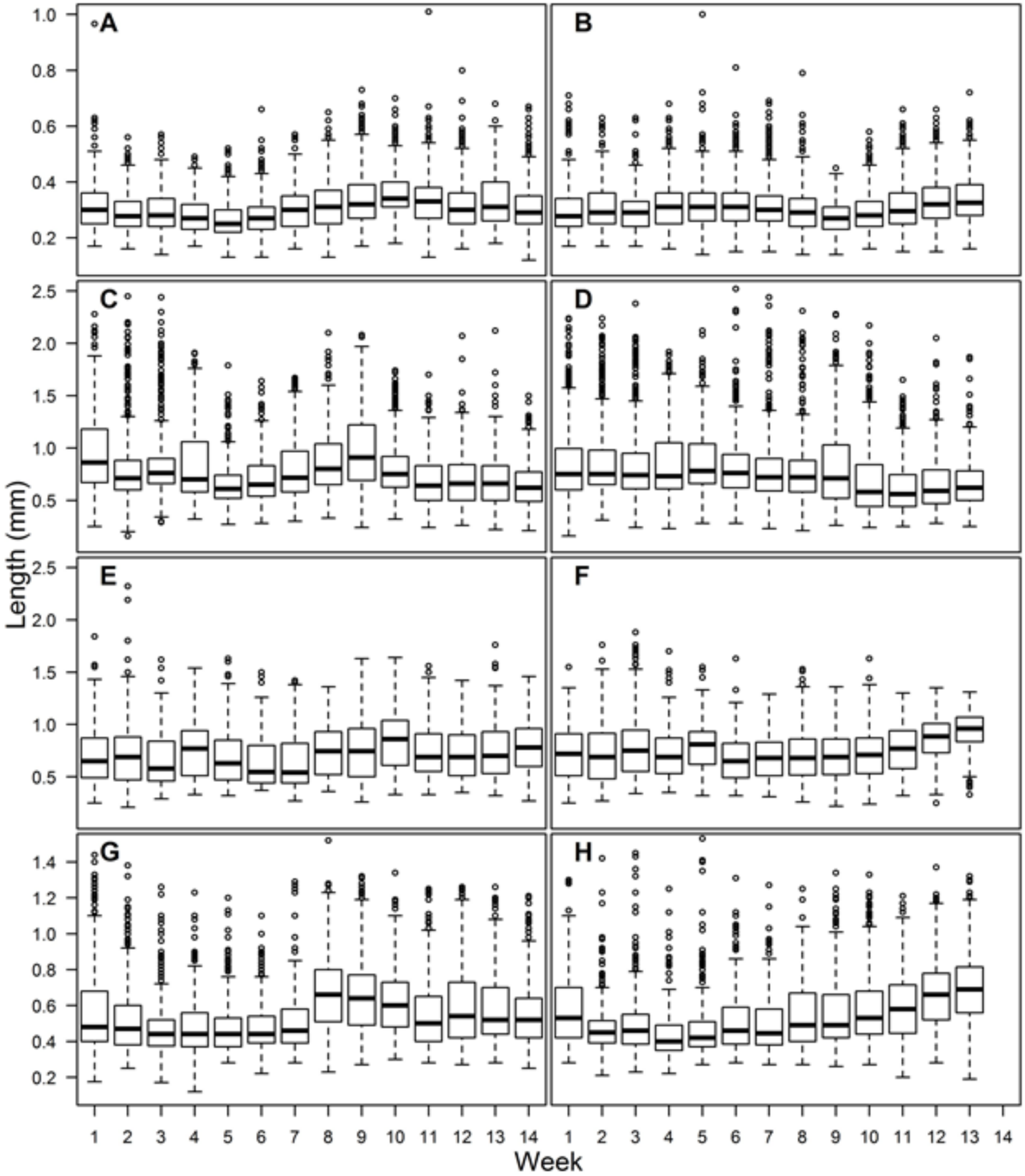

Figure 23: Temporal trends in zooplankton length-frequency distributions. A: Temporal trends in bosminid length in 2015. B: Temporal trends in bosminid length in 2016. C: Temporal trends in Daphnidae length in 2015. D: Temporal trends in Daphnidae length in 2016. E: Temporal trends in calanoid copepod length in 2015. F: Temporal trends in calanoid copepod length in 2016. G: Temporal trends in cyclopoid copepod length in 2015. H: Temporal trends in cyclopoid copepod length in 2016.

increased in late July through early August (Figure 23E, Figure 23F). Cyclopoid copepod length-frequency also seemed to be related to HAB cell density and water temperature. A large increase in cyclopoid copepod length occurred in late July in 2015, coincident with a peak in water temperature; cyclopoid copepod length then decreased through August, when HAB cell density was highest (Figure 23G, Figure 23H). In 2016, cyclopoid copepod length steadily increased in August, after HAB cell density peaked.

CONCLUSIONS

This study suggests HABs have both positive and negative impacts on various aspects of zooplankton and ichthyoplankton prey production in western Lake Erie. HABs may boost secondary productivity and growth of organisms in low trophic levels (Larson et al. 2016), increasing zooplankton and ichthyoplankton prey production, which is important for fishery production in Lake Erie. Despite the occurrence of the most severe HAB recorded in western Lake Erie (Stumpf et al. 2016), larval fish and zooplankton were more abundant in 2015 than 2016, which contributed to the production of the largest year class of walleye in the past decade (Walleye Task Group 2016).

However, Heckman's selection model (Equation 10) showed that the probability that larval fish CPUE = 0 increased with increasing HAB density later in the summer, suggesting HABs may have direct, negative impacts on larval fish survival. Though HABs influence larval fish presence-absence, they do not impact distribution of larval fishes in western Lake Erie. Rather, larval fish relative abundance is determined by site location relative to spawning and nursery areas, water clarity, and water temperature. Heckman's selection model (Equation 11) shows larval fish are most abundant in early summer soon after hatching, when water temperatures are cooler (Wismer & Christie 1987), and in turbid, nearshore nursery areas

(Roseman et al. 2005) with abundant zooplankton prey (Equation 12) along the western shore of Lake Erie. Larval fish are generally weak swimmers (Houde 1969), relying on water currents for transport (Mion et al. 1998), and are therefore unable to avoid HABs in the epilimnion that cover large spatial extents or develop and move quickly with changing wind conditions (Wynne & Stumpf 2015). In addition, larval fishes are more sensitive to algal toxins produced during HABs (Malbrouck & Kestemont 2005). These results suggest larval fish do not avoid areas affected by HABs, and instead experience increased mortality when HABs overlap with nearshore nursery habitats.

The zooplankton relative abundance model (Equation 12) provided weak evidence ($\alpha = 0.1$) that zooplankton densities increase with increasing HAB cell densities; however, zooplankton relative abundance increased with increasing turbidity and water temperature, conditions consistent with increasing HAB severity and expected future conditions (Michalak et al. 2013). Early in the summer, the zooplankton community was dominated by cladocerans, particularly bosminids and Daphnidae, though calanoid and cyclopoid copepods became dominant in late summer, when HAB cell density increased. This shift from cladocerans, indiscriminant filter feeders (Fulton & Paerl 1987), to copepods, which selectively avoid ingesting toxic *Microcystis* (Ger et al. 2016, Landsberg 2002, DeMott & Moxter 1991), is consistent with a study by Lehman et al. (2010) which showed a low cladocera to calanoid copepod ratio during *Microcystis* blooms, due to a decrease in cladoceran feeding, growth, survival, and repropduction rates. I observed a decrease in cladoceran length, on average, in 2015 when HABs were severe, though in general zooplankton were longer at southern, nearshore sites where HABs cell density was highest. Thus, I cannot conclude the overall impact of HABs on

zooplankton growth from this study, though the changes I observed in length-frequency are so small it is unlikely they are biologically relevant i.e. cause gape limitation in larval fishes.

Overall, I found weak evidence for a HAB-initiated trophic cascade that disrupted larval fish production in western Lake Erie. Rather, this study demonstrated increased zooplankton production associated with HABs, which favors larval fish growth. While a shift from cladocerans to copepods occurred with increasing HAB density, both zooplankton taxa are primary prey for larval fishes (Scott & Crossman 1973, Siefert 1972). I conclude this increase in productivity contributed to increased growth rates for larval *Morone* spp. and yellow perch, which on average were longer in 2015 than 2016, and at southern, nearshore sites associated with high zooplankton and HAB cell densities. However, the severe HAB in 2015 was associated with a decrease in clupeid spp. length. This suggests larval fishes may show differential responses to HABs, as Warlen et al. (1998) observed. In particular, clupeid spp. may experience decreased growth rates when high densities of large *Microcystis* colonies interfere with filter feeding mechanisms (Engstrom-Öst et al. 2006).

Though HABs are associated with a shift in zooplankton community composition, increases in zooplankton prey production associated with HABs promote larval fish production by increasing larval fish growth rates (with the exception of larval clupeids). In addition, Reichert et al. (2010) suggested HABs may increase recruitment by increasing turbidity and providing larval fish with a refuge from visual predators, though Mion et al. (1998) found larval walleye mortality rates increased with increasing turbidity. Consistent with these findings, I observed higher abundances of both zooplankton prey and larval fishes in 2015, when a severe HAB occurred. However, an absence of larval fishes at sites with severe HABs suggests larval fish experience increased mortality rates when HABs spatially overlap with nearshore nursery

habitats. A decrease in clupeid abundance and length with increasing HAB severity suggests some larval fishes are more susceptible to negative effects of HABs and may not benefit from increased zooplankton production. Therefore, I conclude HABs do have some cascading effects on low trophic levels, particularly zooplankton production and larval fish growth, abundance and survival, though these impacts are not always harmful as the name suggests.

SYNTHESIS

LAKE ERIE ECOSYSTEM CHANGES RELATED TO HABS AND THE POTENTIAL FOR A TROPHIC CASCADE

The fishery ecosystem in Lake Erie has been subjected to many changes in recent decades, including eutrophication and subsequent implementation of phosphorus control measures (International Joint Commission 2014), overfishing (Taylor & Ferreri 1999), invasion by *Dreissenid* mussels (Johannsson et al. 2000) and other invasive species, and most recently, re-eutrophication (Scavia et al. 2014) and the recurrence of cyanobacterial HABs (Michalak et al. 2013). These environmental changes have the potential to create cascading effects on many trophic levels in the fishery production chain, impacting fishery recruitment. In this study, I found some evidence of direct and indirect impacts of HABs in a trophic cascade involving zooplankton, ichthyoplankton, and YOY fishes, although the impacts of HABs I observed weren't always harmful as the name suggests.

In the previous chapter, I outlined the beginning of the trophic cascade by describing the impacts of HABs on zooplankton and larval fishes. During a Lake Erie HAB, warm, nutrient-rich conditions favor the growth of the cyanobacteria, *Microcystis* (Paerl & Huisman 2008), which affects the phytoplankton community through allelopathic interactions and microcystin production, forming a monotypic bloom (Legrand et al. 2003). I investigated how this well-documented change in the phytoplankton community might impact the zooplankton community; I found zooplankton relative abundance was higher in 2015, when the most severe HAB recorded occurred on Lake Erie (Stumpf et al. 2016), and at sites near the Maumee River mouth, which often had the highest densities of HAB cells (Wynne & Stumpf 2015). Though I found HABs had a significant ($\alpha = 0.1$) positive affect on zooplankton relative abundance, I also observed HABs were associated with a shift in zooplankton community composition, decreasing

the abundance of cladocerans and increasing the abundance of copepods. I could not assess the trophic interactions between zooplankton and phytoplankton directly; rather I indirectly investigated potential mechanisms underlying these trends. I hypothesized that *Microcystis* blooms would have a negative impact on zooplankton feeding and growth, as large *Microcystis* colonies are difficult for zooplankton to ingest and are a toxic, nutrient-poor food source for zooplankton (Ghadouani et al. 2004, Wilson et al. 2006). To investigate the effect of HABs on zooplankton growth rates, I assessed zooplankton length-frequency trends. I found most zooplankton taxa were longer on average in 2016, when HABs were less severe, suggesting at large temporal and spatial scales HABs and associated toxins have a negative impact on zooplankton growth rates. However, in 2015 and 2016, I found zooplankton were longer on average at southern, nearshore sites, where HAB cell density was typically the highest (Wynne & Stumpf 2015). Therefore, I conclude that conditions that favor HAB formation also favor zooplankton production, though the mechanisms underlying this trend, the impact of HABs on zooplankton growth, and the implications for fish feeding rates are unclear. In addition, HABs are associated with a shift in zooplankton community composition from cladocerans to copepods, though both taxa are important prey for larval and planktivorous fishes (Scott & Crossman 1973).

I would expect this general increase in the availability of zooplankton prey to have a slightly positive cascading effect larval fish feeding, growth, and survival rates; in general, I observed similar trends in both zooplankton and ichthyoplankton communities. The relative abundance of larval fishes was higher in 2015 and at turbid, nearshore sites, coincident with high zooplankton densities. In addition, larval *Morone* spp. and yellow perch in these areas were generally longer than larval fishes captured at northern, offshore sites under the influence of the

Detroit River plume, where HABs were less common and severe. These results suggest conditions that favor HAB formation (i.e. warm, nutrient-rich waters) also promote larval fish production indirectly by increasing the availability of zooplankton prey. However, I found HABs had a negative effect on larval fish presence-absence, which led us to assume HABs have a direct, negative effect on larval fishes. I hypothesized HABs increase larval fish mortality rates via direct or indirect toxicity (Acuña et al. 2012) or, as I propose in the case of planktivorous clupeids (Cramer & Marzolf 1970), which were generally shorter and less abundant when HABs were severe, by interfering with their filter-feeding mechanisms (Engstrom-Öst et al. 2006, Wood et al. 2014).

In chapter 1 I further traced these cascading effects of HABs on zooplankton prey production and larval fish abundance through the YOY stage, focusing on YOY forage fish production measured in August during the annual western basin interagency bottom trawl survey, and walleye year class strength, an early indicator of fishery recruitment (Madenjian et al. 1996, Zhao et al. 2013). I predicted decreases in zooplankton prey availability and ichthyoplankton production would decrease the availability of YOY forage fishes for YOY walleye, decreasing walleye fishery recruitment. However, I did not observe decreases in zooplankton and ichthyoplankton production in association with HABs, and found no discernable effect of HABs on walleye year class strength or distribution in the western basin. Rather, YOY walleye were associated with YOY prey fishes and yellow perch, another percid species with similar life history traits (Scott & Crossman 1973). Secchi depth, in particular, was a significant influence on both YOY walleye and forage fish presence-absence at western basin trawl sites; the probability that YOY fishes were present decreased with increasing Secchi depth (i.e. was lower at sites with clearer water). YOY walleye are very sensitive to light levels due to

specialized structures within their eyes, the *tapetum lucidum*, which enable them to locate prey in low-light conditions (Braekevelt et al. 1989). Moreover, YOY forage fishes may prefer turbid areas to reduce predation risk (Engstrom-Öst et al. 2009, Reichert et al. 2010). While some studies suggest young fishes may use turbid zones created by HABs as a refuge from predation (Engstrom-Öst et al. 2006), in this study I found the probability that YOY forage fishes were present significantly decreased with increasing HAB cell density. This suggests that YOY forage fishes do not respond to turbidity due to suspended sediment and algal turbidity in the same way and may actively avoid areas of dense HABs. Therefore, I found YOY forage fish relative abundance was highest at shallow eastern sites, where HABs were less likely to occur (Wynne & Stumpf 2015). However, since YOY walleye distribution was not affected by HABs, they were most likely to be captured at south-western sites; YOY walleye did not seem to discern between algal turbidity and turbidity due to suspended sediment. I identified this differential response to HABs as a potential mechanism for a spatial mismatch between YOY walleye and their prey. If this spatial pattern persists, I would expect YOY walleye feeding, growth, and survival rates to decrease according to the match-mismatch hypothesis (Cushing 1990).

To assess this hypothesis regarding the impacts of HABs on YOY fish growth rates, I investigated length-frequency trends of YOY percids (walleye and yellow perch) and YOY forage fishes (clupeid and *Notropis* spp.). While increased productivity associated with HABs may favor the growth of primary consumers (Larson et al. 2016) such as YOY forage fishes, I did not observe any clear length-frequency trends in relation to HABs severity. I therefore conclude the influence of HABs and other factors on the growth of YOY clupeid and *Notropis* spp. warrants further investigation. I found, for percids, annual abundance estimates and subsequent severity of competition for prey are more important than HABs in determining

length-frequency distributions; at an annual scale, YOY percid length generally decreased with increasing percid abundance. However, I found HAB cell density has a size-specific influence on the distribution of YOY percids throughout the western basin; walleye were generally longest in areas of high HAB cell density, while yellow perch were longest in areas of moderate HAB cell density. Large YOY walleye may be found in where HAB cell densities are high because the bioenergetic costs associated with toxic HAB exposure are more severe for smaller fishes (Malbrouck & Kestemont 2005). In addition, demersal YOY walleye do not typically spatially overlap with the greatest concentrations of HAB cells which occur in the epilimnion especially during calm conditions (Wynne & Stumpf 2015), allowing them to persist and grow where HAB cell densities are high, given there is adequate prey available. Yellow perch inhabit shallow, open water (Scott & Crossman 1973), increasing their risk of exposure to HAB cells and associated toxins; thus, the largest YOY yellow perch were observed at sites where moderate HAB densities were associated with increased productivity (Larson et al. 2016) and decreased predation risk (Reichert et al. 2010).

Overall, I did not find evidence to support my hypothesis that increasingly severe HABs in Lake Erie's western basin decrease walleye fishery production and walleye year class strength. Rather, in this study I observed a strong relationship between YOY prey availability and walleye year class strength, consistent with findings by Madenjian et al. (1996). However, I did find support for my hypothesis that HABs would negatively affect YOY forage fish availability; I found an inverse relationship between the probability that forage fishes were present in the annual bottom trawl survey and HAB cell density. Since YOY walleye do not avoid areas affected with HABs, instead preferring areas with increased algal turbidity, this creates a potential spatial mismatch between walleye and their prey. This mismatch was most severe

between walleye and their preferred prey, clupeids (Knight et al. 1984). My results suggest HABs have a negative impact on YOY clupeid abundance, distribution, and growth. Considering YOY clupeids filter feed in the meta- and epilimnion (Cramer & Marzolf 1970), where HAB cell densities are highest (Wynne & Stumpf 2015), I infer these affects are due to reduced feeding efficiency (Engstrom-Öst et al. 2006) and algal toxin ingestion and accumulation (Acuña et al. 2012). In addition, though conditions that facilitate HAB formation, i.e. warm, nutrient rich waters (Paerl & Huisman 2008), generally promote zooplankton and ichthyoplankton production and growth, high HAB cell densities were associated with an absence of larval fishes at my sampling sites and a general decrease in clupeid spp. lengths. Therefore, I infer that HABs have a direct, negative impact on larval fish survival and clupeid growth rates, putting the availability of this important forage fish at risk.

Though I did not observe a direct effect of HABs on walleye growth and recruitment, it is important to consider both the positive and negative effects of HABs on fishery ecosystem production. Though HABs do not limit the growth and abundance of larval and YOY fishes by decreasing zooplankton prey availability, much like the *Dreissenid* mussel invasion (Trometer & Busch 1999), HABs may limit the abundance, distribution, and growth of gizzard shad through other mechanisms, e.g. by interfering with the efficiency of their feeding mechanisms (Engstrom-Öst et al. 2006) or through direct or indirect toxicity (Acuña et al. 2012). Since forage fish abundance, in particular gizzard shad, has been shown to be vital to the formation of walleye year class strength (Madenjian et al. 1996), it would be prudent to determine stock-recruitment relationships, and growth and mortality rates for gizzard shad under these changing limnological conditions. Such information could be incorporated into a structural equation modeling

framework to predict both gizzard shad abundance and subsequent walleye fishery recruitment for a more holistic management strategy.

APPENDICES

APPENDIX A:

CHAPTER 1 SUPPLEMENTARY INFORMATION

Table A1: YOY fishes captured by ODNR and OMNR in the annual western basin (Lake Erie) interagency bottom trawl survey, 2002-2015 (LEC 2015).

Species	Catch
Alosa pseudoharengus	2261
Ambloplites cavifrons	54
Aplodinotus grunniens	13849
Carassius auratus	1
Carpoides cyprinus	5
Catostomus commersoni	2
Dorosoma cepedianum	71252
Etheostoma nigrum	8
Ictalurus punctatus	272
Labidesthes sicculus	361
Lepomis gibbosus	1
Lepomis macrochirus	32
Macrhybopsis storeriana	244
Micropterus dolomieu	241
Micropterus salmoides	5
Morone americana	574281
Morone chrysops	16521
Moxostoma macrolepidotum	1
Notropis antherinoides	17771
Notropis hudsonius	2963
Notropis volucellus	5778
Osmerus mordax	31700
Perca flavescens	93050
Percina caprodes	1035
Percopsis omiscomaycus	32725
Pomoxis annularis	19
Pomoxis nigromaculatus	1
Sander vitreus	4944
Unidentified *Morone* sp.	3
Unidentified Sunfish	1
Total	869381

Table A2: Spring water warming rate (ºC/day) 2002-2015, calculated by linear regression using mean daily water surface temperature measurements from the NOAA National Data Buoy Center station in western Lake Erie (NDBC 2017a).

Year	Water Warming Rate
2002	0.1675
2003	0.2800
2004	0.2366
2005	0.2849
2006	0.2004
2007	0.2816
2008	0.2487
2009	0.2550
2010	0.1399
2011	-0.2101
2012	0.1697
2013	0.1107
2014	-0.0477
2015	-0.1096

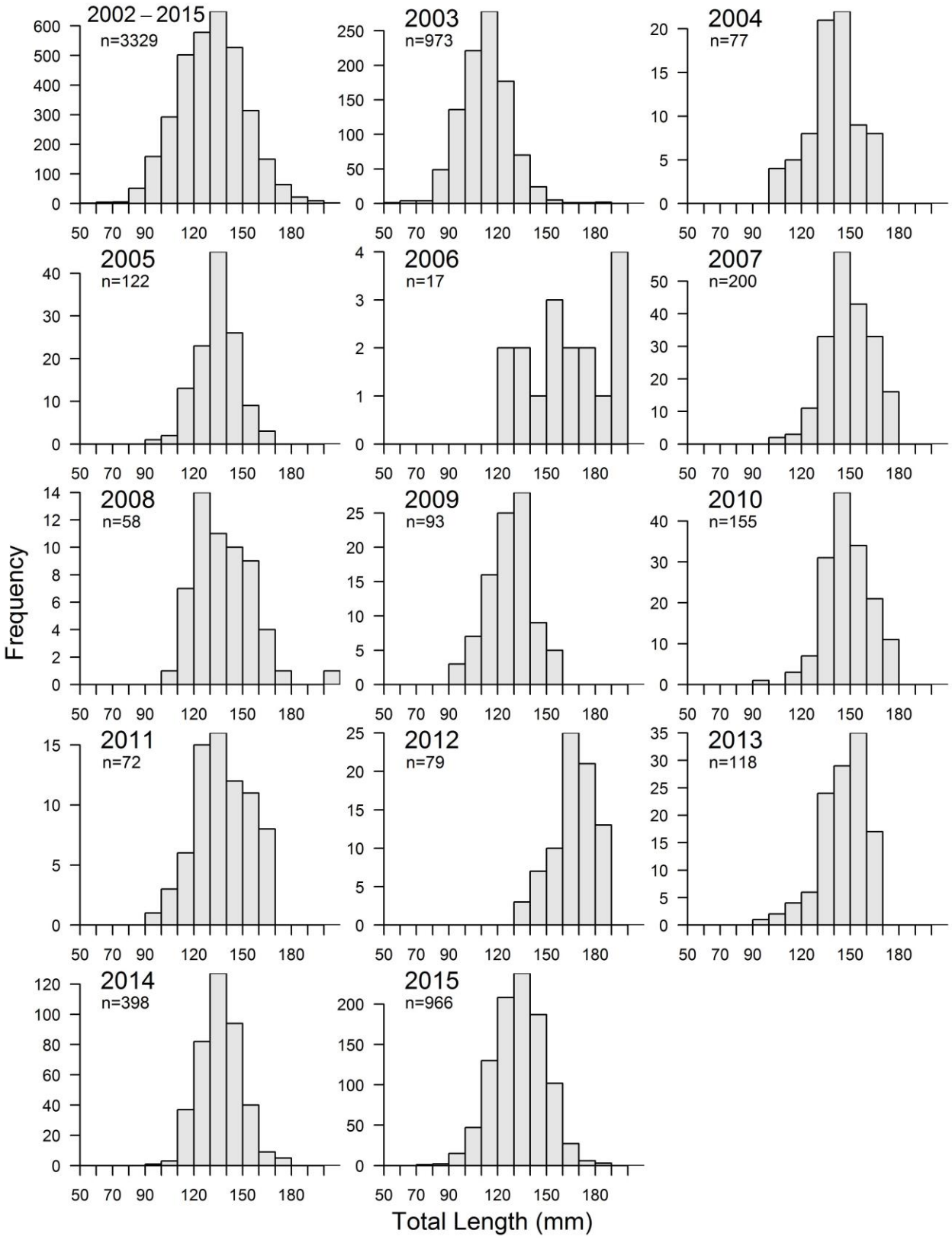

Figure A1: Length-frequency distribution of YOY walleye captured in the annual western basin (Lake Erie) interagency bottom trawl survey, 2002-2015 (LEC 2015).

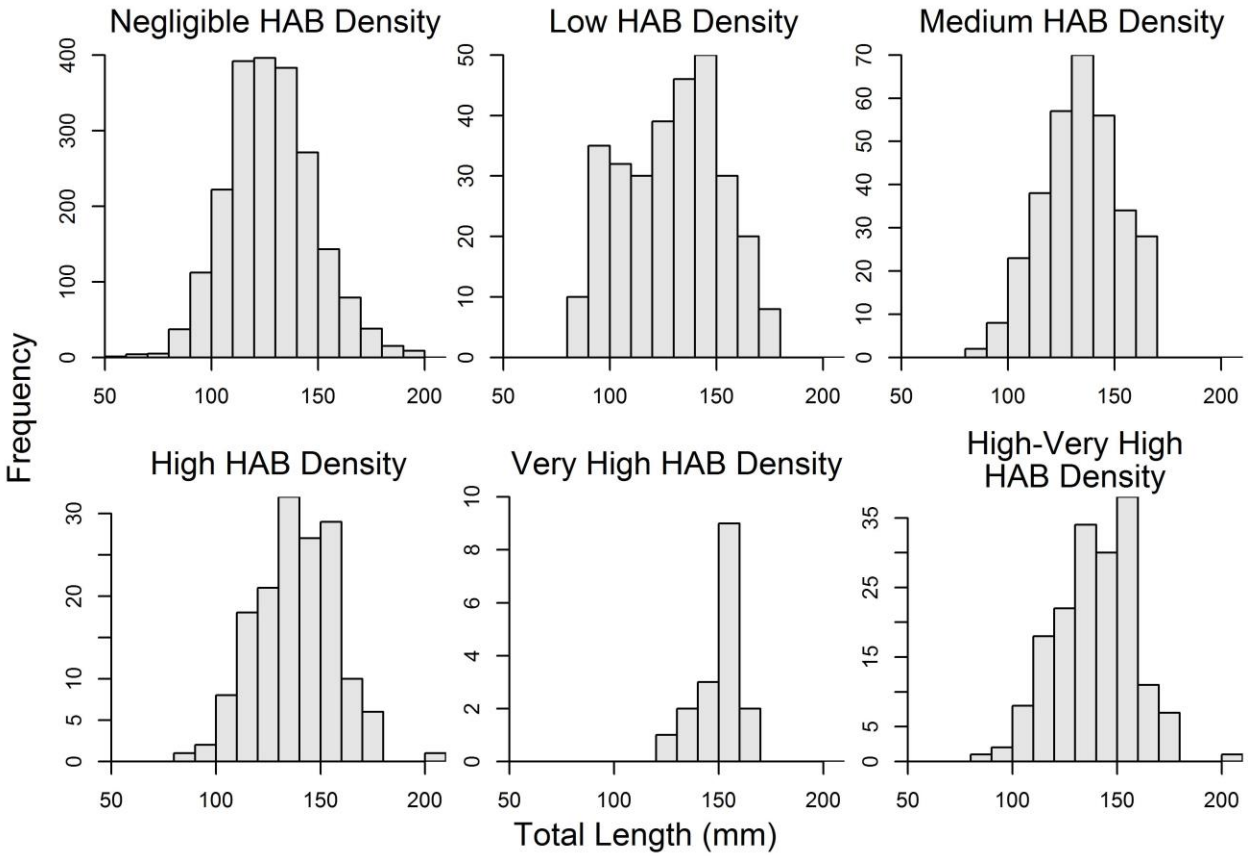

Figure A2: Length-frequency distribution of YOY walleye captured in the annual western basin (Lake Erie) interagency bottom trawl survey, 2002-2015 (LEC 2015), by HAB cell density category. The high-very high categories were combined because of low sample size in the very high category.

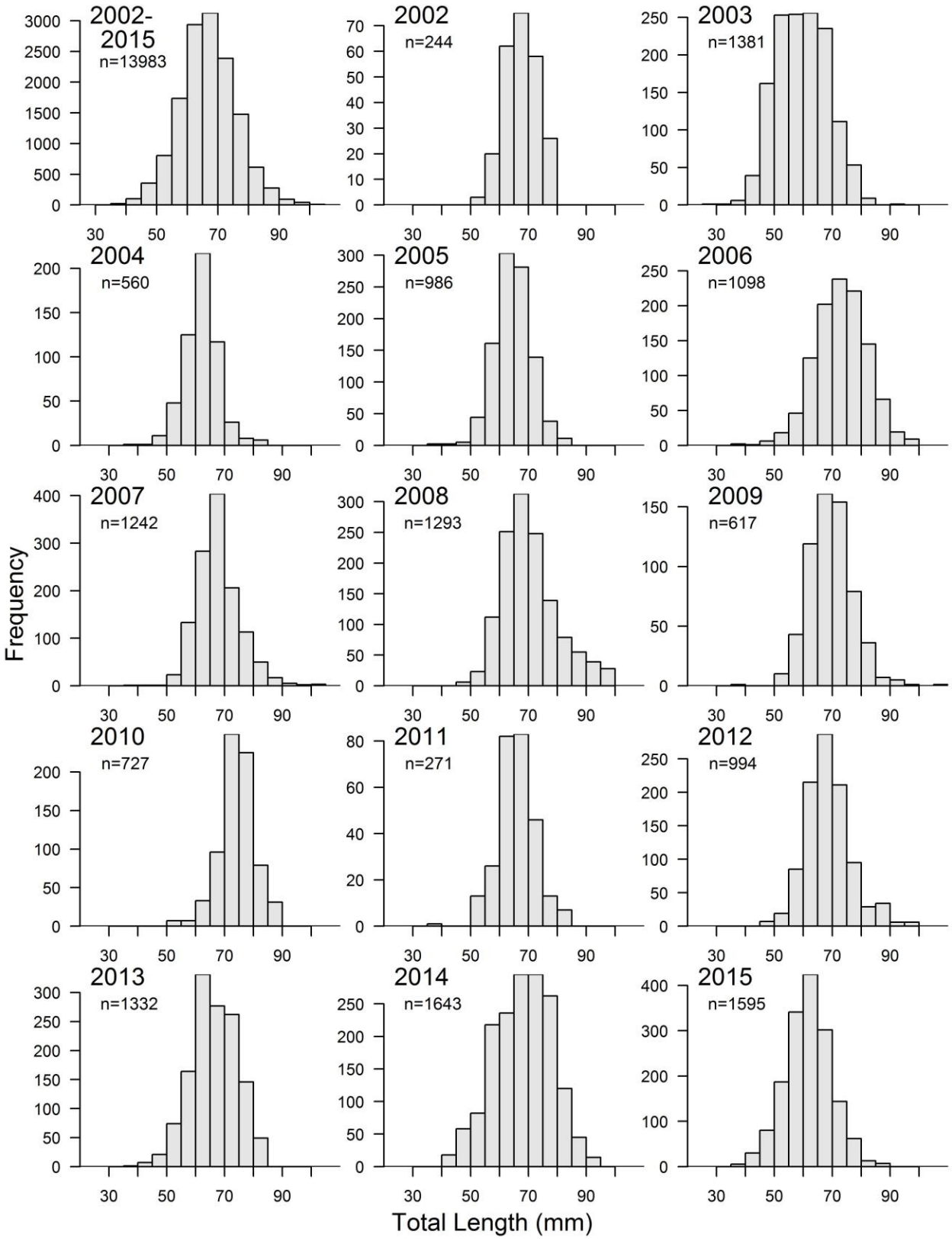

Figure A3: Length-frequency distribution of YOY yellow perch captured in the annual western basin (Lake Erie) interagency bottom trawl survey, 2002-2015 (LEC 2015).

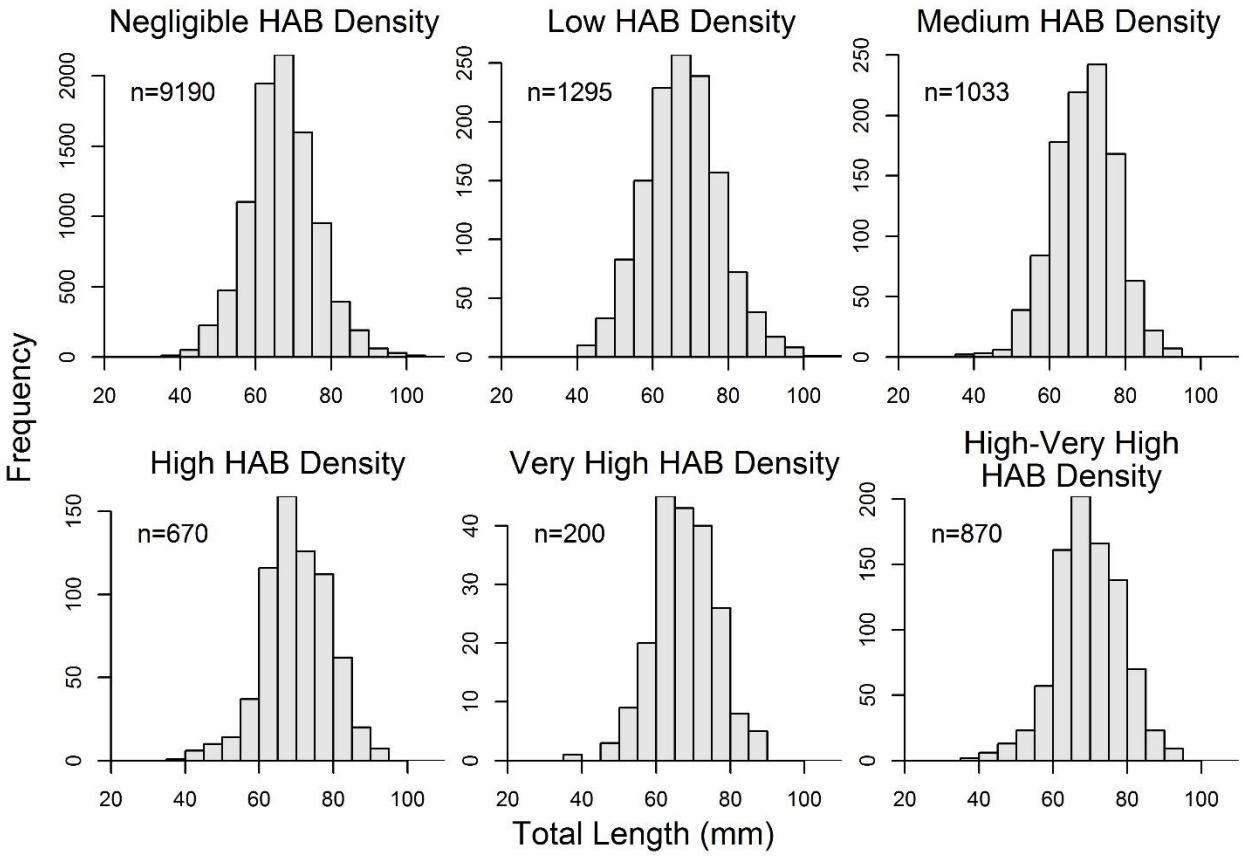

Figure A4: Length-frequency distribution of YOY yellow perch captured in the annual western basin (Lake Erie) interagency bottom trawl survey, 2002-2015 (LEC 2015), by HAB cell density category. The high-very high categories were combined because of low sample size in the very high category.

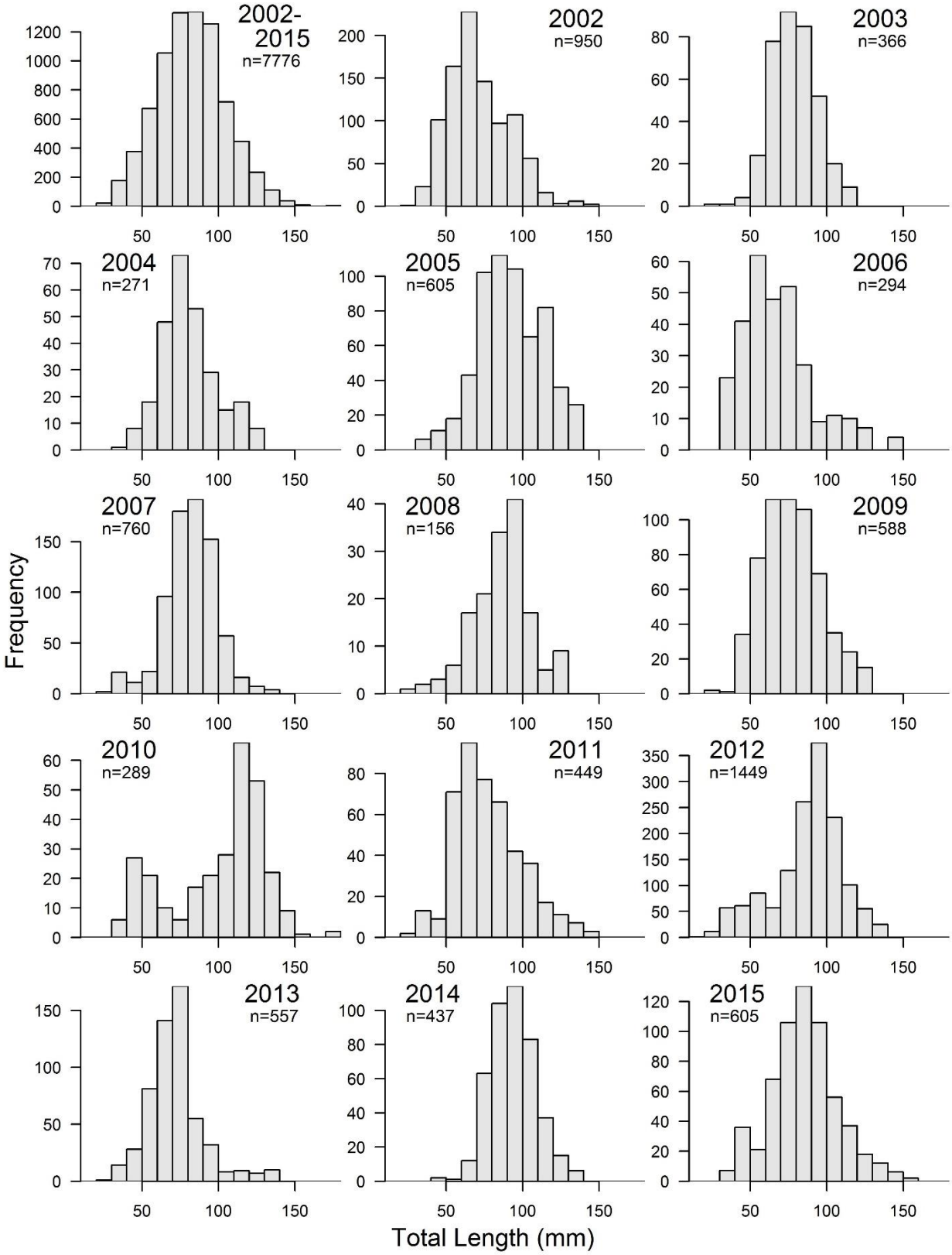

Figure A5: Length-frequency distribution of YOY clupeid species captured in the annual western basin (Lake Erie) interagency bottom trawl survey, 2002-2015 (LEC 2015).

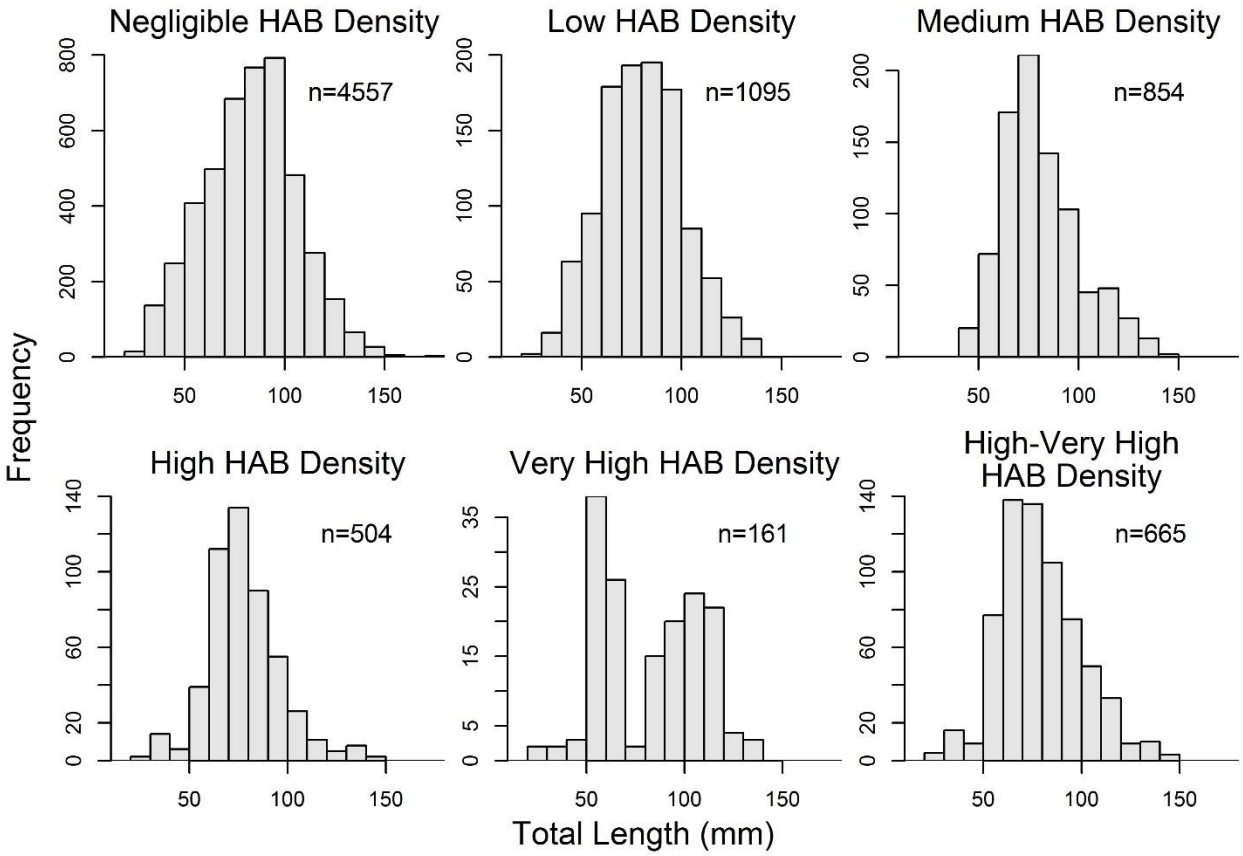

Figure A6: Length-frequency distribution of YOY clupeid species captured in the annual western basin (Lake Erie) interagency bottom trawl survey, 2002-2015 (LEC 2015), by HAB cell density category. The high-very high categories were combined because of low sample size in the very high category.

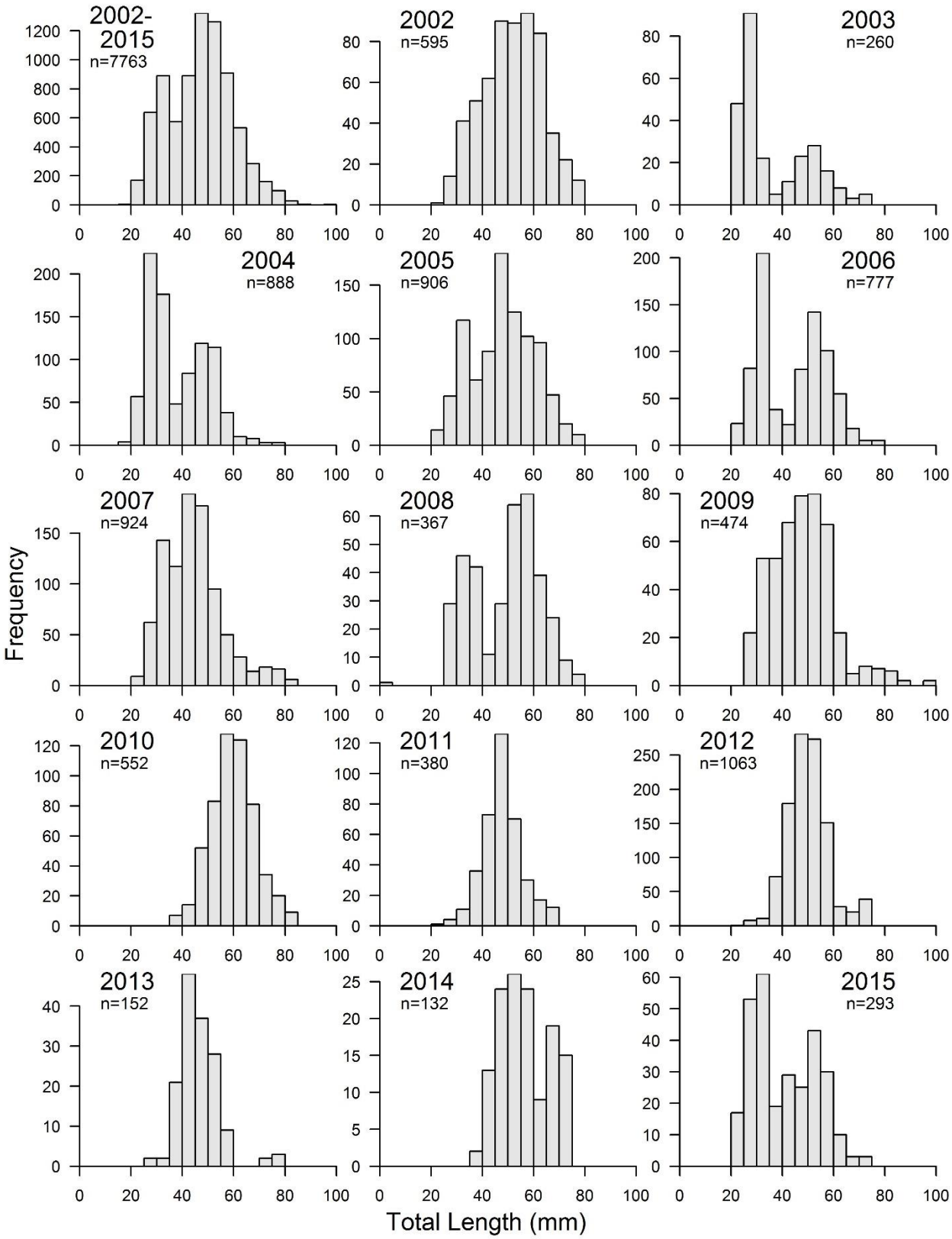

Figure A7: Length-frequency distribution of YOY *Notropis* species captured in the annual western basin (Lake Erie) interagency bottom trawl survey, 2002-2015 (LEC 2015).

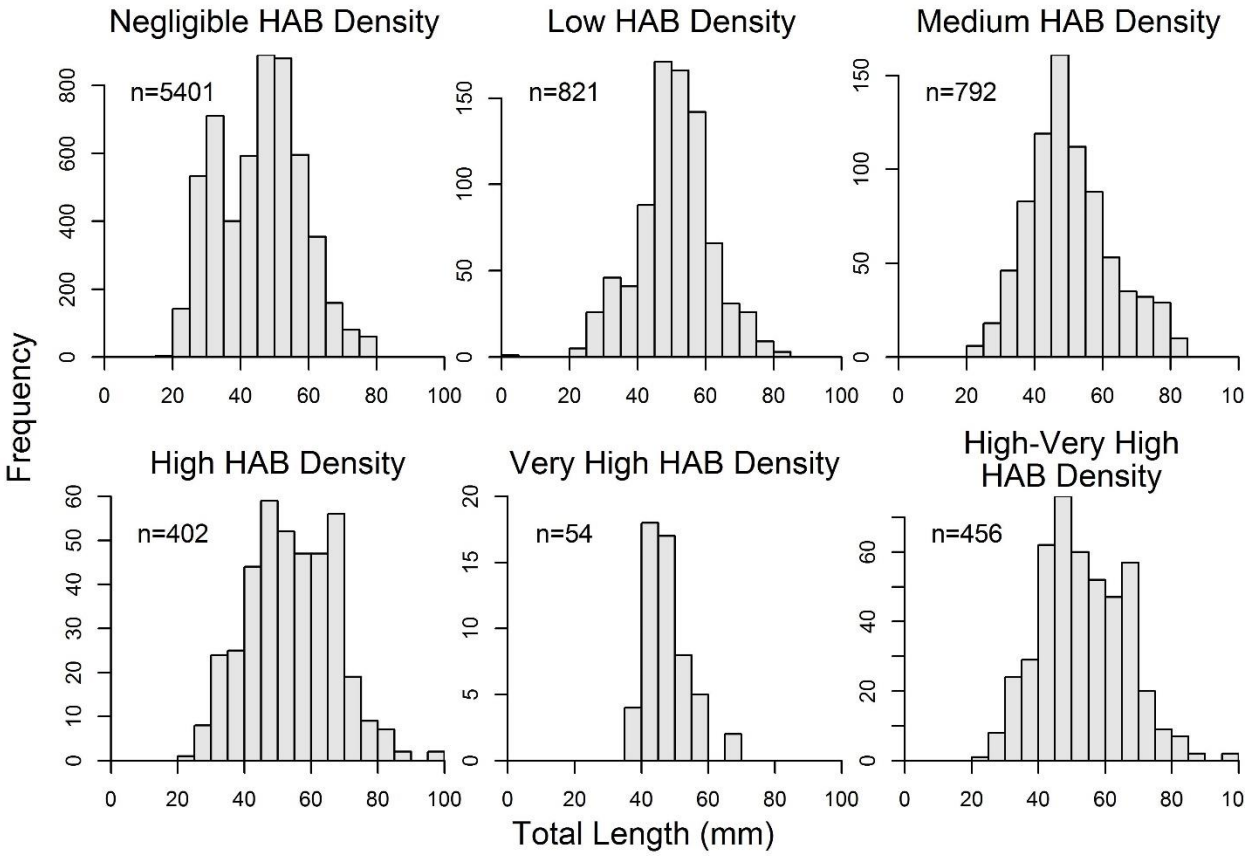

Figure A8: Length-frequency distribution of YOY *Notropis* species captured in the annual western basin (Lake Erie) interagency bottom trawl survey, 2002-2015 (LEC 2015), by HAB cell density category. The high-very high categories were combined because of low sample size in the very high category.

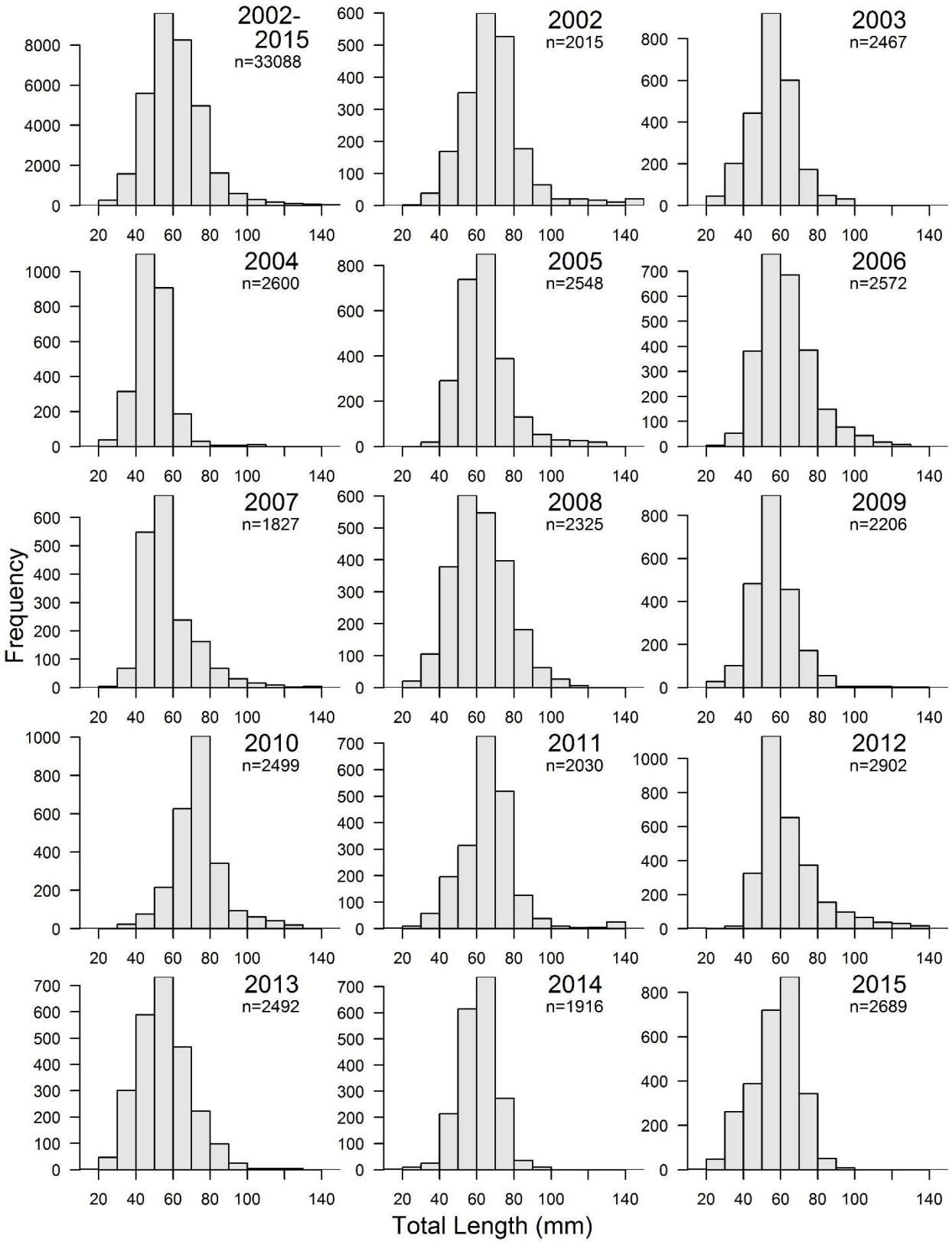

Figure A9: Length-frequency distribution of YOY *Morone* species captured in the annual western basin (Lake Erie) interagency bottom trawl survey, 2002-2015 (LEC 2015).

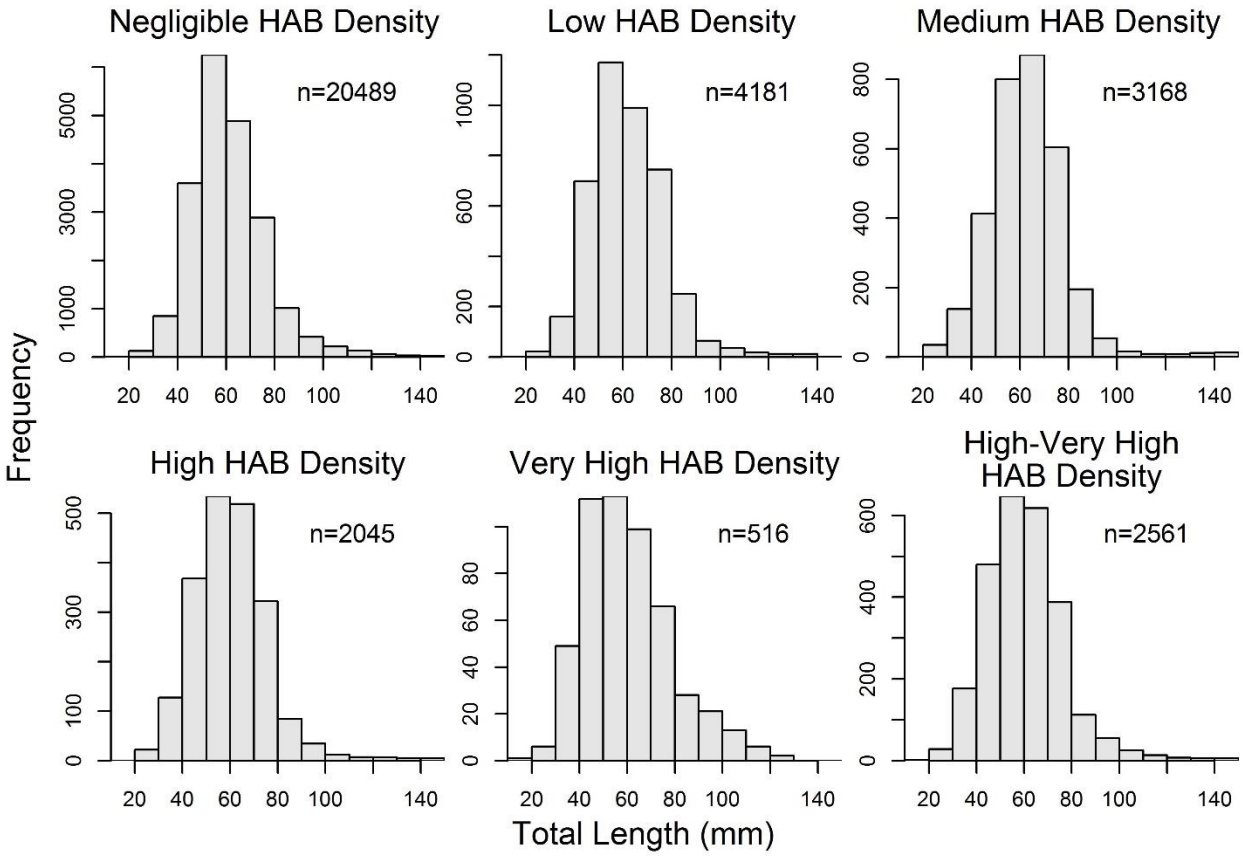

Figure A10: Length-frequency distribution of YOY *Morone* species captured in the annual western basin (Lake Erie) interagency bottom trawl survey, 2002-2015 (LEC 2015), by HAB cell density category. The high-very high categories were combined because of relatively low sample size in the very high category.

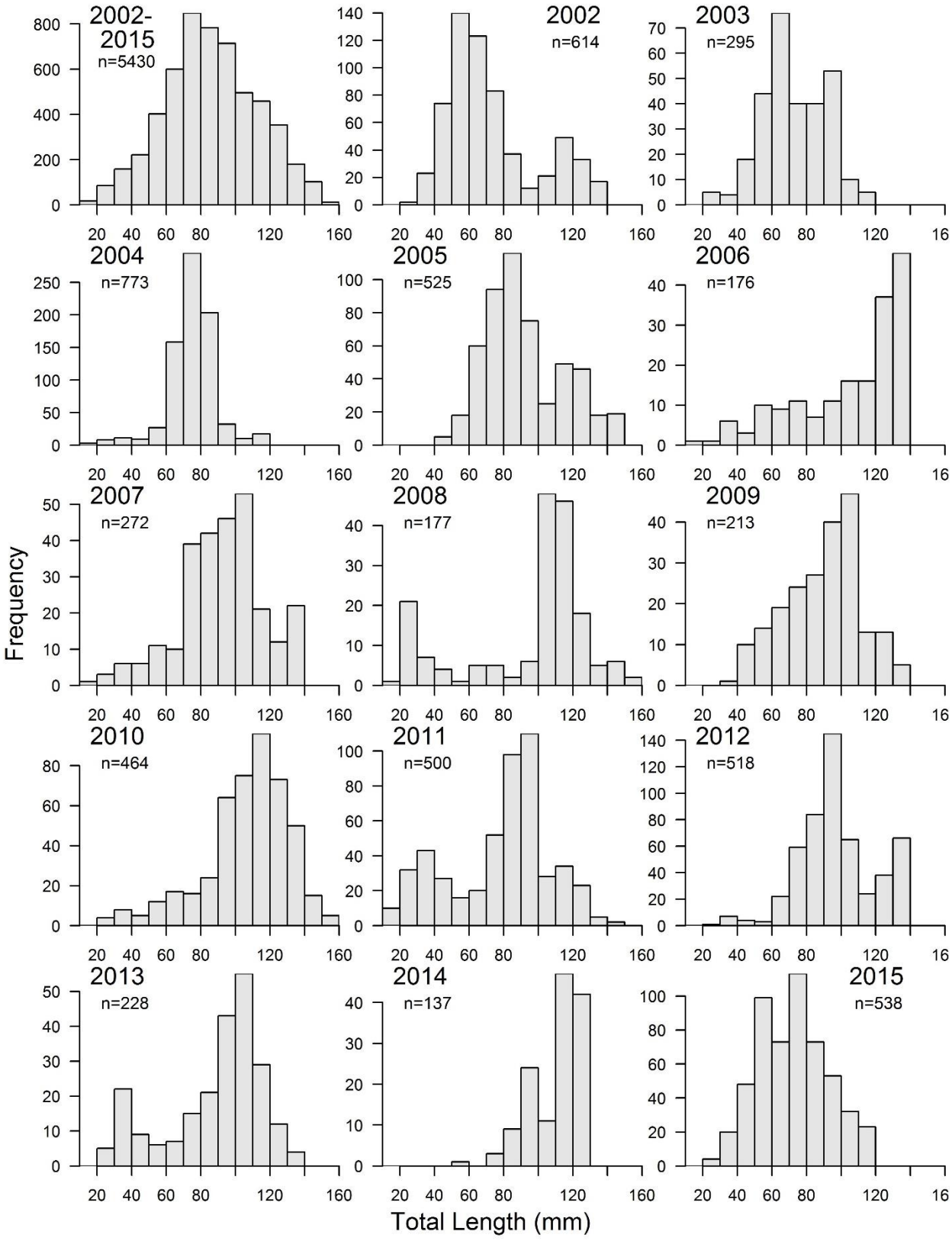

Figure A11: Length-frequency distribution of YOY freshwater drum captured in the annual western basin (Lake Erie) interagency bottom trawl survey, 2002-2015 (LEC 2015).

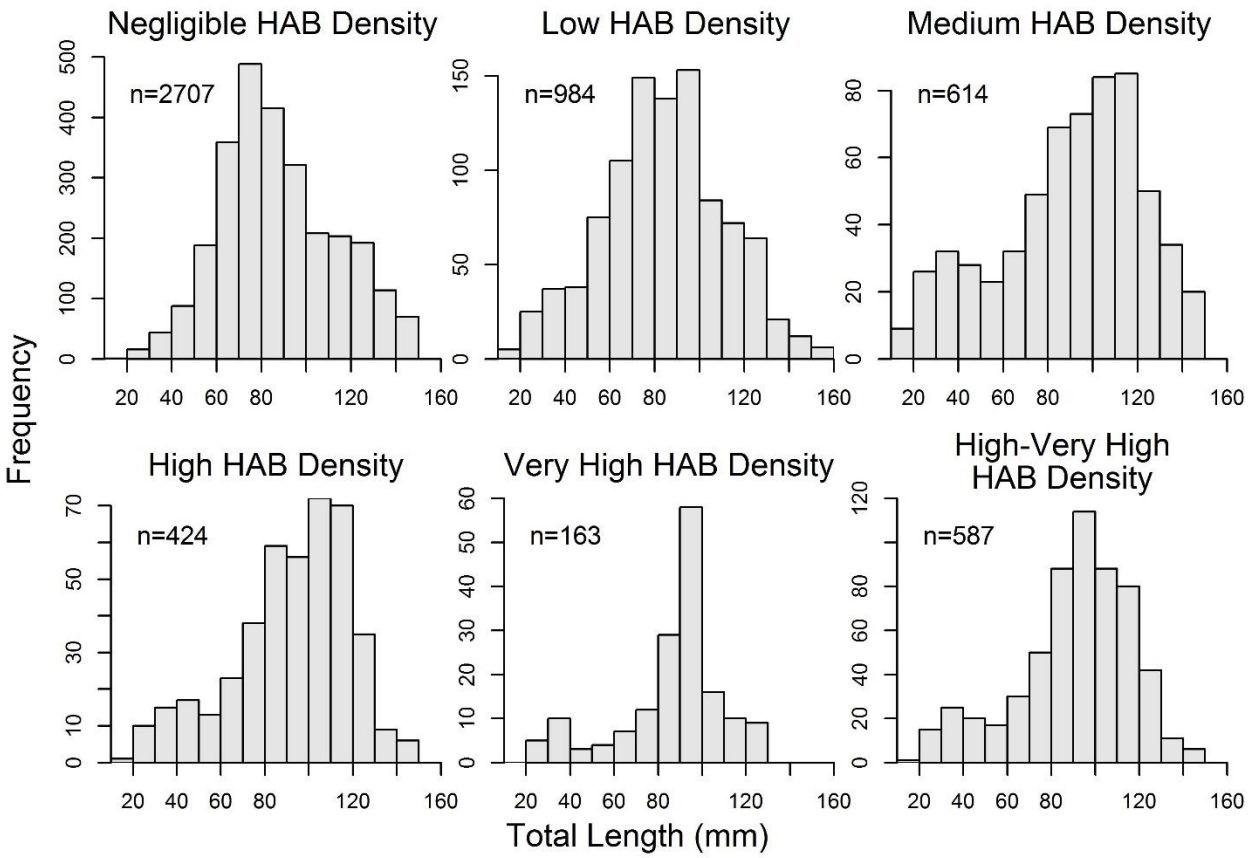

Figure A12: Length-frequency distribution of YOY freshwater drum captured in the annual western basin (Lake Erie) interagency bottom trawl survey, 2002-2015 (LEC 2015), by HAB cell density category. The high-very high categories were combined because of relatively low sample size in the very high category.

APPENDIX B:

CHAPTER 2 SUPPLEMENTARY INFORMATION

Table B1: Larval fishes captured at plankton sampling sites in the western basin of Lake Erie, 2015-2016.

Taxa	2015	2016
Aphredoderidae	1	0
Atherinidae	70	8
Catostomidae	31	0
Centrarchidae	492	85
Cottidae	10	6
Cyprinodontidae	1	0
Fish Eggs	3640	2324
Esocidae	1	0
Freshwater Drum	1138	17
Gadidae	1	0
Clupeid	17727	395
Morone spp.	10768	3907
Notropis spp.	15982	8179
Percopsidae	1	1
Rainbow Smelt	0	119
Unidentified	66	9
Walleye	3	0
Yellow Perch	752	118
Log Perch	2	0
Percid spp.	5	42
Total	47051	12886

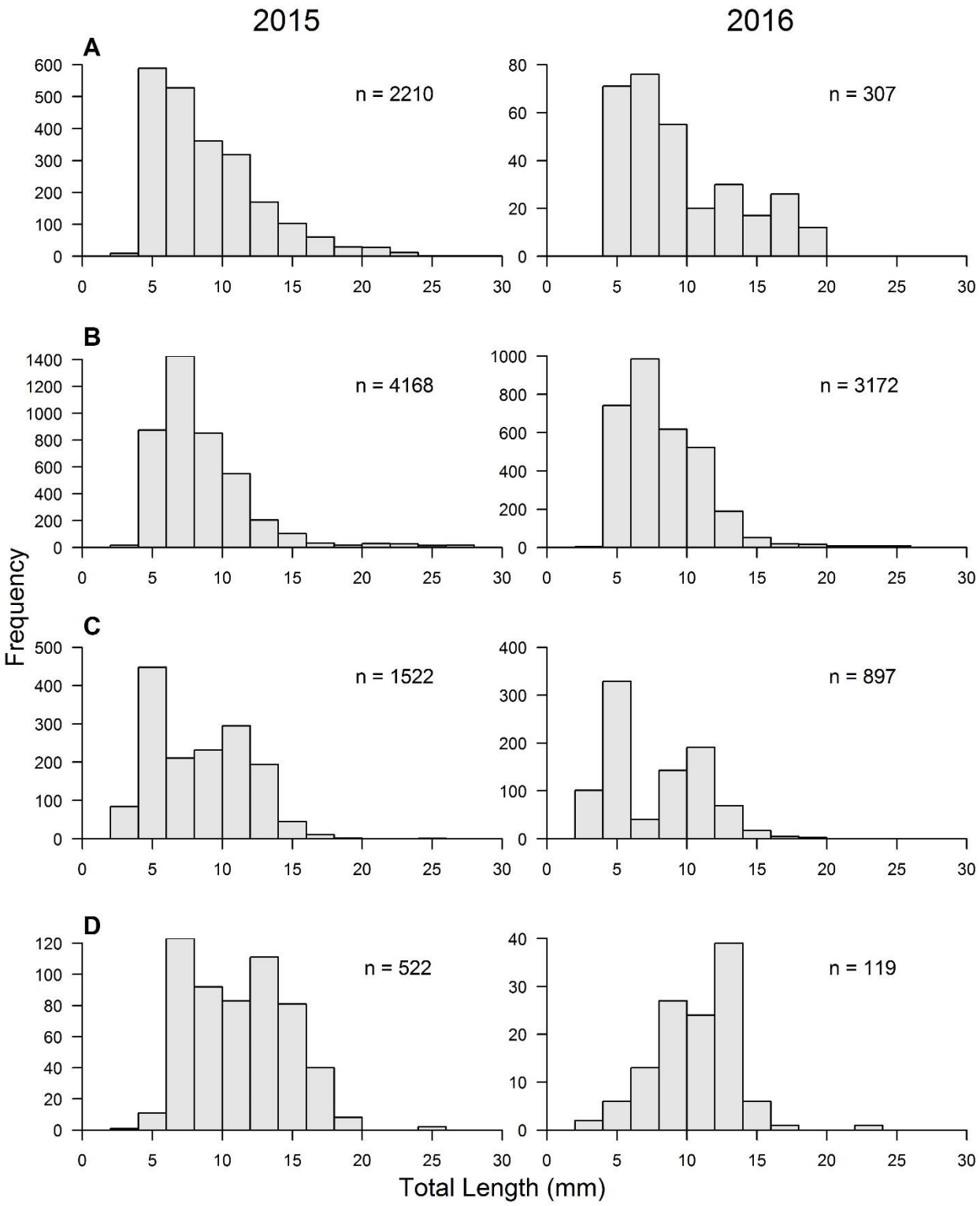

Figure B1: Length-frequency histograms for larval fishes sampled in 2015 and 2016. A: Length-frequency of larval clupeid species, 2015 and 2016. B: Length-frequency of larval *Notropis* spp., 2015 and 2016. C: Length-frequency of larval *Morone* spp., 2015-2016. D: Length-frequency of larval yellow perch, 2015 and 2016.

LITERATURE CITED

LITERATURE CITED

Acuña, S., D. Baxa, and S. Teh (2012). Sublethal dietary effects of microcystin producing *Microcystis* on threadfin shad, *Dorosoma petenense*. *Toxicon* 60:1191-1202.

Auer, N.A., editor (1982). Identification of larval fishes of the Great Lakes basin with emphasis on the Lake Michigan drainage. Great Lakes Fishery Commission, Ann Arbor, MI. *Special Pub.* 82(3): 744 pp.

Backer, L.C., D. Manassaram-Baptiste, R. LePrell, and B. Bolton (2015). Cyanobacteria and algae blooms: Review of health and environmental data from the Harmful Algal Bloom-Related Illness Surveillance System (HABISS) 2007-2011. *Toxins* 7(4): 1048-1064.

Balcer, M.D., N.L. Korda, and S.I. Dodson (1984). *Zooplankton of the Great Lakes.* University of Wisconsin Press. Madison, WI, USA.

Baron, A., W. Zhang, and E. Irwin (2016). Estimating the capitalization effects of harmful algal bloom incidence, intensity, and duration? A repeated sales model of Lake Erie lakefront property values. *2016 Annual Meeting, July 31-August 2, 2016, Boston, MA.* No. 236589. Agricultural and Applied Economics Association.

Bivand, R. (2015). classInt: choose univariate class intervals. R package version 0.1-23. Retrieved from http://CRAN.R-project.org/package=classInt.

Bockstael, N.E., I.E. Strand, K.E. Mcconnell, and F. Arsanjani (1990). Sample selection bias in the estimation of recreation demand functions: An application to sportfishing. *Land Economics* 66(1): 40–49.

Braekevelt, C.R., D.B. McIntyre, and F.J. Ward (1989). Development of the retinal tapetum lucidum of the walleye (*Stizostedion vitreum vitreum*). *Histology and Histopathology* 4(1): 63-70.

Bridgeman, T.B., J.D. Chaffin, and J.E. Filbrun (2013). A novel method for tracking western Lake Erie *Microcystis* blooms, 2002-2011. *J. Great Lakes Res.* 39: 83-89.

Busch, W.D.N., R.L. Scholl, and W.L. Hartman (1975). Environmental factors affecting the strength of walleye (*Stizostedion vitreum vitreum*) year-classes in western Lake Erie, 1960-1970. *J. Fish. Res. Board Can.* 32: 1733-1743.

Cramer, J.D. and G.R. Marzolf (1970). Selective predation on zooplankton by gizzard shad. *Trans. Am. Fish. Soc.* 99(2): 320-332.

Chorus, I. and J. Bartram (1999). Toxic cyanobacteria in water: A guide to their public health consequences, monitoring and management. In Wynne, T.T. and R.P. Stumpf (2015).

Spatial and temporal patterns in the seasonal distribution of toxic cyanobacteria in western Lake Erie from 2002-2014. *Toxins* 7:1649-1663.

Cushing, D.H. (1990). Plankton production and year-class strength in fish populations: An update of the match/mismatch hypothesis. *Adv. Mar. Biol.* 26: 249-293.

DeMott, W.R. and F. Moxter (1991). Foraging cyanobacteria by copepods: Responses to chemical defense and resource abundance. *Ecology* 72(5): 1820-1834.

Engström-Öst, J., M. Karjalainen, and M. Viitasalo (2006). Feeding and refuge use by small fish in the presence of cyanobacterial blooms. *Environ. Bio. Fish* 76:109-117.

Engström-Öst, J., M. Öst, and M. Yli-Renko (2009). Balancing algal toxicity and turbidity with predation risk in the three-spined stickleback. *Journal of Experimental Marine Biology and Ecology* 377(1): 54-59.

Fulton III, R.S. and H.W. Paerl (1987). Toxic and inhibitory effects of blue-green alga *Microcystis aeruginosa* on herbivorous zooplankton. *J. Plankton Res.* 9(5): 837-855.

Gannon, D.P., E. Berens McCabe, S.A. Camilleri, J.G. Gannon, M.K. Brueggen, A.A. Barleycorn, V.I. Palubok, G.J. Kirkpatrick, R.S. Wells (2009). Effects of *Karenia brevis* harmful algal blooms on nearshore fish communities in southwest Florida. *Mar. Ecol. Prog. Ser.* 378: 171-186.

Ger, K. A., Faassen, E. J., Pennino, M. G., & Lürling, M. (2016). Effect of the toxin (microcystin) content of Microcystis on copepod grazing. *Harmful Algae* 52: 34–45.

Ghadouani, A. B.B. Pinel-Alloul, K. Plath, G.A. Codd, and W. Lampert (2004). Effects of *Microcystis* and purified microcystin-LR on the feeding behavior of *Daphnia pulicaria. Limnol. Oceanogr.* 49: 666-679.

Hall, D.J. (1964). A experimental approach to the dynamics of a natural population of *Daphnia galeata mendota*. *Ecology* 45(1): 94-112.

Haney, J.F., and D.J. Hall (1972). Sugar-coated *Daphnia*: A preservation technique for Cladocera. *Limnol. Oceanogr.* 18(2): 331-333.

Hartman, K. J., Vondracek, B., Parrish, D. L., & Muth, K. M. (1992). Diets of emerald and spottail shiners and potential interactions with other western Lake Erie planktivorous fishes. *Journal of Great Lakes Research*, *18*(1), 43–50.

Hjort, J. (1914). Fluctuations in the great fisheries of northern Europe viewed in the light of biological research. *Rapp. P.-v. Reun. Cons. Perm. Int. Explor. Mer.* 20: 228 pp.

Ho, J.C. and A.M. Michalak (2015). Challenges in tracking harmful algal blooms: A synthesis of evidence from Lake Erie. *JGLR* 41:2, 317-325.

Houde, E.D. (1969). Sustained swimming ability of larvae of walleye (*Stizostedion vitreum vitreum*) and yellow perch (*Perca flavescens*). *J. Fish. Res. Board Can.* 26: 1647-1659.

Houde, E. D. (1997). Patterns and trends in larval-stage growth and mortality of teleost fish. *Journal of Fish Biology*, 51: 52–83.

International Joint Commission (2014). A balanced diet for Lake Erie: Reducing phosphorus loadings and harmful algal blooms. Report of the Lake Erie Ecosystem Priority.

Johannsson, O. E., R. Dermott, D.M. Graham, J.A. Dahl, E. Scott Millard, D.D. Myles, and J. LeBlanc (2000). Benthic and pelagic secondary production in Lake Erie after the invasion of Dreissena spp. with implications for fish production. *Journal of Great Lakes Research*, *26*(1), 31–54.

Knight, R.L., F.J. Margraf, and R.F. Carline (1984). Piscivory by walleyes and yellow perch in western Lake Erie. *Trans. Am. Fish. Soc.* 113(6):677-693.

Knight, R.L. and B. Vondracek (1993). Changes in prey fish populations in western Lake Erie, 1969-88, as related to walleye, *Stizostedion vitreum*, predation. *Can. J. Fish. Aquat. Sci.* 50:1289-1298.

Landsberg, J. H. (2002). The Effects of Harmful Algal Blooms on Aquatic Organisms. *Reviews in Fisheries Science* 10(2): 113–390.

Larson, J.H., W.B. Richardson, M.A. Evans, J. Schaeffer, T. Wynne, M. Bartsch, L. Bartsch, J.C. Nelson, and J. Vallazza (2016). Measuring spatial variation in secondary production and food quality using a common consumer approach in Lake Erie. *Ecological Applications* 26(3): 873-885.

LEBS (Lake Erie Biological Station). (2015). Fisheries research and monitoring activities of the Lake Erie Biological Station, 2014. Prepared by B. Bodamer Scarbro, W.H. Edwards, C. Gawne, P.M. Kocovsky, R.T. Kraus, M.R. Rogers, and T.R. Stewart. Report of the Lake Erie Biological Station (LEBS) to the Great Lakes Fishery Commission at the Annual Meeting of Lake Committees, Ypsilanti, MI. 31 pp.

LEC (Lake Erie Committee) (2015). *Interagency western basin trawling catch, effort, and length data.* Ann Arbor, MI: Great Lakes Fishery Commission.

Legrand, C., K. Rengefors, G.O. Fistarol, and E. Graneli (2003). Allelopathy in phytoplankton: Biochemical, ecological and evolutionary aspects. *Phycologia* 42: 406-419.

Lehman, P. W., S. J. Teh, G. L. Boyer, M.L. Nobriga, E. Bass, & C. Hogle (2010). Initial impacts of Microcystis aeruginosa blooms on the aquatic food web in the San Francisco Estuary. *Hydrobiologia* 637: 229–248.

Lim, J.Y., H.H. Lee, and Y.H. Hwang (2011). Trust on doctor, social capital and medical care use of the elderly. *European Journal of Health Economics*, 12: 175–188.

Ludsin, S.A., J. Lee, S. Lee, M. Manubolu, J.F. Martin, L. Collart, K.M. Riedl (2016). Fish flesh and fresh produces as sources of microcystin exposure to humans. Oral presentation at Understanding Algal Blooms: State of the Science Conference; Toledo, OH, USA.

Lumley, T. and A. Miller (2009). leaps: regression subset selection. R package version 2.9. Retrieved from http://CRAN.R-project.org/package=leaps.

Madenjian, C.P., J.T. Tyson, R.L. Knight, M.W. Kershner, and M.J. Hansen (1996). First-year growth, recruitment, and maturity of walleyes in western Lake Erie. *Trans. Am. Fish. Soc.* 126(6): 821-830.

Malbrouck, C. and P. Kestemont (2006). Effects of microcystins on fish. *Environmental Toxicology and Chemistry* 25(1): 72-86.

Michalak, A.M., E.J. Anderson, D. Beletsky, S. Boland, N.S. Bosch, T.B. Bridgeman, J.D. Chaffin, K. Cho, R. Confesor, I. Daloglu, J.V. DePinto, M.A. Evans, G.L. Fahnenstiel, L. He, J.C. Ho, L. Jenkins, T.H. Johengen, K.C. Kuo, E. LaPorte, X. Liu, M.R. McWilliams, M.R. Moore, D.J., Posselt, R.P. Richards, D. Scavia, A.L. Steiner, E. Verhamme, D.M. Wright, and M.A. Zagorski (2013). Record-setting algal bloom in Lake Erie caused by agricultural and meteorological trends consistent with expected future conditions. *PNAS* 110(16): 6448-6452.

Miller, T.J., L.B. Crowder, J.A. Rice, and E.A. Marshall (1988). Larval size and recruitment mechanisms in fishes: Toward a conceptual framework. *Can. J. Fish. Aquat. Sci.* 45: 1657-1670.

Mion, J.B., R.A. Stein, and E.A. Marschall (1998). River discharge drives survival of larval walleye. *Ecological Applications* 8(1): 88-103

NDBC (National Data Buoy Center) (2017a). *Station 45005 (LLNR 5555) – West Erie – 16 NM NW of Lorain, OH historical data: Standard meterological data, 2002-2015.* Silver Spring, MD: NOAA (National Oceanic and Atmospheric Administration). Web 29 May 2017.

NDBC (2017b). *Station MRHO1 – Marblehead, OH historical data: Standard meterological data, 2005-2015.* Silver Spring, MD: NOAA. Web 23 May 2017.

NDBC (2017c). *Station SBIO1 – South Bass Island, OH historical data: Continuous winds data, 2002-2015.* Silver Spring, MD: NOAA. Web 22 May 2017.

Neumann, R.M., and M.S. Allen (2007). Size structure. In Guy, C.S. and M.L. Brown, editors, *Analysis and Interpretation of Freshwater Fisheries Data*, chapter 9, pp 375-421. American Fisheries Society, Bethesda, MD.

Neumann, R.M., C.S. Guy, and D.W. Willis (2012). Length, weight, and associated indices. In Zale, A.V., D.L. Parrish, and T.M. Sutton, editors, *Fisheries Techniques*, Third Edition, chapter 14, pp 637-676. American Fisheries Society, Bethesda, MD.

Obenour, D.R., A.D. Gronewold, C.A. Stow, and D. Scavia (2014). Using a Bayesian hierarchical model to improve Lake Erie cyanobacteria bloom forecasts. *Water Resour. Res.* 50.

Paerl, H.W. and J. Huisman (2008). Blooms like it hot. *Science* 320: 57-58.

Peng, F., L. Kang, and J. Jiang (2013). Selection and institutional shareholder activism in Chinese acquisitions. *Management Decision*, 51(1), 141–162.

Polis, G.A., A.L.W. Sears, G.R. Huxel, D.R. Strong, and J. Maron (2000). When is a trophic cascade a trophic cascade? *TREE* 15(11): 473-475.

Pritt, J.J., M.R. DuFour, C.M. Mayer, E.F. Roseman, and R.L. DeBruyne (2014) Sampling little fish in big rivers: Larval fish detection probabilities in two Lake Erie tributaries and implications for sampling effort and abundance indices. *Trans. Am. Fish. Soc.* 143: 1011-1027.

R Core Team (2014). R: A language and environment for statistical computing. R Foundation for Statistical Computing, Vienna, Austria. http://www.R-project.org/.

Ramsdell, J.S., D.M. Anderson, and P.M. Gilbert (2005). HARRNESS: Harmful algal research and response: A national environmental science strategy 2005-2015. *Ecological Society of America*, Washington, D.C.

Reichert, J.M., B.J. Fryer, K.L. Pangle, T.B. Johnson, J.T. Tyson, A.B. Drelich, and S.A. Ludsin (2010). River-plume use during the pelagic larval stage benefits recruitment of a lentic fish. *Can. J. Fish. Aquat. Sci.* 67:987-1004.

Reiger, H.A., V.C. Applegate, R.A. Ryder, J.V. Manz, H.D. Van Meter, R.G. Ferguson, and D.R. Wolfert (1969). *The ecology and management of walleye in western Lake Erie*. Great Lakes Fishery Commission Technical Report No. 15.

Rockel, M.L. and M.J. Kealy (1991). The value of nonconsumptive wildlife recreation in the United States. *Land Economics* 67(4): 422-434.

Roseman, E.F. (2000). *Physical and biological processes influencing walleye early life history in western Lake Erie*. (Doctoral dissertation). Retrieved from http://search.proquest.com.proxy2.cl.msu.edu/docview/304609056.

Roseman, E.F., W.W. Taylor, D.B. Hayes, R.C. Haas, R.L. Knight, and K.O. Paxton (1996).

Walleye egg deposition and survival on reefs in western Lake Erie (USA). *Annales Zoologici Fennici*, 33:3-4, PERCIS II: Second International Percid Fish Symposium, Vaasa, Finland, 21-25 August 1995 (1996) pp. 341-351.

Roseman, E.F., W.W. Taylor, D.B. Hayes, J.T. Tyson, and R.C. Haas (2005). Spatial patterns emphasize the importance of coastal zones as nursery areas for larval walleye in western Lake Erie. *J. Great Lakes Res.* 31(1): 28-44.

Roseman, E.F., J. Boase, G. Kennedy, J. Craig, and K. Soper (2011) Adaptation of egg and larval sampling techniques for lake sturgeon and broadcast spawning fishes in a deep river. *J. Appl. Ichthyol.* 27(2): 89-92.

Scavia, D., J.D. Allan, K.K. Arend, S. Bartell, D. Beletsky, N.S. Bosch, S.B. Brandt, R.D. Briland, I. Daloglu, J.V. DePinto, D.M. Dolan, M.A. Evans, T.M. Farmer, D. Goto, H. Han, T.O. Höök, R. Knight, S.A. Ludsin, D. Mason, A.M. Michalak, R.P. Richards, J.J. Roberts, D.K. Rucinski, E. Rutherford, D.J. Schwab, T.M. Sesterhenn, H. Zhang, and Y. Zhou (2014). Assessing and addressing the re-eutrophication of Lake Erie: Central basin hypoxia. *J. Great Lakes Res.* 40(2): 226-246.

Schmidt, J.R., S.W. Wilhelm, and G.L. Boyer (2014). The fate of microcystins in the environment and challenges for monitoring. *Toxins* 6(12): 3354-3387.

Scott, W.B. and E.J. Crossman (1973). *Freshwater Fishes of Canada*. Ottowa, ON: Fisheries Research Board of Canada.

Sekhon, J.S. (2011). Multivariate and propensity score matching software with automated balance optimization: The Matching package for R. *J. Stat. Software*. 42(7): 1-52.

Selgeby, J.H. (1975). Life histories and abundance of crustacean zooplankton in the outlet of Lake Superior, 1971-1972. *J. Fish. Res. Board Can.* 32: 461-470.

Siefert, R.E. (1972). First food of larval yellow perch, white sucker, bluegill, emerald shiner, and rainbow smelt. *Trans. Am. Fish. Soc.* 101(2): 219-225.

Stumpf, R.P., T.T. Wynne, D.B. Baker, and G.L. Fahnenstiel (2012). Interannual variability of cyanobacterial blooms in Lake Erie. *PLoS ONE* 7:8.

Stumpf, R.P, L.T. Johnson, T.T. Wynne, and D.B. Baker (2016). Forecasting annual cyanobacterial bloom biomass to inform management decisions in Lake Erie. *J. Great Lakes Res.* 42:1174-1183, Supplementary Material.

Taylor, W.W., and C.P. Ferreri, editors (1999). Great Lakes Fisheries Policy and Management. Michigan State University Press, East Lansing, MI.

Therneau, T., B. Atkinson, and B. Ripley (2014). rpart: Recursive partitioning and regression trees. R package version 4.1-8. Retrieved from http://CRAN.R-project.org/package=rpart.

Tilahun, U., and A. Bedemo (2014). Farmers' perception and adaptation to climate change: Heckman's two stage selection model. *Ethiopian Journal of Environmental Studies and Management,* 7: 832–839.

Trometer, E.S. and W.D.N. Busch (1999). Changes in age-0 fish growth and abundance following the introduction of zebra mussels *Dreissena polymorpha* in the western basin of Lake Erie. *N. Am. J. Fish. Manage.* 19: 604-609.

Walleye Task Group (2016). Report for 2015 by the Lake Erie Walleye Task Group. Prepared by T. Wills, J. Robinson, M. Faust, A.M. Gorman, M. Belore, A. Cook, R. Drouin, T. MacDougall, Y. Zhao, C. Murray, and M. Housak. Report of the Walleye Task Group to the Great Lakes Fishery Commission at the Annual Meeting of Lake Committees, Niagara Falls, ON. 26 pp.

Warlen, S.M., P.A. Tester, and D.R. Colby (1998). Recruitment of larval fishes into a North Carolina estuary during a bloom of the red tide dinoflagellate, *Gymnodinium breve*. *Bull. Mar. Sci.* 63(1): 93-95.

Ware, D.M. and R.E. Thomson (2005). Bottom-up ecosystem trophic dynamics determine fish production. *Science* 308: 1280-1284.

Wiegand, C. and S. Pflugmacher (2004). Ecotoxicological effects of selected cyanobacterial secondary metabolites a short review. *Toxicology and Applied Pharmacology* 203:201-208.

Wilson, A.E. O. Sarnelle, and A.R. Tillmanns (2006). Effects of cyanobacterial toxicity and morphology on the population growth of freshwater zooplankton: Meta-analysis of laboratory experiments. *Limnol. Oceanogr.* 51: 1915-1924.

Winslow, C.J. (March 2015). *Ecological and economic importance of Lake Erie and the impacts of harmful algal blooms*. Oral presentation at the 2015 Great Lakes Conference: Advancing Knowledge and Improvement, East Lansing, MI.

Wismer, D.A. and A.E. Christie (1987). Temperature relationships of Great Lakes fishes: A data compliation. *Great Lakes Fish. Comm. Spec. Pub.* 87(3): 165p.

Wituszynski, D.M. (2014). *Variation of microcystin concentrations in fish related to algae blooms in Lake Erie, and public health impacts.* (Master's thesis). Retrieved from https://etd.ohiolink.edu/!etd.send_file?accession=osu1406224138&disposition=attachment.

Wood, J. D., Franklin, R. B., Garman, G., Mcininch, S., Porter, A. J., & Bukaveckas, P. A. (2014). Exposure to the Cyanotoxin Microcystin Arising from Interspecific Differences in Feeding Habits among Fish and Shell fish in the James River Estuary, Virginia. *Enviromental Science & Technology*, *48*, 5194–5202.

Wooldridge, J.M. (2012). *Introductory Econometrics A Modern Approach.* Mason, OH: South-Western.

Wynne, T.T. and R.P. Stumpf (2015). Spatial and temporal patterns in the seasonal distribution of toxic cyanobacteria in western Lake Erie from 2002-2014. *Toxins* 7:1649-1663, Supplementary Material.

Zhao, Y., P.M. Kocovsky, and C.P. Madenjian (2013). Development of a stock-recruitment model and assessment of biological reference points for the Lake Erie walleye fishery. *North American Journal of Fisheries Management* 33(5): 956-964.